IDENTIFICATION, CHARACTERIZATION AND EVALUATION OF POTENTIAL VACCINE CANDIDATES FOR THE CONTROL AND MANAGEMENT OF PESTE DES PETITS DISEASE IN RUMINANTS

WILLIS ABWAO ADERO

DOCTOR OF PHILOSOPHY IN MEDICAL BIOTECHNOLOGY

THE JOMO KENYATTA UNIVERSITY OF AGRICULTURE AND TECHNOLOGY

2026

Identification, Characterization and Evaluation of Potential Vaccine Candidates for the Control and Management of Peste Des Petits Disease in Ruminants

Willis Abwao Adero

A Thesis Submitted in Partial Fulfillment of the Requirements for the Degree of Doctor of Philosophy in Medical Biotechnology of the Jomo Kenyatta University of Agriculture and Technology

2026

DECLARATION

This thesis is my original work and has not been presented for a degree in any other University.

Signature……Date……

Willis Abwao Adero

This thesis has been submitted for examination with our approval as the University Supervisors:

Signature……Date……

Dr. Steven Ger Nyanjom, PhD

JKUAT, Kenya

Signature……Date……

Dr. Martin Kiogora Mwirigi, PhD

KALRO, Kenya

Signature……Date……

Dr. Yattinder Sigh Binnepal, PhD

KALRO, Kenya

DEDICATION

To my late parents, Mr. and Mrs. Joash Adero, my dear children, brothers, sisters, wife, and my Golden shemeji, who were my source of encouragement during my study period and thesis writing and to my children Meshack, Shadrack, Dylan, Lilly and Favor for the emotional support they accorded me during this entire period.

ACKNOWLEDGEMENT

I would like to acknowledge the Jomo Kenyatta University of Agriculture and Technology for granting me the opportunity to pursue this training within the University.

My sincere gratitude goes to the Director General Kenya Agricultural and Livestock Research Organisation (KALRO) for granting me the opportunity to pursue these studies. Special thanks also go to my supervisors: Dr. Steven Ger Nyanjom, Dr. Martin K. Mwirigi, and Dr. Yatinder S. Binnepal, who have been working tirelessly to guide me through this research process by facilitated the implementation of my objectives as captured in this thesis and writing of this thesis.

I would also like to appreciate Dr. Catherine O. Taracha for providing technical and moral support during this time, not to forget my colleagues who helped me with ideas towards achieving my objective.

I would specifically wish to acknowledge Kenya Climate Smart Agricultural Project (KCSAP) and United States Agency for International Development (USAID project for their financial support and for enabling me to actualize the whole PhD Programme.

I would also wish to acknowledge Mr. Paul Kirui, and Mr. Sam Guya for their dedicated effort they accorded me during my lab work.

TABLE OF CONTENTS

LIST OF TABLES

LIST OF FIGURES

LIST OF APPENDICES

ACRONYMS AND ABBREVIATIONS

ASAL Arid and Semi-Arid Lands

BCA Bicinchronic Acid

BCG Bacillus Calmente Guarin

Bepi-Pred B-cell Epitope Prediction Tool

BoLA Bovine Leucocyte Antigen

BSA Bovine serum Albumin

CDV Canine Distemper Virus

CMV Cartecian Mobillivirus

CTL Cytotoxic T Lymphocytes

CTL Cytotoxic T-Lymphocyte

DAB Diamino Benzidin**e**

DISO Disordered Region

DIVA Differentiating Infected from Non-infected animals

DNA Deoxyribonucleic Acid

ER Endoplasmic Reticulum

FAO Food and Agriculture Organization

FAOSTART United Nation Food and Agricultural Organization Statistical Database

FASTA	Bioinformatic Data Format Used to Store Nucleotide or Amino Acid Sequence
F	Fusion Gene
GDT-HA	Global Distance Test High Accuracy
GF-TAD	Global Framework for the Progressive Control of Transboundary Diseases
GRAVY	Grand Average Hydropathy
HLA	Human Leucocyte Antigen
HN	Hemagglutinin Nur amidase
HRP	Horseradish Peroxidase
IACUC	Institutional Animal Care and Use Committee.
IEDB	Immune Epitope Data Base Tool
KALRO	Kenya Agricultural and Livestock Research Organization
KEVEVAPI	Kenya Veterinary Vaccine Production Institute
LB	Luria Bartani Media
M	Matrix Gene
MHC-1	Major Histocompatibility Complex-1
mRNA	Messenger ribonucleic Acid
Mw	Molecular Weight

Nig/75	Nigerian Strain of PPRV
Ni-NTA	Nickel–Nitrilotriacetic Acid Agarose
N	Nucleocapsid
WOAH	World Organization of Animal Health
PAGE	Poly acrylamide Gel Electrophoresis
PBS	Phosphate Buffer Saline
PDV	Phocine Distemper Virus
PMSF	Phenylmemthyle Suphonylflouride.
P	Phosphoprotein
PPR	Peste des Petite ruminant
PPRV	Peste des Petite Virus
PSIPRED	Protein Structure Prediction Server
rDNA	Recombinant Ribonucleic acid
RMS	Root Mean Score
RNA	Ribonucleic Acid
RP	Rinder Pest
RPV	Rinder Pest Virus
RT	Room Temperature

SLAM	Signal Lymphocyte Activation Molecule
TBE	Tris-Borate-EDTA buffer
TLR-1	Toll Like Receptors
TT	Thermotolerance
Vc-RNA	Virus Complimentary Ribonucleic Acid

ABSTRACT

Peste des petits ruminants (PPR) is a highly contagious transboundary viral disease affecting small ruminants and causing major economic losses in sub-Saharan Africa, including Kenya. Current vaccines require strict cold-chain storage, limiting effective disease control in tropical regions. This study aimed to develop and evaluate a thermostable multi-epitope subunit vaccine targeting the Fusion (F) and Hemagglutinin (H) proteins of Peste des petits ruminant virus (PPRV). Bioinformatics tools were used to predict B- and T-cell epitopes from selected immunogenic amino acid sequences. A total of 82 H-protein and 94 F-protein sequences were retrieved from the National Centre for biotechnology information (NCBI) database and analyzed using bioinformatics and immunoinformatics tools. Conserved B- and T-cell epitopes were identified, characterized for antigenicity, allergenicity, toxicity, and immunogenicity, these were assembled into a multi-epitope vaccine construct with suitable linkers and adjuvant sequences (Gotsman et al., 2006). The final construct had 620 amino acid residues amongst which 51.6% were predicted to be exposed, 20.7% to be medium exposed while (28.2%) were predicted to be buried. A total of 70 amino acid residues were predicted to be located in disordered regions while 550 were predicted to be located in ordered regions. The Model with the lowest Root-mean-square-deviation of atomic position (RMSD) score of 9.6982, was later chosen for refinement. The predicted vaccine construct had a molecular weight (MW) of 65361.99 Da with a theoretical isoelectric point (pI) of 5.70. The Grand Average of Hydropathy (GRAVY) was predicted to be -0.165 and a half-life of more than >10h *in vivo* in *E. coli* and >30h *in vitro* in mammalian reticulocytes. The vaccine was predicted as stable with instability Index of 21.20, estimated aliphatic index of 92.34 and GDI-HA scores slightly above 0.9, with MolProbability score of 2.619. There was positive correlation between Test vaccine candidate and a Positive (N/75), which was statistically significant ($r=+0.95$, $n=10$, $p<0.001$, (2-tailed). Close similarity was observed between the tested strains. These findings indicate that the vaccine candidate is a promising thermostable subunit vaccine for controlling PPRV in small ruminants.

CHAPTER ONE

INTRODUCTION

1.1 Importance of Peste des Petits Ruminants

Peste des petits ruminant (PPR) was first reported in Kenya in 2006, with initial outbreaks occurring in Turkana County, after which the disease spread rapidly across the arid and semi-arid lands (ASALs). Subsequent studies have demonstrated that the rate of spread varies considerably between regions, ranging from 30% to 70% depending on the county. For instance, Turkana County reported infection rates of approximately 40% in goats and 32% in sheep, while Kwale County recorded a seroprevalence of 48.6% in goats (Kihu[a] et al., 2015; Mutua et al., 2023). Several risk factors have been identified as key drivers of PPR transmission within pastoral production systems. These include high levels of pastoral mobility, communal grazing practices, and the presence of porous international borders with neighbouring countries such as Ethiopia, Somalia, and Uganda, all of which facilitate transboundary disease spread (FAO & WOAH, 2016). In response to the outbreaks, vaccination campaigns were initiated in Kenya in 2008. However, vaccination coverage has remained inconsistent, resulting in recurrent outbreaks in susceptible populations. Beyond Kenya, PPR is endemic across sub-Saharan Africa, the Middle East, South Asia, and parts of China, where it continues to pose a significant threat to small ruminant production systems (Banyard, A.C., et al., (2010). The disease is characterized by high morbidity rates of up to 100% and mortality rates ranging from 50% to 90% in naïve populations, thereby severely undermining food security and rural livelihoods.

The presence of Peste des petits ruminants (PPR) across Africa, Asia, and Europe continues to interfere with food security, livelihoods, and trade, posing significant threats to biodiversity and the health of ecosystem, especially in developing countries where diseases are endemic and difficult to control (Rossiter and Al Hammadi, 2009). The Transboundary Animal Diseases (TAD), which include Peste des petits

(PPR), Foot and Mouth disease (FMD), Classical swine fever (CSF), Contagious bovine pleuro-pneumonia (CBPP) and Rift Valley fever (RVF), are of great concern and contribute to a high rate of morbidity and mortality with rapid spread across borders affecting poor and the most vulnerable farmers (Seyoum and Teshome, 2017; Negesso et al., 2016). The disease affects small ruminants, especially goats and sheep (Bwihangane et al., 2017), and is caused by a virus of the genus morbillivirus (Mariner et al., 2017). The virus is a single-stranded RNA virus of the family Paramyxoviridae (subfamily Paramyxovirinae) under the order Mononegavirales (Diallo, 2007). Due to its nature, the disease has since been declared the next target for eradication by the Food and Agriculture Organization (FAO) of the United Nations and the World Organization for Animal Health (WOAH). The disease is of great economic importance causing mortality rates of up to 100% especially in naïve population (Hailat et al., 2018) and mortality rate of 0 to 90% in susceptible animals (Rojas et al., 2017).

In the year 2015, the international community set a target to eradicate PPR disease by 2030 and since then, FAO and WOAH have jointly developed and implemented the Global Control Eradication Strategy for PPR (Benfield et al., 2023). Conventionally, PPR has been controlled through vaccination using a tissue culture-attenuated Kabate 'O' strain of RPV (Rinderpest Virus) (both mobilliviruses), originally developed by Plowright and Ferris (Baron et al., 2005). However, the vaccine is highly heat-labile, limiting its use in field vaccination programs. Hence, it is of significant importance to develop alternative homologous vaccines against PPR (Kamel & El-Sayed, 2019). To be effective, sanitary regulations require an efficient veterinary service to regulate animal movement which is costly for most developing countries. Medical prophylaxis involves vaccination and campaigns which are costly to implement for most poor, small-scale livestock farmers in developing countries. Hence, the need to develop alternative vaccines against PPR (Kamel and El-Sayed, 2019). Traditional antigen production strategies require the cloning and expression of several hundred proteins (Pizza et al., 2000) and their purification before evaluation in immunogenicity assays. These methods are often laborious and challenging due to

the many complications associated with expression of outer membrane proteins including issues of low solubility, formation of inclusion bodies, protein instabilities and toxicity to the expression host (McAllister et al., 2018). Significant advancement in technologies over the past two decades and the approaches used for vaccine design have emerged.

Advancements in the field of bioinformatics and immunology have led to disciplines in vaccine design against diseases via computer-aided (*in silico*) epitope predictions. This technology has enabled the development of specific peptide-based vaccines and employs the construction and analysis of algorithms for mapping possible B- and T-cell epitopes. The technology has been successfully used in the identification of vaccine candidate against Omicron variant of SARS-CoV-2 using immunoinformatic approaches (Aasim et al., 2022). The availability of whole genome sequencing has also shifted the focus towards *in silico* antigen prediction for the development of third generation vaccines (Klima et al., 2019). The reverse vaccinology (RV) approach starts from the genome rather than the whole organism and identifies the entire catalogue of proteins within an organism with the potential to express at any point in time (Palumbo et al., 20111). This strategy has the added advantage of being applied to cultivatable and non-cultivatable species (McAllister et al., 2018).

The PPRV has a genomic sequence of ~16kb in length, composed of 15,948 nucleotides that are characterized into contiguous, non-overlapping and transcription units, encoding for six transcriptional units (Bailey et al., 2005), arranged from 3′to 5′ as nucleoprotein (N), phosphoprotein (P), matrix (M), Fusion (F), haemagglutinin (H) and large polymerase protein (L). The virus genome is arranged in the order of 3 N–P/C/V–M–F–H–L 50 separated by inter-genic region (Balamurugan et al. 2014) that is divided into six transcriptional units encoding two non-structural proteins (V, C) and six structural proteins: the surface glycoproteins include the fusion (F) and Haemagglutinin (H) proteins, the matrix protein (M), the nucleoprotein (N), and the phosphoprotein (P) forms the polymerase complex in association with large (L) protein (Balamurugan et al., 2014). The nucleoproteins of morbilliviruses are highly

immunogenic proteins produced in large quantities within the cells during virus infection (Haas et al., 1995). This makes it a suitable target for the host's immune response. This study identified, characterized and evaluated a multi-epitope vaccine candidate against PPRV using immunoinformatics approaches targeting the H and F proteins.

1.2 Statement of the Problem

Small-scale livestock production systems in sub-Saharan Africa are critical to household food security, income generation, and socio-economic resilience, particularly among women, pastoralists, and resource-constrained communities in Sub-Saharan Africa. Sheep and goats provide meat, milk, manure, skins, and financial security, making them indispensable livelihood assets in arid and semi-arid regions. However, the sustainability of small ruminant production is severely threatened by transboundary infectious diseases, notably Peste des Petits Ruminants (PPR) (Pope et al., 2013). The disease is a highly contagious viral disease caused by the PPR virus (PPRV), a member of the genus Morbillivirus, which primarily affects goats and sheep and is characterized by fever, stomatitis, pneumonia, diarrhea, and high mortality rates (FAO and WOAH, 2023). The disease continues to spread across Africa, the Middle East, and Asia despite ongoing global eradication efforts. Globally, PPR threatens more than 300 million rural families that depend on small ruminants for their livelihoods, with annual economic losses estimated at between US$ 1.4 and 2.1 billion (FAO & WOAH, 2023). In sub-Saharan Africa, recurring outbreaks continue to undermine livestock productivity through mortality, reduced milk production, poor growth performance, reproductive losses, and restrictions on livestock trade. In Kenya, PPR remains endemic in pastoral and agro-pastoral regions, including Turkana, Marsabit, Mandera, Garissa, and Kajiado counties, where the disease periodically causes devastating socio-economic losses. Previous outbreaks in Turkana County reportedly resulted in destruction of up to 65% of household livestock assets and annual economic losses exceeding USD 2 million (Kihu[b] et al., 2015; Jemberu et al., 2022). Recent epidemiological studies further

indicate continued circulation of diverse PPRV lineages in East Africa, raising concerns regarding viral evolution, transboundary spread, and vaccine effectiveness (Banyard et al., 2024). Vaccination remains the primary strategy for PPR prevention and control. Currently licensed vaccines, including PPRV/Nigeria/75 and PPRV/Sungri/96, are live-attenuated vaccines that confer long-lasting immunity and have played a significant role in disease reduction (Singh et al., 2019). However, these vaccines possess several limitations that hinder their effectiveness in endemic regions. First, they require strict cold-chain maintenance during transportation and field deployment, a major challenge in remote pastoral areas with limited infrastructure and unreliable electricity supply. Second, live-attenuated vaccines are associated with biosafety concerns, including the theoretical risk of reversion to virulence, contamination during production, and difficulties in differentiating infected from vaccinated animals (DIVA), which complicates disease surveillance and eradication programmes (Diallo et al., 2021). Although thermostable formulations have recently been developed to improve vaccine stability under tropical conditions, vaccination coverage in many endemic regions remains inadequate due to logistical, financial, and infrastructural constraints.

In addition, conventional vaccine development approaches for PPR have largely relied on empirical laboratory-based methods involving virus isolation, attenuation, and antigen production in cell culture systems. These approaches are often labor-intensive, time-consuming, costly, and may fail to identify transiently expressed or poorly immunogenic viral proteins that could serve as potential vaccine candidates. Advances in genomics, immunoinformatics, reverse vaccinology, and structural bioinformatics now offer opportunities for rational vaccine design through identification of highly conserved immunogenic epitopes capable of inducing robust cellular and humoral immune responses (Deeba et al., 2023). Despite these advances, limited studies have explored computationally designed multiepitope vaccines targeting the immunodominant fusion (F) and hemagglutinin (H) proteins of PPRV, particularly in the context of African circulating strains. Therefore, there remains an urgent need to develop safer, thermostable, cost-effective, and broadly protective

next-generation PPR vaccines that can overcome the limitations of current live-attenuated vaccines while supporting the global PPR eradication strategy targeted for 2030. The application of immunoinformatics and recombinant vaccine technologies presents a promising alternative for the development of novel multiepitope subunit vaccines with improved safety, stability, and immunogenicity against PPRV (Dhanda et al., 2018; Glick & Patten, C. L. (2022).

1.3 Justification

Recent advancements in bioinformatics and genomics approaches in biomedical sciences has led to the sequencing of many pathogen genomes, as well as the increase in nucleotide and protein sequence databases. Availability of genes and protein motifs that control critical biological processes in pathogens can be identified, characterized and manipulated to develop synthetic-based vaccine. Synthetic peptide vaccines that offer many advantages, which include absence of any potentially infectious material, such as that present in live attenuated vaccines, ability to include multiple epitopes, accounting for multiple variants of a pathogen, economical production on a large scale, ability to manufacture vaccines for pathogens that are difficult or impossible to culture in the laboratory and ability to minimize the amount and complexity of a well-defined antigen.

An appropriate peptide-based vaccine would also decrease the chance of stimulating a response against self-antigens (Purcell et. al., 2007). The conventional approach to vaccine development requires cultivation of the pathogenic microorganism and its dissection using biochemical, immunological, and microbiological methods to identify the components important for immunity. This method, in many cases, has failed to provide a solution for pathogens with no vaccines. In this study, the reverse vaccinology approach was used for PPRv vaccine development since it reduces the time required for the identification of vaccine targets.

The development of PPR vaccine using an immunoinformatics approach helps to predict the epitopes from the antigenic regions of the respective pathogens, which is

particularly useful for developing multi-epitope-based vaccines targeting antibiotic-resistant strains (Mugunthan & Harish, 2021). Specific epitopes are identified which can effectively stimulate the immune responses against resistant strains (Alharbi et al., 2022). To effectively vaccinate against PPR, it is crucial to utilize safe, low-risk, and low-complication vaccines. PPR vaccine development using an immunoinformatics approach allows for the prediction of epitopes from antigenic regions of the virus, enabling the design of multi-epitope vaccines. These vaccines stimulate specific immune responses and minimize risks associated with conventional live vaccines, such as reversion to virulence (Bouazzaoui et al., 2021). These new improved PPR vaccines offer significant benefits to small-scale farmers by providing enhanced protection, improved vaccine stability, and cost-effectiveness which lead to increased livestock productivity, reduced disease-related losses, and improved livelihoods, especially for vulnerable communities reliant on small ruminants. Additionally, the vaccines are often thermostable thus enhancing their efficacy and use in ASAL areas where most small-scale farmers are found (Zhao et al., 2021).

1.4 Research Objectives

1.4.1 General Objective

To identify, characterise and evaluate potential vaccine candidates for the control and management of PPR

1.4.1 Specific Objectives

i. To determine appropriate immune epitopes from the PPR virus whole genome sequence
ii. To clone, express and Molecular characterize the selected immune epitopes
iii. To computationally and experimentally assess the immunogenicity, allergenicity, toxicity, and physicochemical characteristics of the selected and

expressed protein candidates for their suitability as vaccine targets against PPRvirus.

1.5 Research Question

i. Does reverse vaccinology accurately predict immunogenic epitopes in PPRV enabling the development of a subunit vaccine?
ii. Are immunogens identified through bioinformatic tools immunogenic and suitable as vaccine candidates for PPR?
iii. Do expressed proteins demonstrate protective potential as vaccine candidates against PPRV?

1.6 Scope and Limitations of the Study

1.6.1 Scope

This study involved bioinformatic analysis of the complete PPRV genome sequence to identify immunogenic regions using computational tools. Selected epitopes were assessed for immunogenicity, toxicity, stability, and hydropathy. The identified sequences were then cloned and expressed in an expression vector before being purified and assessed for their potential as subunit vaccine candidates through *in-vivo* and *in-vitro* evaluation.

1.6.2 Limitation of Study

The research predominantly relied on in silico approaches to predict the immunogenicity, allergenicity, toxicity, and physicochemical properties of selected protein candidates, and while these tools are efficient and cost-effective, they may not fully capture the complexity of biological responses in vivo. In addition, the study focused on a limited number of proteins, which may not represent the full antigenic diversity of Peste des petits ruminant virus (PPRV), potentially affecting the broad applicability of the results across different viral strains and geographical regions. Experimental validation was also limited, with minimal or no in vivo

assessment of immune responses, protective efficacy, or long-term immunity in target animal species. Furthermore, the lack of extensive field-based epidemiological data and constraints in resources restricted large-scale protein characterization and real-world applicability. Finally, critical aspects such as vaccine delivery systems, thermostability, and large-scale production feasibility were beyond the scope of this study, yet remain essential for practical implementation in endemic settings.

1.7 Hypothesis

Alternative Hypothesis (Ha)

Selected and expressed protein candidates of Peste des petits ruminant virus (PPRV) will exhibit high immunogenicity, while remaining non-allergenic, non-toxic, and possessing favorable physicochemical properties, thereby making them suitable candidates for vaccine development.

Null Hypothesis (H_0)

Selected and expressed protein candidates of PPRV do not exhibit adequate immunogenicity and/or demonstrate allergenic, toxic, or unfavorable physicochemical properties, rendering them unsuitable for vaccine development.

CHAPTER TWO

LITERATURE REVIEW

2.1 Historical Development of Peste des Petits Ruminants Virus (PPRV)

Peste des petits ruminant viral disease was first described in the Republic of Côte d'Ivoire in West Africa in 1942 (Gargadennec and Lalanne, 1942). However, there are indications that the disease existed much earlier. The disease is considered one of the main constraints to small ruminants' production and is listed as a reportable disease by the Office International des Epizooties (OIE) (Tenuche, et al., 2023). Sheep and goats are the most affected contributing to high economic losses (Kwiatek *et al.,* 2011). The disease is an acute and highly contagion affecting sheep and goats, with subclinical manifestations in ruminants. It represents one of the most important ruminant diseases that poses a great challenge to sustainable small-scale agriculture productivity, particularly in small ruminant farming in developing countries (Banyard et al., 2014).

However, the disease has also been found to affect other wild ruminant species. The virus was first identified in West Africa, and has since spread to other regions, including Central Africa. The disease is characterised into lineages which include Lineage I-IV with the common lineage being Lineage I and II. Amongst the lineages, lineage-IV is the most widespread lineage present in Southern Asia, the Middle East, and many countries of Africa (Banyard et al., 2010). In the last 20 years the disease has shown rapid spread throughout large parts of the developing world (Banyard et al., 2010; Kwiatek et al., 2011) and has since spread to sub-Saharan Africa, the Middle East, Turkey and the Indian subcontinent.

During the last decade, the disease has been reported for the first time in China, Kenya, Uganda, Tanzania, Morocco and Tunisia (Banyard et al., 2010: Lamp & Haq, 2016) Lamb & indicating that the virus is highly infectious, and is of emerging transboundary nature. Initially, according to (Yadav[a] et al., 2020). The disease has,

however, gained attention during a recent rinderpest outbreak that was observed in sheep and goats and could not be transmitted to another large ruminant (McVety et al., 2018). It was not until Gibbs and others (1979) revealed that it is biologically and physico-chemically distinct; hence, it was considered a new member in the genus Morbillivirus, alongside RPV, canine and phocine distemper viruses (CDV and PDV), measles virus (MV) and morbilliviruses of porpoises, dolphins and cetaceans (PMV, DMV and CMV).

Since PPR and Rinderpest (RP) are clinically related diseases and the viruses are antigenically similar, it is believed that PPR remained undiagnosed due to the high prevalence of RP and the availability of the available diagnostic tests to differentiate PPR from RP (Baron et al., 2016). The disease is characterized by fever, oculonasal discharge, stomatitis, diarrhea, bronchopneumonia, and sometimes death. Goats and sheep are the natural targets. (Shankar, 2016).

PPRV is characterized and phylogenetically analysed based on the fusion gene (F), which classified all the strains of PPRV into four distinct lineages however, it appeared that phylogenetic analysis based on the nucleoprotein gene (N) presents a much better molecular epidemiological pattern (Kwiatek et al., 2007) hence, is currently preferred over F gene- classification. However, all the strains are in the same group regardless of what gene is used as a basis for classification, except that the F gene-based lineage I (i.e. Nig/75) became lineage II on the N gene-based tree. Other recent suggestions have been made based on the use of haemagglutinin neuraminidase (HN) gene F and N genes, which could give better solutions and permit tracing of virus transmission within outbreaks. (Balamurugan et al., 2014). Nevertheless, it is still unclear whether differences between lineages merely reflect geographical speciation or if they are also correlated with variability in pathogenicity between isolates (Banyard et al., 2010).

There is currently no effective curative treatment available for this viral disease. Consequently, disease control and prevention primarily rely on the implementation of stringent sanitary and phytosanitary measures, including the provision of efficient

veterinary services, surveillance, biosecurity practices, movement control, and vaccination programs where applicable. The implementation of animal movement regulations, with stamping out policy that come with a high cost during outbreaks especially in developing countries. Therefore, the only way to effectively control PPRV is through employment of vaccination programmes. Currently, efficient attenuated vaccines are available for its control, unfortunately, in most cases they are used only during outbreaks to limit spread of the disease, despite the fact that vaccination campaigns need to be systematic. The cost associated with their implementation is also too high for most developing countries, hence the only feasible way to cut down this cost is through the development of cheaper thermostable subunit vaccine that would enable, protection in one shot making it an economic viable venture for most developing nations.

Conventionally available vaccines consist of attenuated or killed agents that poses risk of reversion to live viruses (Andey, et al., 2024, as well as take a long time for their development which includes cultivation of the desired microorganism at a larger scale and under proper conditions, as well as an effective inactivation with appropriate inactivating agent and subsequent evaluation of vaccine immunogenicity.

In Kenya, it was first confirmed in 1992 (Mantipe et al., 2019) and confirmed in the Turkana district in 2007 (Kihu et al., 2012). The disease has a significant economic burden to the farmers leading to multiple losses (Kihu et al., 2013). PPRV has now spread to over 70 countries in Africa, the Middle East, and Asia, and is currently threatening more than 1.7 billion sheep and goats, amounting to 80 % of the global population (Baro *et al.,* 2017). Impacting negatively on the pastoral community, their livelihoods, and their food security (Kotchofa et al., 2021). Women and children are the most affected group of the population (Kumar *et al.,* 2003). During infection goats are more susceptible to the infection than sheep (Abubakar et al., 2008). Incidence of peste des petits ruminants (PPR) virus in sheep and goat as detected by immuno-capture *ELISA has* a morbidity rate of 80-90% and mortality rates of 50 - 80% (Kumar et al., 2014). Sero-prevalence and associated risk factors of peste des

petits ruminants among ovine and caprine in selected districts of Afar region in Ethiopia, have been associated with a high rate of abortions in infected goats (Kardjadj et al., 2016; Dubie, et al., 2022). The causative agent is a highly contagious paramyxovirus of the *genus Morbillivirus* that is closely related to measles virus (MeV) in humans, rinderpest virus in cattle and canine distemper virus in canines (Prajapati et al., 2019). Infection is by direct contact of healthy animals with the secretions or excretions from infected animals, or contaminated fomites. The disease is relatively new in Kenya, and limited information is available regarding the factors contributing to its spread. Approximately 44,869,759 small ruminants are considered at risk of infection (Kihu, 2014). Efforts to control the disease in Kenya have been constrained by insufficient epidemiological data, inadequate funding, and limited technical support. Consequently, the effectiveness of current control measures in curbing the spread of the disease remains uncertain.

2.2 Geographical Distribution of PPR

PPRV has a widespread distribution spanning West and Central Africa, Arabia, the Middle East and southern Asia (Banyard et al., 2010). Initial discovery of the disease was in West Africa but has since spread to other sub-Saharan African countries, the Middle East, Turkey and the Indian subcontinent. (Banyard et al., 2010; Munir *et al.,* 2013), indicating its highly infectious and transboundary nature, and over the last 20yrs the disease has shown rapid spread throughout large parts of the developing world (Baron et al., (2014). Peste des petits ruminants (PPR) have been documented across multiple regions of Africa, underscoring its extensive geographic distribution and progressive spread OIE/WOAH (2021). The disease is endemic in West Africa, where countries such as Nigeria, Senegal, and Mali have reported recurrent outbreaks linked to transboundary livestock movements (Munir et al., 2013). In Central Africa, confirmed cases in Cameroon and Chad highlight the persistence of the virus in pastoral systems characterized by high animal mobility. Similarly, East African nations including Ethiopia, Kenya, and Uganda have experienced significant outbreaks, threatening millions of small ruminants that form the backbone of rural

livelihoods (Kihu, 2014). In North Africa, the occurrence of PPR in Morocco, Algeria, and Tunisia demonstrates that the disease has penetrated the Maghreb region, which was previously considered free of infection (Baazizi et al., 2017;). Recent epidemiological analyses further indicate a southward trajectory of PPR spread, raising concerns about its potential incursion into Southern African countries where small ruminant populations remain highly vulnerable (FAO, 2016). This evidence collectively justifies the assertion that PPR is not only entrenched across West, Central, East, and North Africa but is also advancing toward Southern Africa, thereby posing a continental threat to food security and livestock-dependent economies.

Countries in Central and southern Africa who have reported their first ever PPR outbreaks include; Gabon, Democratic Republic of Congo and Angola (Diallo et al., 2019). In Kenya, the disease was first suspected by pastoral communities and other livestock in Oropoi and Lokichoggio divisions of Turkana County, Rift Valley province of Kenya in 2006, and has since spread to Kakuma, Loima and Kibish divisions of Turkana districts as described in a risk map developed by the VSFB-Belgium. The disease has since spread to other areas beyond Turkana into the neighbouring districts (Kihu *et al.*, 2012), as well as in other arid and semi-arid areas within Northern and southern parts of Kenya, with several other outbreaks being reported to OIE as late as 2013 (Griffith, et al., 2024). Spatial analysis of risk factors and their effects on peste des petits ruminants control strategies in Kajiado and Marsabit pastoral systems of Kenya (Gitonga, 2015).

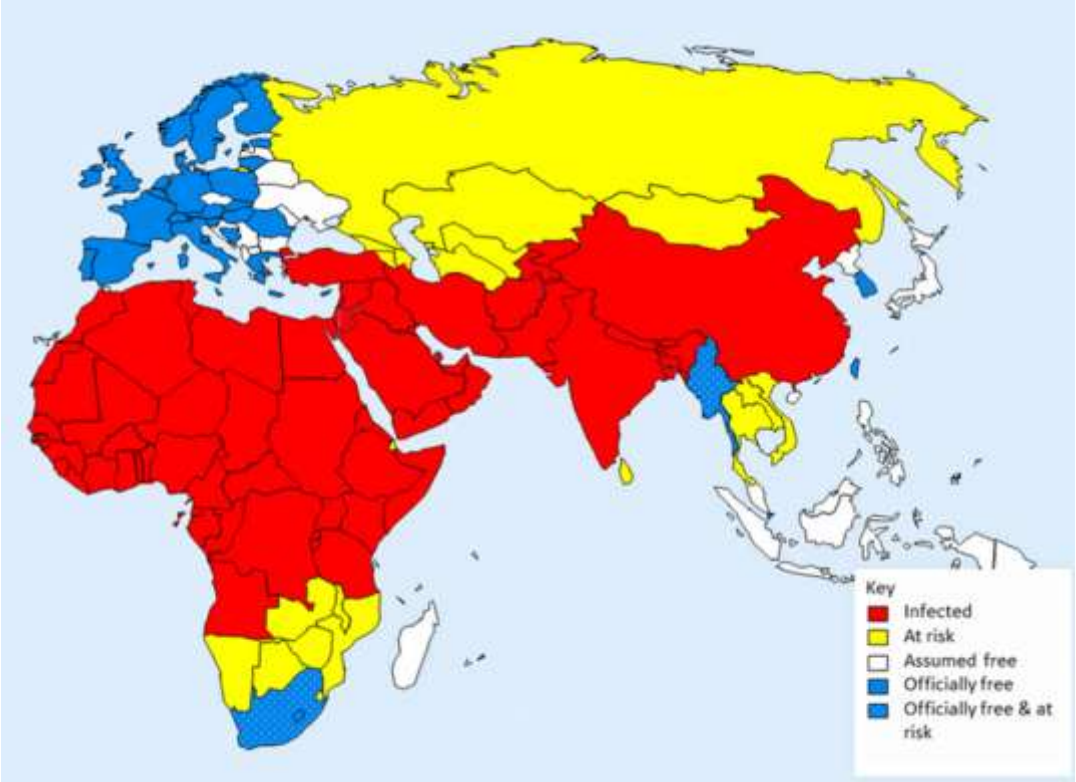

Figure 2.1: Spatial Distribution of Peste des Petits Ruminants Globally. Source: (Bryony Anne Jones https://doi.org/10.1371/journal.pone.0149982.g001)

2.3 History and Classification

Peste des petits ruminant (PPR) is classified as a notifiable terrestrial animal disease by the World Organization for Animal Health (OIE). Globally, PPR has infected 66 countries, including 38 countries in Africa, 27 countries in Asia, and one country in Europe. According to 2018 data from the United Nations Food and Agriculture Organization Statistical Database (FAOSTAT). There are a total of 2.5 billion heads of cattle worldwide, out of which over 1.74 billion sheep and goats are in PPR infected zones i.e., 56.4% (982.3 million) in Asia, 43.6% (759.1 million) in Africa, 0.1% in Europe (1.57 million) (Figure 2.1). The disease was earlier mistaken to be Rinderpest (RP) due to its close antigenic similarities and lack of a DIVA test that could be able to differentiate PPR from RP; this led to the disease remaining

undiagnosed for a long time as a result contributing to its high prevalence rate (Baron et al., 2014).

The disease has however gained attention during recent rinderpest outbreak which was observed in shoats but could not be transmitted to cattle reared in the same herd or proximity, this led to its first recognition by Gibbs et al. (1979) who revealed that it was biologically and physio-chemically distinct from other member of the genus Morbillivirus which included: canine and phocine distemper viruses (CDV and PDV), measles virus (MV) morbilliviruses of porpoises, dolphins and cetaceans (PMV, DMV and CMV), hence the disease was then referred to as 'goat plague' (Muniraju, M. B. 2015) that has contributed to major constraint in the production of small ruminants (Balamurugan et al., 2014).

Initial viral replication involves virus–host receptor interaction. The virus interacts with the host though the HN protein due to sialic acid present on the host cell membrane (linked in a 2–3 linkage), (Moss and Griffin 2006) The H protein is responsible for the attachment of the virus to the cell surface through recognition of and binding to host cell receptor molecules, e.g., salicylic acid, immune cell marker signalling lymphocyte activation molecule (SLAM)/CD 150 (Parida, et al., (2015) or the epithelial cell receptor Nectin-4 (Krishnan et al., 2019). Attachment of the H protein to receptors activates the fusion activity of the F protein, enabling fusion of the viral envelope with the host cell membrane and releasing of the viral genetic material into the Cell cytoplasm. (Leroy et al., 2020).

2.4 Virus Replication

Morbilliviruses replicate solely in the host cytoplasm. The genome of Peste des petits ruminant virus is never found as naked RNA and is fully encapsulated by the N protein forming the helical ribonucleoprotein complex which also protects the RNA from host RNAses. The ribonucleoproteins may consist of genome-sense (–ve) or antigenome-sense (+ve) strands. The ribonucleo protein complex containing the RNA encapsulated by N, in conjunction with L proteins constitute the minimal

replicative unit for this virus. Once in the infected cell, viral genome is released into the cytoplasm and acted upon by the viral polymerase complex, which binds to the genome promoter and starts transcribing short leader RNAs.

The viral polymerase produces mRNAs 50 methylated and 30 poly-adenylated by the viral polymerase which are translated by the host cell machinery. At a certain time point post-infection, the polymerase complex switches its action from the production of mRNA to the production of a full-length positive-sense RNA. This switch is thought to be linked to the accumulation of viral proteins within the host cell, although the precise mechanism for an alteration in polymerase activity remains unclear.

2.5 PPR Genome Characterisation and Classification

Previously, according to (Shaila et al., 1996; Dhar et al., 2002) PPRV was characterized and phylogenetically analyzed based on the fusion gene (F), this classified all the strains into four distinct lineages however, it appeared that phylogenetic analysis based on the nucleoprotein gene (N) presented a much better molecular epidemiological pattern (Sahu et al., (2017), Hence, is currently preferred over F gene.

All PPRV strains are grouped together regardless of which gene is used for classification. The only exception is that the strain Nig/75, which falls under lineage I when classified by the F gene, shifts to lineage II when classification is based on the N gene. Other recent suggestions have been made based on the use of haemagglutinin neuraminidase (HN) gene F and N, which could give better solutions and permit tracing of virus transmission within outbreaks (Gattani, 2019). Nevertheless, it is still unclear whether differences between lineages merely reflect geographical speciation or if they are also correlated with variability in pathogenicity between the isolates (Banyard et al., 2010).

Viral genome of PPRV (Figure 2.2.) is ~16kb in length and is composed of 15,948 nucleotides that are characterized into contiguous, non-overlapping and transcription units and encodes for six structural proteins (Bailey *et al.,* 2005) arranged from the 3′ to 5′ as nucleoprotein (N), phosphoprotein (P), matrix (M), fusion (F), haemagglutinin (H) and large polymerase protein (L).

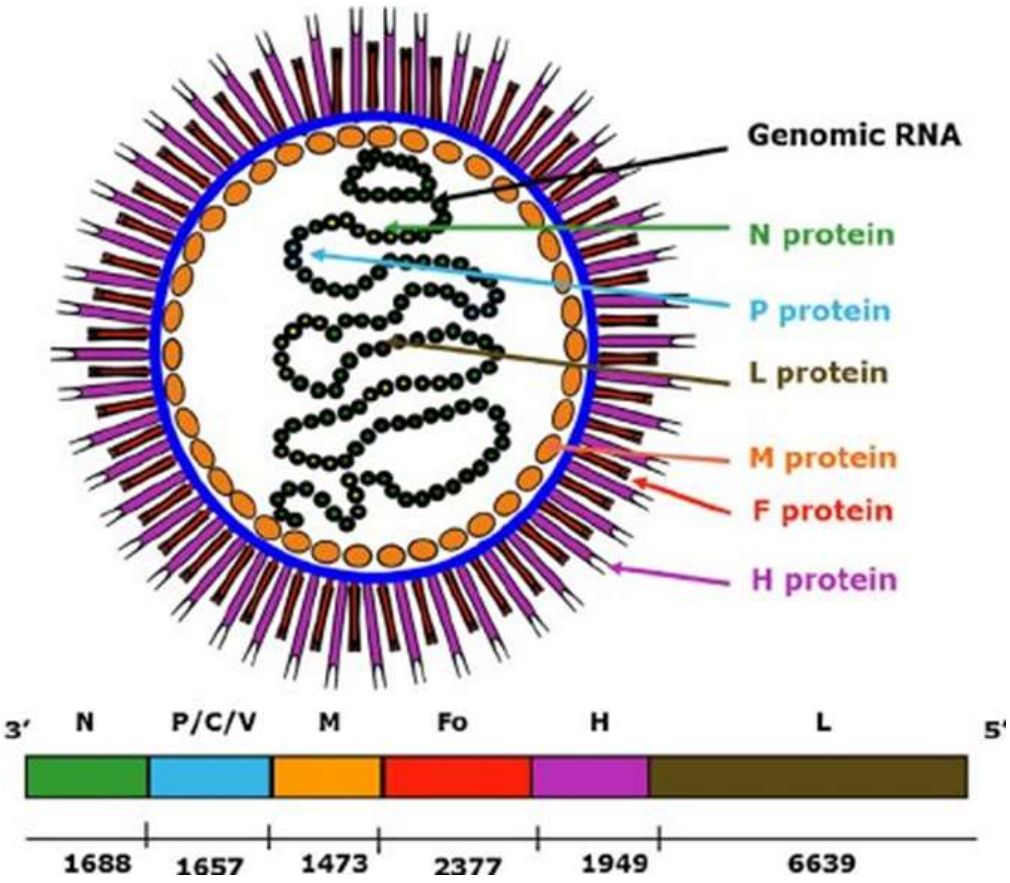

Figure 2.2: Schematic Representation of the PPR Morbillivirus Genome. Source: (Bailey et al., 2005)

2.6 Pathogenesis

The main route of infection is respiratory and hence, infection is via the respiratory tract. All secretions and excretions from infected animals are contagious throughout the disease; once in the host, the virus targets lymphoid tissue. The first step in virus infection is the attachment of a virion to a host cell surface receptor which leads to

the fusion of viral and cellular membrane (Figure 2.3).Negative sense RNA genome is then released into the cell cytoplasm and transcription is initiated to produce viral gene transcripts (mRNAs), that are later translated using the host cell transcriptional machinery after penetrating the caprine endometrial epithelial cells via the caveolae-mediated endocytosis pathway (Yang *et al*,. (2018). Following the production of the necessary viral proteins, a switch to a replicative mode occurs, which results in the production of a positive-sense (+) viral complementary RNA (vcRNA +ve), which is a replicative intermediate that acts as a template for the generation of progeny negative-sense genome RNA. The encapsidated genomes then interact with the M protein and the viral glycoproteins, leading to budding of new virions at the host cell plasma membrane. ER: reticulum. The incubation period usually is 2 to 6 days; however, it can be up to 10 days.

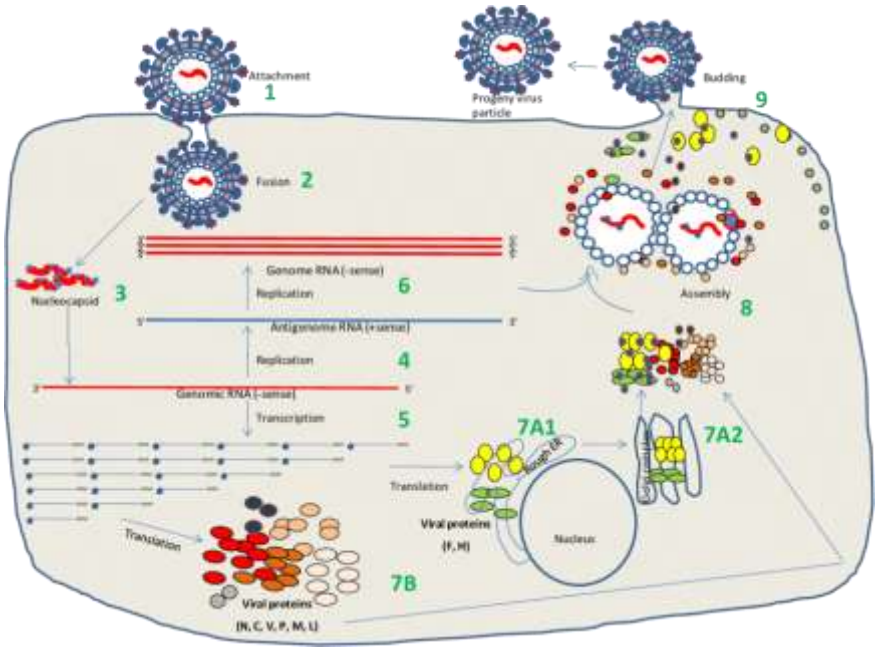

Figure 2.3: Schematic Replication of the Life Cycle of a Morbillivirus. Source: (Yang et al., 2018)

2.7 Clinical Symptoms and Transmission of PPR

Clinically, the disease is characterized by fever, oculonasal discharge, stomatitis, diarrhea, bronchopneumonia, and sometimes death (Figure 2.4). Symptoms produced by the PPR virus in sheep and goats closely resemble that of Rinderpest, but the course is much more rapid. With the acute form, sheep and goats typically display a sudden increase in temperature of between 40° - 41°C and diarrhea, resulting to 80 - 100% morbidity (Bukar & Mabu, 2023). After few days (2-3 days) of infection, the infected animal develops nasal and lacrimal discharge, depression, thirst, anorexia, leukopenia, oral erosions with necrotic foci, which results in excessive salivation and diarrhoea (Figure 2.5), that may be profuse but rarely is hemorrhagic, and usually accompanied by abdominal pain, tachypnea, emaciation, and severe dehydration, death usually occur within 5-10 days post infection. The infection may also cause abortion in pregnant sheep and goats.

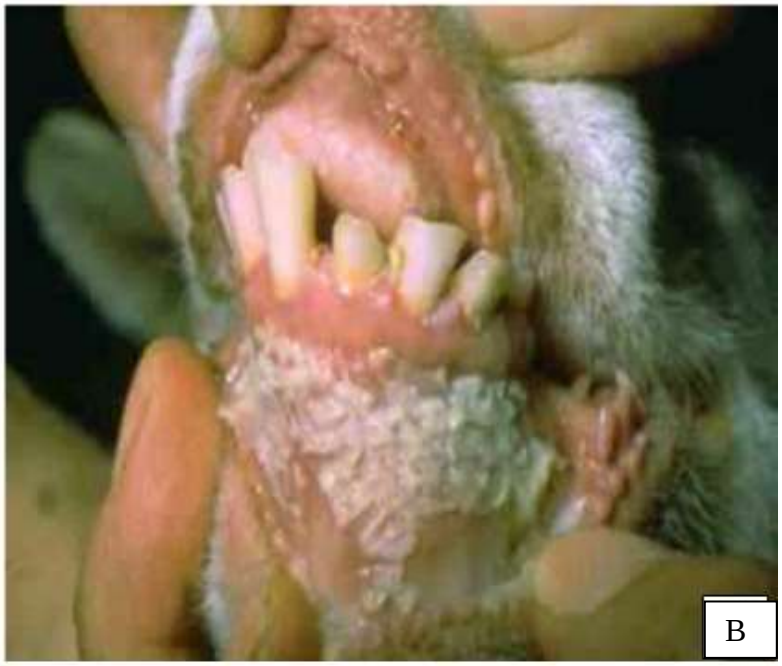

Figure 2.4: (A) Goat Infected with PPR Virus and showing sero-Mucopurulent Nasal Discharges Resulting from Bacterial superinfection as Well as Erosive gum (B) with Dead Cells on the Gums Involving the Inside of the Lower Lip and Sero-Mucopurulent Nasal Discharges resulting from bacterial superinfection. *Source*: *(Bukar & Mabu, 2023).*

Figure 2.1: A Case of PPR Showing Soiled Perianal, Emaciated, Depressed and Nasal Discharges. Source*:* (Courtesy Dr Njiru of Moyale County)

2.8 Morphological Classification of PPRV

Peste des petit ruminants' virus, like other Morbilliviruses, is an enveloped, non-segmented negative-strand RNA virus Encoding six structural proteins which include: (nucleocapsid (N), phosphoprotein (P), matrix (M), fusion (F), hemagglutinin (H), and polymerase (L)), and two non-structural proteins (C and V), which are in the order of 3′-N-P/C/V-M-F-H-L-5′ on the genome (Su *et al.*, 2015). The PPRV genome is 15,984 nucleotides long (Kinimi, et al., 2021) and the size of the virion ranges between 400 and 500 nm, which is larger than RPV (300 nm). All the genes follow the order of 3' N–P/C/V–M–F–H–L 5' (Banyard et al., .2005). Where each gene is separated by an intergenic region of variable length (Colinas, et al., 2008). It encodes two non-structural proteins (V, C) and six structural proteins Fusion (F) protein, Haemaglutinin (H) protein, the matrix protein (M), the

Nucleoprotein (N), and the Phosphoprotein (P), which form the polymerase complex in association with large proteins (L) (Baron et al., 2005). The M protein, located inside the envelope, stabilizes the virus structure and surrounds the viral RNA, which is associated with the N protein. Untranslated regions at the 3' and 5' ends of both genomic and antigenomic RNA serve as promoters, which play a crucial role during transcription and replication of Paramyxoviruses Lamb, (Noton, & Fearns, 2015). During virus budding, the viral envelope is derived from an infected cell membrane and studded with glycoprotein peplomers consisting of F and H proteins. The H and F proteins are the spike glycoproteins, which are inserted into the viral envelope. The matrix protein M serves as a link between the glycoproteins and ribonucleo-protein complex (RNP), mainly containing the viral RNA and the N protein surrounding it. In the virions, P, N, and L proteins constitute the nucleocapsid, which encloses the viral RNA. There is only one single serotype of PPRV.

However, phylogenetic analysis based on the small region of the N/F gene showed that the virus can be classified into four distinct lineages (I–IV). In general, Lineages I and II are present in West-Africa, Lineage III in Arabia and East Africa, and Lineage IV in Asia and the Middle East (Dhar et al., 2002). Initially, PPRV virus was characterized and phylogenetically analyzed based on the fusion gene (F), which classified all the strains into four distinct lineages however, it appeared that phylogenetic analysis based on the nucleoprotein gene (N) presented a much better molecular epidemiological pattern (Kumar *et al.,* 2014) Hence, currently preferred over F gene. However, all the PPRV strains are in the same group regardless of what gene is used as a basis for classification, except that the F gene-based lineage I (i.e. Nig/75) became lineage II on the N gene-based tree. Other recent suggestions have been made based on the use of haemagglutinin neuraminidase (HN) gene F and N genes, which could give better solutions and permit tracing of virus transmission within outbreaks. Kamel and El-Sayed (2019). Nevertheless, it is still unclear whether differences between lineages merely reflect geographical speciation or if they are also correlated with variability in pathogenicity between isolates (Banyard *et al.,* 2010).

2.9 Control and Management of PPRV

There is no curative medical treatment against this viral infection. Hence, the only way of dealing with it is by means of sanitary measures and vaccination. Sanitary prophylaxis requires an efficient veterinary service that can effect animal quarantine and the stamping out policy; however, for most developing countries these control measures are quite expensive hence, the only way to effectively control the disease is through medical Veterinary prophylaxis, which involves vaccination. Currently, an efficient live attenuated vaccine, the N/75, a Nigerian strain is available. Unfortunately, in most cases, it is only used during outbreaks to control the spread of the disease. Vaccination campaigns must be implemented in a systematic manner, despite the substantial financial burden associated with their execution, given the considerable economic importance of individual small ruminants such as goats and sheep .Conventionally produced vaccine have saved lives despite of the time taken during their production due to the nature work which includes; cultivation of the desired microorganism at a larger scale and under proper conditions as well as an effective inactivation with a subsequent evaluation of its immunogenicity. The vaccines are also associated with some unfavourable consequences (Hassan et al., 2023).

2.9.1 Attenuated Vaccines Developed for Peste des Petits Ruminant's Virus

Initial attempts to attenuate PPRV in vitro were conducted by Gilbert and Monnier (1962) using primary sheep liver cell cultures. These studies demonstrated that PPRV infection induced a characteristic cytopathic effect (CPE), predominantly manifested by the formation of multinucleated giant cells or syncytia resulting from virus-induced cell fusion. Subsequent investigations by Harris, J. R. (1993). in different cell culture systems further characterized the cytopathic alterations associated with PPRV infection, describing the progressive appearance of refractile, rounded cells that eventually detached from the monolayer.

Efforts to attenuate the virus through serial tissue culture passage revealed gradual reduction in virulence. (PPR, A. P. D. P. R., 2006). Reported that after six serial passages, the virus retained high pathogenicity in vivo; however, following twelve passages, infected animals exhibited only mild pyrexia, indicating partial attenuation of the virus. These pioneering studies laid the groundwork for the subsequent development of safe and efficacious live attenuated PPR vaccines, such as the Nigeria 75/1 strain, which remains one of the most widely used vaccines in global PPR control and eradication programs.

2.9.2 Conventional Live-Attenuated Vaccines

Success in the development of live-attenuated vaccine was demonstrated by (Diallo, et al., 2007) who together developed a live attenuated vaccine for ruminants, leading to progress in vaccine development for control of the disease. Vaccine, 25(30), 5591-5597., developed a homologous live-attenuated PPR vaccine by serial passage of the Nigeria/75/1 isolate in Vero cells. The virus strain used was isolated in sheep liver cell culture from a goat that had died from PPRV infection (Kashem, 2010). They were able to demonstrate that continuous passages caused mutations that led to true attenuation which could vary at subsequent passage levels. Initially, syncytia were not observed until 4–6 days following infection; however, further passage of the virus in cell culture appeared to enhance the replicative efficiency of the virus, with a reduction in the time to observation of syncytia to almost 2 days. By passage 20, the *in vivo* virulence is greatly reduced, while by 55 passages, the virus only causes a mild hyperthermia in animals, this was finally reported as being completely attenuated by 63rd passage. Importantly, at this passage level, the vaccine is able to induce neutralizing antibodies. (Singh et al., 2015). Numerous field trials have been conducted using this vaccine with more than 98,000 sheep and goats being vaccinated between 1989 and 1996 (Ithinji, 2011). The vaccine was found to be safe even in pregnant animals and produced solid immunity following a single vaccination that lasted for a minimum of 3 years and was also able to protect ruminants against RPV in a manner similar to that seen through the application.

(Holzer et al., 2016).

2.10 Current Vaccines against PPRV in the Field

A number of vaccines have been developed and used to manage PPRV (Table 2.1). Initially, heterologous rinderpest vaccine was used to control PPR disease, however after eradication of rinderpest, its use was restricted. Initial vaccine to be used was the attenuated vaccine that was developed against PPR and it involved using the Sungri, Nigeria 75/1 strain (Mahapatra, et al., (2020). Three more attenuated vaccines were further developed by using other lineages.

Table 2.1: Current Vaccines, Type and Strain in Use for the Control and Management of PPRV

Product	Vaccine type	Strain	Country Deployed
PESTEVAC	Modified Live	Live Nigeria 75/	Afghanistan, Albania, Bahrain, Ethiopia, Iraq, Jordan, Kuwait, Kenya, Lebanon, Libya, Yemen, United Arab Emirates, Syria, Pakistan and Oman
PPR-VAC	Live PPRV 75/1	PPRV 75/1	Botswana, Kenya
Not available	Live Attenuated	Egypt 87	Egypt
Not available	Live	PPRV 75/1	Nepal, Kenya
Not available	Live	PPRV 75/1	Nigeria
PESTDOLL- S	Live	Nigeria 75/1	Turkey
Sungri 96 IVRI	Live	Sungri 96 IVRI	India
PPR vaccine	Live	Arasur/87	India
PPR vaccine	Live	Coimbatore/97	P India

2.11 Progress in PPR Vaccine Development

When it first emerged due to its similarity with rinderpest the rinderpest vaccines were used for vaccination programmes that was able to protect against PPRV. Nigeria 75/1, however following the introduction of a live attenuated vaccine for PPRV in 1989, rinderpest vaccines have since been banned since Rinderpest has been declared eradicated (Zhao *et al.,* 2021*).* At present, the PPRV Nigeria 75/1

lineage II live attenuated vaccine is currently being used in all affected regions basically in Africa, Asia and the Middle East. (Tenuche et al., 2023). Sungri 96, an Indian strain have since been introduced that gives a longer protection at least 6 years (Balamurugan et al., 2023). Status Paper on Peste des petits ruminants Indian Perspective, ICAR-National Institute of Veterinary Epidemiology and Disease Informatics (NIVEDI), pp: 1-47 Copyright©: ICAR-National Institute of Veterinary Epidemiology and Disease Informatics (NIVEDI)(2023). All rights are reserved by the Organization.) Other experimental challenges conducted have also shown that the two vaccines have the ability to induce protective immunity against all four genetic lineages of PPRV when challenged subcutaneously or intranasally (Mahapatra et al., 2020).

Other inactivated vaccines are currently under development, for example, the Morocco /2008 PPRV inactivated vaccine (Zhao et al., 2021) formulated with delta inulin adjuvant (Ronchi et al., 2016). However, they are faced with challenges of not being able to provide long lasting immunity when compared to live attenuated vaccines, with limited use in non-endemic areas due to the risk of reversion. (Lewis et al., 2021). The existing attenuated vaccines are widely used, but there are still some deficiencies, including low thermal tolerance and inability to differentiate infected from vaccinated animals (DIVA). Thermotolerant (TT) vaccines and DIVA vaccines need to be developed to facilitate the widespread use of PPR vaccines for enhanced herd immunity as well as differentiate between vaccinates and naturally infected animals. (Zhao *et al.*, 2021).

2.12 Future Vaccine Opportunities

Recombinant marker vaccines serve as valuable tools for effective disease control, the establishment of disease-free zones, and post-outbreak sero-surveillance. To enable such surveillance, these vaccines are paired with companion diagnostic tests capable of distinguishing natural infection from vaccination. DIVA (Differentiating Infected from Vaccinated Animals) vaccines, therefore, play a critical role in control and eradication programs (Ranjitha et al., 2023). Therefore, although the current

live-attenuated vaccine is efficacious against clinical disease, they heavily rely on cold chain for their survival and administration especially in the tropical regions hence, to facilitate the sero-surveillance and sero-monitoring, a recombinant marker vaccine (either positive or negative marker) approach may be beneficial (Selvaraj *et al.*,2021). Inactivated vaccines are currently under development; however, they face some challenges, of not being able to provide the same lasting immunity as live attenuated vaccines, with limited use in non-endemic areas due to the risk of reversion hence not safe. (Lewis *et al.,* 2021). The existing attenuated vaccines are widely used, but there are still some deficiencies, including low thermal tolerance and inability to differentiate infected from vaccinated animals (DIVA). Thermotolerant (TT) vaccines and DIVA vaccines need to be developed to facilitate the widespread use of PPR vaccines for enhanced herd immunity as well as differentiate between vaccinated and naturally infected animals. (Zhao *et al.*, 2021).

2.13 Vaccination in Kenya

FAO has continued to support the Government of Kenya in animal disease surveillance, focusing mainly on prevention of disease outbreak which threatens the country's food security, as well as loss of livelihoods for livestock keepers and to this regard, the FAO has been supporting the vaccination programme, by handing over two million vaccines, for Peste des Petits Ruminants (PPR) to the Ministry of Agriculture, Livestock Fisheries and Cooperatives. Since 2006 when PPR first broke out in Turkana County, FAO, through various donors has invested approximately USD 20 Million in response and prevention measures. This has averted an estimated loss of 10 million small sheep and goat stock worth Ksh 45.58 billion in revenue. (Njeumi, et al., 2020). Eradicating the scourge of peste des petits ruminants from the world. Viruses, 12(3), 313.

FAO has since launched and rolled out the 2017-2020 PPR Control and Eradication Strategy roadmap for control and eventual eradication of PPR in Kenya by 2027, three years ahead of the Global target of 2030 (Ayebazibwe, et al., 2022). Garissa, Tana River, Kitui, Isiolo, Samburu, Turkana and Marsabit are among the counties

FAO is supporting to build their disease surveillance capacity by training 139 community disease reported and 30 veterinarians on participatory disease search method. In the same counties, FAO enhanced their diagnostic capacity by equipping their laboratories with the necessary diagnostic kits and reagents, in addition to adoption of ICT, through a mobile phone and web interface tool called Epicollect, which has improved the monitoring, reporting and information sharing of PPR and other diseases. (Mtema, Z. J. 2013).

2.14 Summary and Research Gaps

Current PPR situation is that approximately 70 countries have cases or have reported infection and of this, more than 60% are in Africa. Globally it is estimated that 330 million of the poorest people in Africa, the Middle East and Asia keep livestock, including small ruminants (Doganay, M. (2018). Sheap and goats play an important role in the livelihoods and food security of these communities as well as contributing significantly to the national economic development. However, PPR-related morbidity is as high as 100%, with a mortality rate that can reach 90% (Liu et al., 2018). In areas where the disease is endemic, the mortality rate may be lower, but the disease has a more insidious impact on flock productivity. Each year, PPR causes economic losses worth an estimated USD 1.2 to 1.7 billion, due to animal deaths, reduced production and the cost of fighting the disease (Govindaraj et al., 2023). Current live-attenuated vaccine are efficacious against clinical disease, however, they heavily rely on cold chain for their survival and administration especially in the tropical regions hence, are unable to facilitate the sero-surveillance and sero-monitoring of the disease, it is therefore important to develop a thermostable subunit vaccine for the control and management of the disease.

CHAPTER THREE

MATERIALS AND METHODS

3.1 Bioinformatics Analysis and Sequence Retrieval

3.1.1 Study sites: The study sites was include mainly from large public databases and repositories such as NCBI, EMBL-EBI, while sampling criteria in NCBI was involve in obtaining data sets such as (genomic sequences, metadata) this followed standardized practices to ensure reproducibility and quality.

3.1.2 Conceptual Frame Work: NCBI data → Bioinformatics prediction → Protein expression → Lab immunogenicity testing → Animal validation.

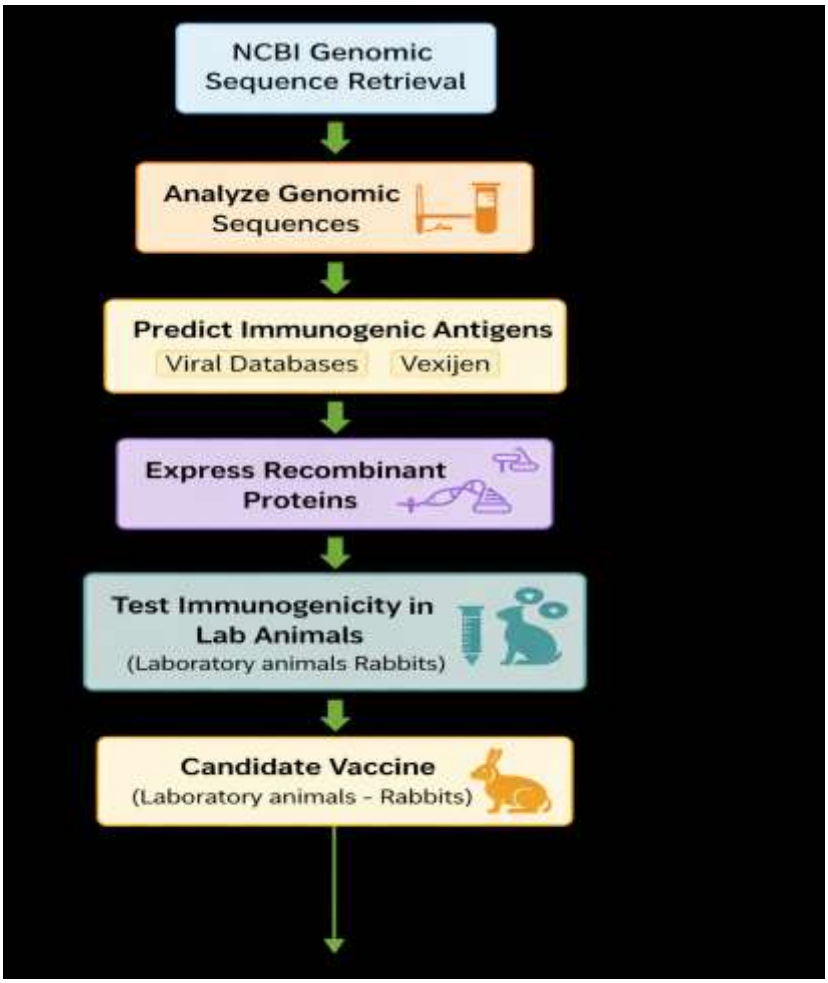

Two immunogenic protein sequences of PPRV were retrieved from GenBank of the National Centre for Biotechnology Information (NCBI) (http://www.ncbi.nml.nih.gov/protein) on the 23rd of March 2021. These included 82 and 94 sequences of the hemagglutinin protein (H protein) and Fusion protein (F protein) mainly because they are the virus's major surface glycoproteins responsible for host cell entry and immune recognition (Sinnathamby et al., 2001). The sequences were retrieved to identify regions of similarity that may be functional and conserved within them that could be used as immune epitopes. All sequences were retrieved in the FASTA format. The retrieved sequences, their accession numbers and geographical locations are listed in Tables 3.1 and 3.2

Table 3.1: Retrieved Strains of the Hemagglutinin Protein of PPRV with their Date of Collection, Accession Numbers, and Geographical Regions

No.	Acc. number	Country	Year	No.	Acc. number	Country	Year	No.	Acc. number	Country	Year
1	AEH25644	China	2011	29	ATS17278	Sierra Leone	2017	57	ASN64042	China	2017
2	ABY71271	China	2008	30	AMX28327	India	2017	58	ASN64036	China	2017
3	AAS68031	India	2009	31	AMX28319	India	2017	59	ASN64030	China	2017
4	ABX75304	Cote d'Ivoire	2008	32	AMX28311	India	2017	60	ASN64024	China	2017
5	ABX75312	Nigeria	2008	33	ANS54233	Liberia	2016	61	ASN64018	China	2017
6	ADM32488	India	2012	34	AKT04315	Benin	2016	62	ASN64012	China	2017
7	AEX61013	India	2012	35	AKT04307	Benin	2016	63	ASN64006	China	2017
8	ASY05923	Georgia	2017	36	AKR81281	India	2015	64	ASN64000	China	2017
9	ARB50221	China	2017	37	AKT04323	Cote d'Ivoire	2015	65	ASN63994	China	2017
10	ANS59483	India	2016	38	AJT59441	Senegal	2015	66	ASN63988	China	2017
11	AKQ09544	India	2015	39	AID07002	Ghana	2015	67	ASN63982	China	2017
12	AIL54036	UAE	2014	40	AIN40492	Kenya	2014	68	ASN63976	China	2017
13	AIL54028	Oman	2014	41	AHG50444	India	2014	69	ASN63970	China	2017
14	AIL54020	Uganda	2014	42	ACQ44671	China	2011	70	ASN63964	China	2017
15	AIL53996	Ethiopia	2014	43	ABY61988	India	2008	71	ASN63867	China	2017
16	AIL54012	India	2014	44	ABY61986	India	2008	72	ASN63861	China	2017
17	AIL54004	Ethiopia	2014	45	CAH61258	Turkey	2005	73	ASN63855	China	2017
18	CAD54790	India	2004	46	ANG60369	Nigeria	2016	74	ASN63849	China	2017
19	AHA58209	Iraq	2018	47	ANG60361	Nigeria	2016	75	ART66998	Algeria	2017
20	ARP51875	Mongolia	2018	48	AJE30413	China	2015	76	ALM55670	China	2016
21	AOO35467	China	2018	49	AJE30404	China	2015	77	ALA65398	China	2015
22	AIL29370	Turkey	2014	50	AUP34040	Nigeria	2018	78	AKN58853	China	2015
23	AGG09146	Morocco	2014	51	ASN64078	China	2015	79	AJA39814	China	2015
24	ADN03213	India	2013	52	ASN64072	China	2017	80	AIK97759	China	2014
25	ACN62119	India	2015	53	ASN64066	China	2017	81	AIK19904	Senegal	2014
26	CAJ01700	Nigeria	2005	54	ASN64060	China	2017	82	ADX95995	Nigeria	2011
27	YP_133827	Turkey	2018	55	ASN64054	China	2017				
28	AUO30190	Bangladesh	2018	56	ASN64048	China	2017				

Table 3.2: Retrieved Strains of the Fusion Protein of PPRV with their Date of Collection, Accession Numbers, and Geographical Regions (https://www.ncbi.nlm.nih.gov/)

No.	Accession number	Country	Year	No.	Accession number	Country	Year	No.	Accession number	Country	Year
1	AHA58208	Iraq	2018	**33**	ASN63969	China	2017	**65**	AIL54019	Uganda	2014
2	AOO35466	China	2016	**34**	ASN63963	China	2017	**66**	AIL53995	Ethiopia	2014
3	AGJ84028	Morocco	2013	**35**	ASN63872	China	2017	**67**	AIK97758	China	2014
4	CAJ01699	Nigeria	2005	**36**	ASN63866	China	2017	**68**	AIK19903	Senegal	2014
5	AHN53450	India	2014	**37**	ASN63860	China	2017	**69**	AIL54011	India	2014
6	ADN03216	India	2012	**38**	ASN63854	China	2017	**70**	AIL54003	Ethiopia	2014
7	ADM32487	India	2012	**39**	ASN63848	China	2017	**71**	AHG50445	India	2014
8	ACN62118	India	2012	**40**	ARP51874	Mongolia	2017	**72**	AGP04219	Bangladesh	2013
9	AEX61012	India	2012	**41**	AMX28326	India	2017	**73**	AGG09145	Morocco	2013
10	ADX95994	Nigeria	2011	**42**	AMX28318	India	2017	**74**	AFR66765	China	2012
11	YP_133826	Turkey	2017	**43**	AMX28310	India	2017	**75**	ACV31220	India	2012
12	ATS17277	Sierra	2017	**44**	APD77392	China	2016	**76**	ACV31219	India	2012
13	ASY05922	Georgia	2017	**45**	ANS59482	India	2016	**77**	ACQ44670	China	2011
14	ASV72322	China	2017	**46**	AHF58487	India	2016	**78**	ADJ05518	China	2010
15	ASN64077	China	2017	**47**	ALM55669	China	2016	**79**	CAH61257	Turkey	2005
16	ASN64071	China	2017	**48**	AKT04314	Benin	2016	**80**	AXE28383	Israel	2018
17	ASN64065	China	2017	**49**	AKT04306	Benin	2016	**81**	AWD71675	Pakistan	2018
18	ASN64059	China	2017	**50**	ALA65397	China	2015	**82**	AWD71669	Pakistan	2018
19	ASN64053	China	2017	**51**	AKN58852	China	2015	**83**	AWD71663	Pakistan	2018
20	ASN64047	China	2017	**52**	AKR81280	India	2015	**84**	AUP34039	Nigeria	2018
21	ASN64041	China	2017	**53**	AKQ09543	India	2015	**85**	AUO30189	Bangladesh	2018
22	ASN64035	China	2017	**54**	AKT04322	Cote d'Ivoire	2015	**86**	ANG60368	Nigeria	2016
23	ASN64029	China	2017	**55**	AJT59440	Senegal	2015	**87**	ANG60360	Nigeria	2016
24	ASN64023	China	2017	**56**	AKG94168	India	2015	**88**	ANS54232	Liberia	2016
25	ASN64017	China	2017	**57**	AJA39813	China	2015	**89**	ART66997	Algeria	2017
26	ASN64011	China	2017	**58**	AID07001	Ghana	2015	**90**	ABX75303	Cote d'Ivoire	2008
27	ASN64005	China	2017	**59**	AJE30412	China	2015	**91**	ABX75311	Nigeria	2008
28	ASN63999	China	2017	**60**	AJE30403	China	2015	**92**	ABY71270	China	2008
29	ASN63993	China	2017	**61**	AJE30396	China	2015	**93**	AAS68030	India	2009
30	ASN63987	China	2017	**62**	AIN40491	Kenya	2014	**94**	AEH25643	China	2011
31	ASN63981	China	2017	**63**	AIL54035	UAE	2014				
32	ASN63975	China	2017	**64**	AIL54027	Oman	2014				

3.2 Multiple Sequence Alignment (MSA) and Construction of Phylogenic tree

Two exterior immunogenic protein of PPRV were retrieved in FASTA format from NCBI (http://www.ncbi.nml.nih.gov/protein) (Accession numbers YP_133827.2 for the H-protein and F-protein YP_133826.1). Multiple sequence alignment (MSA) was performed to assess genetic variation among different PPRV strains and to identify conserved and variable regions within the selected proteins. The conserved regions identified through sequence alignment were considered important for epitope prediction and vaccine candidate selection. Furthermore, phylogenetic trees were constructed using the Maximum Likelihood method to determine the evolutionary relationships and genetic diversity among the selected PPRV strains. This analysis provided insights into the genetic relatedness and evolutionary patterns of circulating PPRV isolates relevant to vaccine design and development. (Tamura et al., 2011).

3.3 Epitope Prediction

Several immuno-informatics tools were used for the prediction of multiple epitopes from the H and F proteins of PPRV. Those epitopes that were predicted to be immunogenic were subjected to the Immune Epitope Database (IEDB) tools (http://www.iedb.org/) (Vita et al., 2015) for analysis of identified epitopes. The inputs that were submitted to these epitope analysis resources included **YP_133827.2** for the H protein and **YP_133826.1** for the F protein.

Cytotoxic T lymphocyte epitopes prediction based on the reference sequences of polymerase, envelope, and transacting factor, multiple epitopes were predicted against human alleles (HLA-A, HLA-B, HLA-C) using IEDB MHC-1 binding prediction tools. Antigenic, allergenic, and toxic effects were then assessed for the predicted epitopes. A total of 6, 11, and 15 epitopes were obtained from the polymerase, envelope, and transacting factor proteins, respectively. They were selected as Tc cell epitopes due to their high antigenicity scores, non-allergenicity, non-toxicity and the allelic interactions. Helper T lymphocyte epitopes and the reference sequence of each of the three proteins (polymerase, envelope, and

transacting factor) was analysed against the human alleles (HLA-DR, DQ, DP) using IEDB MHC-1I binding prediction tools with a percentile rank of (≤ 10) lower percentile ranking means a better binding ability higher than 10 means that the epitope has lower binding ability hence is not considered. A vast number of epitopes were predicted from the three proteins. The predicted epitopes were analysed for antigenic, allergenic, and toxic outcomes.

3.4 Cytotoxic T lymphocyte Epitope Prediction

The epitopes prediction focused on three key components, i.e., MHC-I binding peptide prediction, proteasomal C-terminal cleavage, and the transportation efficiency Transporter Associated with Antigen Processing (TAP). Immune Epitope Database (IEDB) tools (http://tools.iedb.org/mhci) were used to predict different Cytotoxic T cell (CTL) epitopes that bind to the Major Histocompatibility Complex class I alleles (MHC class I) (Anandhan, et al., 2023). Analysis were done using 8 cow alleles (BoLA-1:00902, BoLA-2 012:01, BoLA-D18.4, BoLA –HD6, BoLA-JSP.1, BoLA-T2a, BoLA-T2b and BoLA-T2c). The peptide length of all selected epitopes was set at 9 amino acids (9mers) with percentile ranking range of 0-2. Potentially selected MHC class I T cell epitopes were further analysed for conservancy, immunogenicity, allergenicity, potential toxicity and antigenicity to get candidate for MHC class I T-cell epitopes (Beavis et al., 2017).

3.5 Prediction of Linear-B Cell and Conformational Epitopes

The linier B-cell epitopes of the F and H proteins of PPRV were identified through the online BepiPred 2.0 server (http://www.cbs.dtu.dk/services/BepiPred/) (Jespersen et al., 2017). The random forest algorithm trained on epitopes annotated from antibody-antigen reactions and protein structures was the basis of development of BepiPred-2.0 (Jespersen et al., 2017). Potential linier B cell epitopes were analysed for conservancy, antigenicity, non-toxicity, allergenicity and surface accessibility with epitopes qualifying in these preliminary criteria undergoing further analysis for hydrophobicity and flexibility to get candidate B cell epitopes. Conformational

epitopes, on the other hand, were analysed by the online Ellipro IEDB server (http://tools.iedb.org/ellipro/) (Khan et a., .2019) was determined using an online server the Ellipro IEDB server (http://tools.iedb.org/ellipro/) (Anand *et al.*, 2020).

3.6 Prediction of the Epitope Conservancy

Conservancy of the epitopes was done using the IEDB tool (http://tools.iedb.org/ conservancy/) with a threshold value of 0.5 being considered. The Immune Epitope Database and Analysis Resource (IEDB) prediction tool was used in the development of a vaccine candidate. Immunogenicity score prediction was performed at the threshold value of 1.00. (Calis et al., 2013). IEDB tool for conservancy (http://tools.iedb.org/conservancy/) was used for immunogenicity score prediction, with a threshold value of 1.00 being applied (Jeyachandran et al., 2024).

3.7 Epitope Antigenicity Prediction

Immunoinformatics was used in the prediction of a variety of specific epitopes for B-cell recognition and T-cell through MHC class I and II molecules. Amino acid sequences of potential Linear B and MHC class I were submitted to the VaxiJen v2.0 server in FASTA format (http://www.ddgpharmfac.net/vaxijen/ VaxiJen/ VaxiJen.html) to determine and predict their antigenicity (Doytchinova & Flower 2007). Residues with scores greater than the threshold (the default value is ≤0.5) are predicted to be antigenic epitopes. Highly antigenic epitopes were subjected to further downstream analysis.

3.7.1 Allergenicity and Toxicity extrapolation of the Potential Epitopes

The allergenic potentials of the constructed vaccine were estimated using the Allergen FP v1.0 (https:// ddg- pharm fac. net/ Aller genFP/) (Allergen fp v1.0 server 2022) and Aller TOP v2.0 (https://www.ddg-pharmfac.net/ Aller TOP/) (AllerTOP v2.0 server 2022). The antigenicity of the constructed vaccine was determined using the Vaxi Jen v2.0 server (http:// www. ddg- pharm fac. net/ vaxij en/ VaxiJ en/ VaxiJ

en. html) (VaxiJen v2.0 server 2022). The selected server's prediction accuracy was set at 88.7% (Dimitrov et al., 2014).

3.7.2 Toxicity Prediction

To ensure the non-toxic nature of the selected epitopes an online tool ToxinPred was used for prediction of epitopes toxicity. The server predicts the toxicity of epitopes based on the physiochemical properties (http://crdd.osdd.net/raghava/toxinpred/) (Gupta et al., 2013). The toxicity of the peptides was predicted through the ToxinPred (http://www.imtech.res.in/raghava/toxinpred/) web server based on machine learning techniques and quantitative matrix performed using different peptides properties (Gupta et al., 2013).

3.7.3 Homology Modelling Refinement and Validation of the H and F Proteins and Epitope Mapping

The 3D model of the vaccine structures for the predicted H and F proteins of PPRV were predicted using the raptorX server (http://raprtorx.uchicago.edu/structure predition/predict/) based on the amino acid sequences and provided distance-based protein folding powered by deep learning (Xu, 2019). Construction of the multi-epitope vaccine's 3D structure was done using appropriate bioinformatic tools, The PHYRE2 server (http:// www. sbg. bio. ic. ac. uk/ phyre2/ html/ page. cgi? id= index) (PHYRE2 server 2022) was used to model the 3D structure of the H and F proteins. From the PHYRE2 server, it was further refined by the Galaxy Refine server (https:// galaxy. seokl ab. org/ cgi- bin/ submit. cgi? type= REFINE) (Galaxy Refine Server 2022) to enhance its structural quality. The vaccine candidate protein structure was further validated using the ProSA-web (https:// prosa. services. came. sbg. ac. at/ prosa. php) server (ProSa-web-protein structure analysis, 2022). The positive Z-score was used as a metric for the 3D protein model that was created and visualized using PyMOL molecular graphics system version 4.0 (downloaded from https://pymol.org) this was done for the purposes of epitope mapping.

3.7.4 Construction of Multi-epitope Subunit Vaccine

The primary assembly of the vaccine sequence was accomplished by fusing the B and T cells predicted epitopes that demonstrate conservancy, antigenicity score of more than 1 and were shown to be non-allergenic and non-toxic. Nine candidates CTL epitopes obtained from the previous analysis of the H- protein and seven of the F- protein were used in designing a multi-epitope vaccine. The peptide sequences of these epitopes were fused using poly AAY linkers. A *flagellin* protein from *Salmonella enterica subsp. enteritica serovar Dublin*, retrieved from the NCBI database (accession no. OMB76318.1), which is a TLR5 (PDB ID: 3J0A) agonist was chosen as an adjuvant. The adjuvant was added to the N terminal of the vaccine peptide and linked using an EAAAK linker in order to potentiate antigen-specific immune responses (Jahangirian *et al.*, 2022). A 6His tag was added to the C terminal of the vaccine to aid in easy purification and identification of the recombinant protein.

3.7.5 Analysis of Physiochemical Properties, Antigenicity, Solubility, Allergenicity and Toxicity of the Vaccine Construct

Physiochemical properties of the vaccine candidate determined included molecular weight, theoretical isoelectric point, total number of negative and positive residues, extinction coefficient, half-life, aliphatic index, instability index and the Grand Average Hydropathy (GRAVY) and were computed using Expasy's ProtPram server (Bouqellah & Farag, 2023). Antigenicity of the predicted vaccine construct was done using a freely accessible VaxiJen2.0 server (http://www.ddgpharmfac.net/ vaxijen/ VaxiJen/VaxiJen.html), the server used was based on auto and cross-covariance (ACC) transformation of protein sequences into uniform vectors of principal amino acid properties (Doytchinova & Flower 2007). AllerTOP v2.0 (http://www.ddg-pharmfac.net/AllerTOP) was used to assess the allergenicity of the vaccine construct. ToxinPred was used in the toxicity extrapolation of the vaccine construct. Solubility was evaluated using the SolPro server (http://scratch.proteomics.ics.uni.edu) (Gupta et al., 2015).

3.7.6 Molecular Docking of Vaccine Constructs with Antigenic Recognition Receptor

Docking studies (https:// www. unipr ot. org/) were used to predict the binding affinity between the vaccine construct and the antigenic recognition domain of the toll-like receptor-3 (TLR3, UniProt id-2A0Z) (Uniprot database 2022). The PDB file of TLR3 was obtained from the Protein Data Bank (https: //www. rcsb. org/) (RCSB PDB 2002). The protein was prepared using the protein preparation wizard of Maestro 11.2 software of Schrodinger with default parameters using OPLS3 force field. Further, protein–protein blind docking between vac cine construct and TLR3 was performed using Maestro 11.2 software of Schrodinger

3.8 *In-silico* Codon Optimization of the Vaccine Construct

In order to achieve maximal expression in *E. coli*, codon optimization was performed (strain K-12). The Java Codon Adaptation tool (http:// www. jcat. de/) was employed to get the GC content and Codon Adaptation Index (CAI) score for the vector with the highest expression. The parameters were calculated such as avoiding rho-independent transcription terminators and prokaryotic ribosome binding sites to generate optimal and complete protein expression, also avoided cleavage sites of EcoRI and BamHI restriction enzymes. Restriction endonuclease sites EcoRI and BamHI were appended to the N and C terminals of improved DNA, respectively. The sequence of the final vaccine construct was derived from three additional options to avoid the ***rho***-dependent transcription termination in prokaryote ribosome binding site and restriction enzyme cleavage site.

The *Jcat* output included the Codon Adaptation Index (CAI) and percentage GC content, was used to assess protein expression levels. *Nde I* and *Xho I* restriction sites were introduced to the N and C terminal of the sequence, respectively, using CLC Sequence viewer v8.0 (http://www.cacbio.com) Further, *In-silico* cloning was performed by inserting optimized improved DNA into the pET28a (+) vector

between the EcoRI and BamHI site. Finally, *In-silico* cloning of constructed vaccine was done using SnapGene tool to ensure vaccine expression.

3.8.1 Prediction of the Secondary and Three-Dimensional Structure of the Vaccine Construct

The secondary structure of the vaccine was generated using the PSI-BLAST based Secondary Structure Prediction PSIPRED server (http://bioinf.cs.ucl.ac.uk/psipred/), an excellent tool for prediction of secondary structure, with access to Gen-THREADER for protein fold recognition and MEMSAT-2 transmembrane topology prediction. PSIPRED incorporates two feed-forward neural networks which analyses an output obtained from position-specified iterated-BLAST (PSI BLAST).The three-dimensional structure of the vaccine was predicted using the Raptor-X prediction server (Sheng et al., 2017).

3.8.2 Molecular Docking Simulation of the Predicted Vaccine Candidate

The PatchDock (http://bioinfo3d.cs.tau.ac.il/PatchDock/) server was used for TLR-3 (PDB ID: 1ziw) – vaccine docking (SchneidmanDuhovny et al., 2005). The calculation by PatchDock involves three basic stages, i.e. atomic shape portrayal; surface fixes coordinating, as well as separating and scoring. Patch Dock separates the surface of both the input molecules into small patches according to the proper surface shape. Fire Dock (Fast Interaction Refinement in Molecular Docking) (Andrusier et al., 2007) web tool (http://bioinfo3d.cs.tau.ac. il/FireDock/) wasused to optimize as well as re-score the rigid body molecular docking solutions. All of the highly refined models were entirely based on the binding value. CAST-p server (http;//sts.bioe.uic.edu/castp/) was used to predict the binding pockets/cavities in the TLR-5. CAST-p server is excellent in identifying and providing measurements of binding pockets that are surface accessible, alongside information on inaccessible cavities for protein molecules (Xiao et al., 2020). Molecular docking of the multiepitope vaccine peptide with the TLR5 receptor (PDB ID: 3J0A) was done using ZDOCK (Gupta et al., 2020). The model with the lowest energy score was then

selected as the best docked complex.

3.8.3 Molecular Dynamics Simulation of the Vaccine Candidate Receptor Complex

Molecular dynamics simulation was performed using the iMODS server (http://imods.chaconlab.org) (López-Blanco et al., 2014). Which does the exploration of models like these generating transitional models that are feasible between two homologous structures (López-Blanco et al., 2014). The stability of the protein was evaluated by this server and is usually represented in terms of elastic network model, main-chain deformity plot, eigenvalue, B-factor values and covariance matrix (López-Blanco et al., 2014).

3.8.4 Refinement and Validation of the Tertiary Structure

The 3D structure for the predicted multi-epitope subunit vaccine was refined using an online web tool, Galaxy Refine (http://galaxy.seoklab.org/)

The validation of the 3D model of the vaccine construct was performed on ProSA-web, ERRAT and RAMPAGE.

3.8.5 Molecular Dynamics Simulation of the Vaccine Receptor Complex

Molecular dynamics simulation was done by the iMODS server (http://imods. chaconlab.org). iMODS which does the exploration of models generating transitional models that are feasible between two homologous structures (Lopez *et al.*, 2014). The stability of the protein was evaluated by this server and is usually represented in terms of elastic network model, main-chain deformity plot, eigenvalue, B-factor values and covariance matrix (Lopez et al., 2014).

3.8.6 Codon Optimization and *In-silico* cloning of the Vaccine

Java codon optimization tool (Grote et al., 2005) was used in analysing the cloning and expression efficiency in *Escherichia coli* strain K 12. The adapted codon

sequence was then inserted into a pET28a (+) vector (Figure 3.1). The final vaccine codon sequence is represented in yellow while the remaining construct represents the pET28a (+) expression vector. A clone containing 7152 approx. 72kDa base pairs in length was then formed.

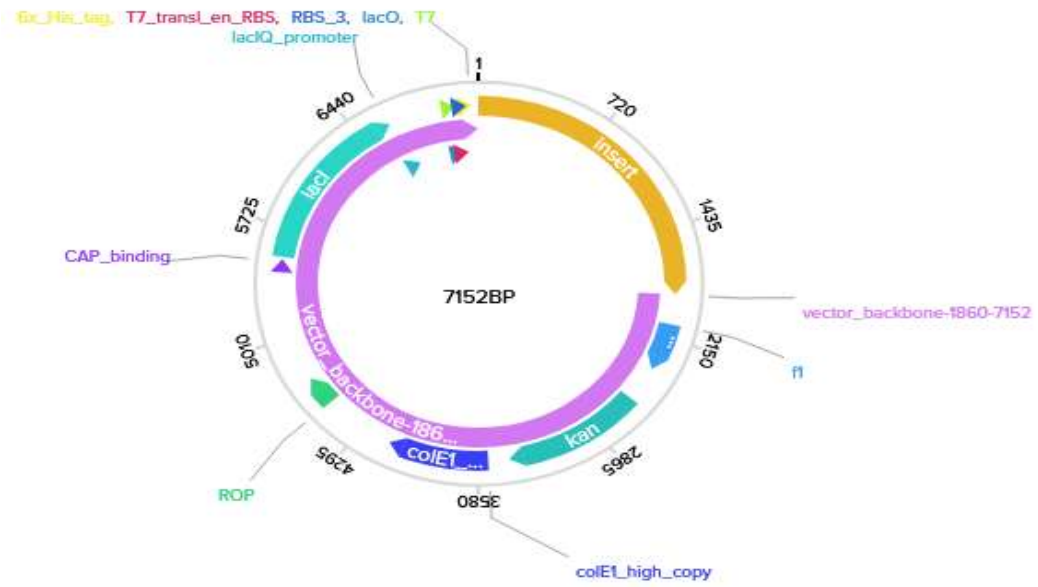

Figure 3.1: *In-Silico* Restriction cloning of the Final Vaccine Sequence into the pET28a (+) Expression Vector. The final vaccine codon sequence is represented in yellow while the remaining construct represents the pET28a (+) expression vector. A clone of 7152 base pairs was then formed.

3.8.7 Plasmid Preparation and Analysis

3.8.7.1 Transformation of Competent DH5-Alpha *Escherichia coli* cells

Competent DH5-Alpha *Escherichia coli* cells (stored in a -80^{o}C freezer) were left to thaw on ice for 20 min. After which, 5µL of pET-28a (+) plasmid DNA was added to 50µL of the competent cells in a micro-centrifuge tube. The competent cell/DNA mixture was then incubated on ice for 30 min. before being incubated again at 42^{o}C in a water bath for 45 sec. and later again on ice for 2 min.

The culture was added to 250µl of Luria–Bertani broth media broth containing antibiotics (*Kanamycine)* and incubated at 37ºC a shaker bath for 45 minutes, at 220 rotations per minute (rpm). Transformed cells were plated (spread plate technique) onto three, initially prepared, 10 cm Luria–Bertani agar plates containing 100 µg/ml kanamycin (50µL of the cells per plate). The competent cell/DNA mixture was then incubated on ice for 30 minutes. Thereafter, the bottom 2/3 of the transformation tube was inserted in a 42ºC water bath for 45 seconds (heat-shock step), immediately followed by incubation on ice for 2 minutes. Afterwards, 250µl of LB media (without antibiotic) was added to the bacteria, followed by incubation in a 37ºC shaking incubator, for 45 minutes, at 220 rotations per minute (rpm). Transformed cells were plated (spread plate technique) onto three, initially prepared, 10 cm LB agar plates with 50 µg/ml kanamycin (50µL of the cells per plate). Non-transformed DH5-Alpha *E. coli* cells were also plated on one LB agar plate (media lacked kanamycin), acting as a negative control in the experimental set-up.

3.8.7.2 Expression of Recombinant PPRV Proteins

The expression of the PPRV proteins was performed using Baby Hamster Kidney-21 (BK21) cells. The initial LB agar plates containing 100µg/ml Kanamycin were streaked with recombinant plasmids contained in glycerol stocks and incubated overnight in a HERACELL 150i CO_2 incubator (ThermoScientific, Germany). After overnight incubation, the desired isolate was inoculated in 5ml culture of Luria broth (LB from Sigma Life Sciences, USA) containing 100µg/ml Kanamycin and incubated at 37^0C while shaken at 220 rpm. 5 ml of O/N culture was added to 250 ml of broth containing Kanamycin and incubated at 37^0C until an OD reading of 600 nm was achieved. The culture was induced by adding 0.4 mM isopropyl β-D-1-thiogalactopyranoside (IPTG) from Promega Corporation, USA, and further incubating for 3,4 and 6 hours at 37^0C, while shaking at 220 rpm. The culture was then spun using Beckman Coulter Avanti J-301 at 8000 rpm for 15 min. The supernatant was discarded and pellets re-suspended in 1 ml of 25% sucrose and 50 mM tris pH 8.0 before being transferred to a 50 ml Falcon tube and kept at -80^0C for

further analysis. Lysis buffer at pH 8.0 was then added to the cells and span down for 1 hour to break open the cells before being broken down further using a sonicator (Ultrasonic Homogenizer Model 150VT, Biologicals, Inc., USA) at 50% amplitude for 2 min to further break the remaining cells. The lysate was later span at 10,000 x g for 30 min at 15^{o}C, the supernatant was collected and the pellet re-suspended in 10 ml PBS. 5ul of supernatant and/or pellet were mixed with 5x SDS sample buffer at a ratio of 1:3 and placed in a water bath at 95^{o}C for 4 min and thereafter loaded on wells of 10% SDS-PAGE gel before running it for 1 hr 50 min. The gel was later stained using coomassie blue and distained before visualizing it by Bioanalytical Imaging System (Azure Biosystems, USA) to confirm the presence of proteins.

3.8.7.3 Isolation of Plasmid DNA

The overnight *Escherichia coli* cultures of 0.5 ml were distributed to 10 micro-centrifuge tubes (5 for transformed and 5 for non-transformed bacteria). Transformed cells had been grown on LB media containing Kanamycin (50µg/ml). Non-transformed cells were grown on LB media without the antibiotic. 0.5 ml of phenol: chloroform: isoamyl alcohol (25: 24: 1) was added to each micro-centrifuge tube before being vortexed at maximum speed for 1 minute to break down the cells and later Spun down at 12000 g for 5 minutes. Later 0.45ml of the supernatant was removed carefully and 0.5 ml of isopropanol added onto it before being spun down at 12000g for five minutes. The supernatant was poured off and 0.5 ml of 70% ethanol was added carefully by the side to avoid interfering with the DNA at the bottom of the micro-centrifuge tube. It was spun at 12,000g for 5 minutes. The supernatant was carefully poured off and the pellets vacuum dried before being re-suspended in 100 µl of nuclease-free water for downstream DNA analysis.

3.8.7.4 Electrophoresis of the Isolated Plasmid DNA

Agarose gel of 1% solution in 1X TBE was prepared and poured into Gel casting try that was pre-set along with combs, this was allowed to polymerize and the combs removed carefully without breaking the wells. The gel was then submerged into the

horizontal electrophoresis tank containing 1X TBE buffer. The gels were loaded with 15 µl of plasmid DNA and 20 µl of sample buffer to make a volume of 35 µl . This was loaded into the wells alongside a marker DNA. The gel was then run at a constant voltage of 20 MA in 1xTBE buffer and keeping track of the dye front. Once the gel had reached it max, it was removed and placed in a solution containing Ethidium Bromide to stain the DNA for 30 min. The gel was later removed using gloves and rinsed using distilled water before being placed in a transilluminator and visualized under UV.

3.8.7.5 Protein Purification

3.8.7.6 Cell Lysing

Two microliters of the lysis buffer were added to the cell pellet and re-suspended by pipetting up and down, to ensure that no chunks remain. 1µl of lysozyme and 1ul of DNase I was then added to helps break down bacterial cell walls and degrades unwanted DNA from bacterial lysis to facilitate protein purification this was later incubated at room temperature for 15 min. and spun down to obtain the lysate. One ml of the lysate was then added into a 1.5ml tube and spun down at maximum speed of 5minites. The Nickel–Nitrilotriacetic Acid Agarose (Ni-NTA agarose) beads was then equilibrated by adding 500 µl water to the 200µL bead slurry (Ni-NTA Agarose) and pipetting up and down gently to mix before being spun down at 3000 rpm for 1min. The supernatant was carefully removed and discarded. 500ul of wash buffer was added to the bead slurry and gently mixed by pipetting up and down avoiding the formation of bubbles the resin was then set centrifugation at 4000rpm for one minute. 50µL of the supernatant was then transferred to a clean 1.5mL tube, label and stored for purification process. During the purification process 100µL of wash buffer was added to the beads and mixed gently by pipetting gently to mix. The entire slurry was then added to a 2ml micro centrifuge tube and incubated at room temperature for 10 minutes being inverted gently to re-suspend the beads. The supernatant was later collected in a clean 1.5mL tube and labelled. Elution was done by adding 200µL of elution buffer to the bead slurry while being gently agitated.

Elutes were collected and tested for binding capabilities as well as to identify the location of the protein of interest.

3.8.8 Determination of the Purified Protein Concentration

Pierce Bicinchoninic Acid (BCA) Protein Assay Kit was used. The content of one ampule was diluted into clean vials, using the same diluent as the samples. Protein concentrations of cell lysates were determined against a standard curve produced using known concentrations of bovine serum albumin (BSA) (Sigma) in 200µl. Quantification was performed as described by BCA Protein Assay Kit (Thermo Scientific, USA). Whereby, 25µl of a sample was pipetted in a replicate in a microplate well (20-2000 µg/ml). 200µl of the working reagent was added to each well and mixed for 30 seconds. The plate was then incubated at 37^0C for 30 min, then absorbance measured at 562 nm in a plate reader (BioTek Synergy HT, USA). This was used to determine the protein concentrations.

Using a microplate 10ul of each standard was added into the well in duplicate. BCA Reagent A was mixed with BCA Reagent B at a 50:1 ratio (50:1, Reagent A: B). this was considered to be a working reagent, 200uL of the working reagent was then added to each well and the plate covered before mixing it gently by tapping and incubating at 37°C for 30 min. After which absorbance readings were taken by measuring at 562 nm. A standard curve was then constructed using the concentration and absorbance to find the equation for the least-squares regression line of data.

3.8.9 Screening for the Binding Capabilities of Novel Antibodies (Dot Blot)

3.8.9.1 Dot Blot

After the protein purification above, dot blot analysis was done to determine the binding capability of the purified protein, during this process, a nitrocellulose membrane was prepared, and grids were drawn using a pencil under sterile conditions to indicate the region to be blotted. Using narrow-mouth pipette tip, 2 µl of the sample was spotted onto the nitrocellulose membrane at the centre of the grid.

The membrane was left to air dry. After drying non-specific sites were blocked using 5% BSA in TBS-T (0.5-1hr, RT) in 10cm Petri Dish as a reaction chamber. The membranes were then incubated with primary antibody at a concentration of (0.1-10 µg/ml for purified antibody, 1:1000 and 1:100000 dilution for antisera) dissolved in BSA/TBS-T for 30 min at RT. This was incubated for 30 min. before washing it 3X with TBS-T, each wash done for a duration of 5min. The membrane was later incubated with secondary antibody conjugated with (Horseradish Peroxidase HRP) for 30 min at room temperature. Washing was done three times with TBS-T (15 min x 1, 5 min x 2), then once with TBS (5 min). Incubation was later done with DAP reagent for 1 min, cover with Saran-wrap to remove excessive solution from the surface and expose the membranes in dark room.

3.8.9.2 Sodium Dodecyl Sulphate–Polyacrylamide Gel Electrophoresis (SDS-PAGE)

Required amount of sample buffer was prepared enough for 25 µl per reaction. The protein concentration was determined using Nano drop technique and the required dilutions calculated to get 150g of protein in 75 µl of buffer. In the fume hood, 25ul of the sample buffer was added to 75 µl of protein sample to make the total volume to 100ul. This was centrifuged at 13000 rpm for 60 sec. and incubated at 90 ^{0}C for 5min. The samples were spun down at 1300pm before being stored loaded onto the gel. The reagents for gel preparation were mixed proper volumes. TEMED and APS were added last to enhance the solidification of the gel. The gel was then added into the already made gel casts up to a height approximately 1 cm below the gels comb. The remaining cast was then filled with isopropanol and allowed to harden for 30-60 min. All isopropanol from the gel casts was then poured off and dried using a paper towel. After running the gels, they were stained using Coomassie Blue Brilliant G-250 on a shaker overnight. After which they were distained sterile distilled water until the background was clear, and the protein bands were light blue. The gel was then placed on a Geldock (InGenius, Syngene, England) for observation and taking the pictures.

3.8.9.3 Loading the Gel

The samples were prepared by mixing 10µL of the E fractions with 30 µl of Wash buffer and 10µL of 5x SDS loading buffer. 10µl of standard marker were loaded carefully into the first well after which 20µL of each prepared sample was then loaded onto the wells using gel-loading tips. The samples were left to settle slowly at the bottom of the well before connecting the power supply.

3.8.9.4 Running the Gel

The gel apparatus were assembled and plugged onto a power supply, the gel was run at 120V. When the dye front had nearly run off the bottom of the gel, the power source was turned off and the apparatus unplugged. The running the gel was removed and the entire apparatus rinsed with distilled water.

3.8.9.5 Visualization of Proteins Separated by SDS-PAGE

Proteins separated by SDS-PAGE were assessed for protein quality and molecular weight by staining the polyacrylamide gels for 30 minutes in 0.1% w/v Coomassie brilliant blue R-250 (Sigma) in 25% methanol (Sigma), 10% acetic acid (Fisher Scientific). After staining, polyacrylamide gels were detained in rapid Coomassie distaining solution which constituted of (acetic acid /methanol/ water at a ratio of (1:3:6 v/v)) overnight, and assessed after sufficient distaining was achieved.

3.8.10 Western Blot Analysis

The gel was carefully moved to a nitrocellulose membrane that was placed face-to-face with the gel and current applied on either side. The charged proteins moved from within the gel onto the membrane while maintaining the organization they had within the gel. Protein binding was based upon hydrophobic interactions, as well as charged interactions between the membrane and protein. A glass stirring rod was used to remove all bubbles before transferring the proteins for 2hrs at 50V in 4^{o}C. The membrane was removed and rinsed with distilled water before blocking it in 5%

skimmed milk/TBS/Tween for one hour at 37^{o}C. Washing was done 3X using PBS/Tween before adding primary antibodies and incubated for 1 hour at room temperature. Washing was repeated 3X times using PBS/Tween for 10 min each before adding secondary antibodies diluted 1:2500 in 5% milk/TBS/Tween and incubated at 37^{o}C for 1 hour. This was washed 3X for 10 min in TBS/Tween. 2mL of substrate was added and incubated in the dark room temperature for 5 minutes before being observed for reactivity.

3.8.11 Detection of the Immune Potential of the Extract (Dot Blot)

The samples were spun and serially diluted in Phosphate buffered saline (PBS) 10^{1}-10^{9} before adding 10µl of different sample onto a nitrocellulose membrane strip. 10 µl of the primary antibody was added at a dilution of 1:500 dilution in PBS. A protein sample from expressed *E. coli* lacking the gene of interest was also blotted on the strip as a negative control. The membrane was incubated for 20 min. at room temperature to dry. After drying, the membrane was inserted in a 50 ml falcon tube and blocked with 45 ml of 5% skimmed milk in PBS for 1 hour at room temperature (on a rotor). Afterwards, the blocking buffer was poured off and the membrane washed 3X times for 10 min. per wash using 0.1% PBS tween 20. The membrane was incubated in 45 ml of positive PPRV goat serum diluted 1:500 in PBS for 1 hour at room temperature on a rotor. Afterwards, the membrane was washed three times (10 min per wash) in 45 ml of 0.1% tween 20 in PBS on a rotor. The membrane was incubated with 45 ml of anti-goat serum at a dilution of (1:500 dilution in PBS) for 1 hour at room temperature in a rotor for 30 minutes. The membrane was washed three times (10 min. per wash) in 45 ml of 0.1% PBS-tween (on a rotor) 10 µl 30% hydrogen peroxide (H_20_2) diluted to 10 ml was added to 0.05% diamino-benzidine (DAB). This was poured into a 50ml Falcon tube and the membrane inserted into the mixture and finally incubated in the dark for 5 minutes. Thereafter, the reaction was stopped by briefly washing the membrane with distilled water then air dried and observed for any reaction.

3.8.12 Immunological Techniques

3.8.12.1Electroblotting Blotting

Following protein transfer, the nitrocellulose membrane was stained with Ponceau S solution (*Thermo Scientific™ Ponceau S Staining Solution Cat. No. A40000279, USA*) for 5-15minutes to confirm efficient protein transfer and assess equal protein loading among the samples. The membrane was subsequently rinsed using phosphate-buffered saline containing Tween-20 (PBS-Tween) to remove excess Ponceau S stain. None specific protein binding was avoided by blocking the membrane using 5% (w/v) skimmed milk, prepared in PBST for 30 min. at room temperature with gentle rocking. Blocking of the membrane was essential to improve assay sensitivity and minimize background signal during immunodetection.

After blocking, the membrane was incubated with the appropriate species-specific primary antibody diluted in 5% skimmed milk prepared in PBST. The membrane was carefully covered with parafilm and incubated on a rocker at 4°C for 1 hour to facilitate specific binding of the antibody to the target protein. Following primary antibody incubation, the membrane was washed three times with PBST for 5 min. each to remove unbound antibodies.

The membrane was then incubated with the corresponding horseradish peroxidase (HRP)-conjugated secondary antibody (*Goat anti-Rabbit IgG (H+L Thermo Fisher Scientific USA*), HRP diluted in either 5% (w/v) skimmed milk or 5% (w/v) bovine serum albumin (BSA) prepared in PBST. Incubation was carried out for 2 hours at room temperature on a rocker. Subsequently, the membrane was washed six times with tris-buffered saline containing Tween-20 (TBST) for 5 minutes each to eliminate excess secondary antibody and reduce non-specific background signals.

Protein detection was performed using enhanced chemiluminescence (ECL) substrate (Millipore). The membrane was incubated with the ECL reagent for approximately 1

minute, sealed in transparent plastic wrap, and exposed to autoradiography film (Kodak) for visualization of the immunoreactive protein bands.

3.8.12.2 Production of Polyclonal Antibodies for Use in the Development of Diagnostic Tests for PPR Virus

Three months old weaner female rabbits (New Zealand White) were used for this part of study. Fourteen rabbits were purchased from Biotechnology Research Institute (BIORI) Muguga small animal facility. The animals were acclimatized for two weeks before the start of the experiment. The rabbits were divided in three treatment groups of four rabbits each (A, B and C) (Table 3.3). Group A consisted of 4 rabbits each that were injected with F/H sub-unit vaccine candidate, Group B consisted of 4 rabbits were used as positive control and were injected with conventional N/75 vaccine from Kenya Veterinary Vaccine Production Institute (KEVEVAPI), while Group C consisted of 4 rabbits used as negative control. The remaining two rabbits were used as a contingency management based on the Institutional Animal Care and Use Committee IACUC requirement and regulations. (Permit number C/ BIORI/4/325/III/45.) Female rabbits were preferred because they are reported to mount a more vigorous immune response than their male counterparts. The rabbits were housed in cages of about 12 square feet (1.1 m^2) of living space with at least 24 inches (60 cm) of height, plus an attached exercise run of 32 square feet (3 m^2) at ambient temperature ranging between 18-24°C which was maintained throughout the experiment. The room was well-ventilated to ensure comfort to the experimental animals. Rhode grass hey was used as bedding and was changed every 2-3 days, to maximize in the animal hygiene. Feeding was done using rabbit pellet supplemented with fresh green vegetables such as cabbages, kale and hay. Health of the experimental was monitored by a qualified resident Veterinary Surgeon throughout the duration of the experiment.

Table 3.3: Grouping and Dosage Framework for PPRV Vaccine Trials in Rabbits

No	Group	No. of Rabbits	Treatment	Concentration of the vaccine candidate
1	A	4	Vaccine candidate	100ug/ml
2	B	4	Conventional vaccine N/75	100ug/ml
3	C	4	Negative control	-
4	Contingency management	2	-	-
	Total	**14**		

3.8.13 Blood Collection Procedures

Approximately 3 mL of pre-immunization blood samples were collected from each rabbit into sterile red-top vacutainer tubes prior to primary immunization to establish baseline serum parameters and to screen the animals for any underlying infections before inclusion in the study. Subsequently, immunized blood samples were collected aseptically from the right marginal ear vein, with the procedure performed rapidly to minimize animal stress and discomfort. The rabbits were securely restrained using a commercial restrainer, and the sampling site was disinfected with 70% ethanol to remove debris and potential contaminants. Gentle pressure was applied to the ear to enhance venous distension, after which blood was collected using a sterile 21-gauge needle. The samples were appropriately labelled with the date of collection and animal identification number, allowed to clot at room temperature, and subsequently centrifuged at 2700 rpm for 10 minutes to separate the serum for downstream immunological analyses.

3.8.14 Determination of Seroconversion for the Vaccine Candidates

Approximately 3 ml of blood was drawn from each rabbit before their vaccination. After which they were injected with 1ml of the developed vaccine candidate (F/H) mixed with an adjuvant Montenide II which create stable water-in-oil emulsions that prolong antigen release, leading to stronger and longer-lasting immune responses

compared to traditional adjuvants. The adjuvant was chosen Montanide ISA ISA 70, commonly used for veterinary medicine, the antigen was prepared to ensure that it has the required dose by mixing with sterile PBS. The antigen was then combined with the adjuvant in a defined ration of 50:50 by volume and later homogenised using a homogeniser to create a stable emulsion. Proper mixing was done to avoid the risk of granulomas and adverse reactions. Blood was collected from the rabbits after every 7 days' post-vaccination and a booster immunization was administered on day 21 (Table 3.4).

3.8.14.1 Immunization Procedures

Three (3) female New Zealand white rabbits (2-4kg) were used for each antigen/Adjuvant mixture (Positive N75, F/H subunit vaccine and N/saline as a negative control). The antigen-adjuvant emulsion was then injected subcutaneously (<0.2 ml per site) at 3 sites per animal using a 23–25-gauge needle. Injection sites were monitored daily for any type of reaction. Observation included an assessment of the injection sites for tissue necrosis and abscess formation was done. The animal's activity, food/water consumption and general body condition was also monitored on a daily basis and in case of any slight observable changes, this was made known to the resident Vet immediately for attention.

3.8.14.2 Anti PPR Conjugate Preparation

The procedure was done according to (Crowther, 2008). Anti-PPR vaccine antisera were pooled and a 33% ammonium sulphate added to form deposit. The deposit was reconstituted in PBS pH 7.2. 10 mg of HRP Sigma P-8375 was weighed and dissolved in 0.2 ml of 1.25% glutaraldehyde in 100 mM sodium phosphate, pH 6.8 and incubated overnight at ambient temperature. After overnight incubation, excess free glutaraldehyde was removed by gel filtration on a Phamacia column 18cm by 3cm internal diameter packed with Sephadex G-25 using PBS as eluting buffer. The enzyme was concentrated back to 10mg/ml by dialysis against 100 Mm sodium carbonate/sodium by carbonate buffer, pH 9.5, containing 30%% sucrose. 0.1ml

antibody was added to the enzyme solution. The mixture was left to incubate at $4^{O}C$ for 24hrs. 0.1ml 0.2M ethanolamine, pH 7.0 was added then incubated for 2hrs.

Table 3.4: Showing Vaccination Schedule Pre and Post Immunized Blood Collection

Date	Activity
Day 0	• **Pre-immune bleed** Bleed 3 ml per Rabbit for control serum collection • Primary injection Injection with purified PPR antigen. Controls will not be injected
Day 7	• **Bleeding** Bleed 3 ml per Rabbit for serum collection
Day 14	• **Booster 1st booster dose** Boost with 1 ml of purified PPR virus protein.
Day 21	• **Bleeding** Bleed 3 ml per Rabbit for serum collection
Day 28	• **Booster 2nd Booster dose** Boost with 1 ml of purified PPR virus protein depending on the amount of titre from day 21.
Day 35	• **Serum neutralization titration** Experimental animals were then euthanized using Isoflurane

3.8.15 Indirect ELISA to Determine Seroconversion

3.8.15.1 Screening of Serum Samples from Immunized Rabbits Using Indirect ELISA

The indirect ELISA (iELISA) was performed in duplicate and repeated on three different occasions. The negative and positive control sera were placed in duplicates in the first and last row of plates coated with 1 µg/ml of each antigen. No serum sample was placed in the second row and the OD of this row was subtracted from the OD containing sera. The ELISA plates were coated with 1 µg/ml antigen in coating buffer (100 µl/well) using 0.05 M carbonate–bicarbonate coating buffer (pH 9.6), which facilitates efficient adsorption of the antigen onto the ELISA microplate wells, and incubated at 4^{0} C overnight. The following day, plates were washed 3x in phosphate-buffered saline-tween (PBS-T Washing steps were performed using 1×

phosphate-buffered saline containing 0.05% Tween-20 (PBS-T) to remove unbound reagents and minimize non-specific interactions. 200 µl blocking buffer (1x PBS-T and 0.5% Horse serum from Gibco Life Technologies TM, New Zealand) was added and serum tested on dilution plates in each well. For anti-IgG, the initial concentration was obtained at 1/100 and diluted 4-fold, plates were incubated at 37^0C with gentle shaking for 1hr, and washed 3x with PBS-T. HRP-conjugated goat anti-rabbit IgG (H+L) secondary antibody (Invitrogen™, Thermo Fisher Scientific, catalog no. PI31460) was used for immunodetection in ELISA and Western blot assays. The antibody was affinity purified and conjugated to horseradish peroxidase for chemiluminescent/colorimetric signal detection. 100 µl of secondary antibody goat anti-rabbit IgG (H+L) secondary antibody (Invitrogen™, Thermo Fisher Scientific, catalog no. (PI31460) conjugated to HRPO at a dilution of 1/10000. Blocking buffer was added in each well and kept for 1 hr with gentle shaking at 37^0C. The plates were again washed 3x in PBS-T and 100µl/well of substrate from Sigma Aldrich, USA added. The plates were placed in the dark for 15 min. and read at a wavelength of 405 nm in BioTek Synergy HT, USA plate reader.

CHAPTER FOUR

RESULTS

4.1 Multiple Sequence Alignment

Considerable degrees of similarities were observed between amino acid sequences of both proteins, illustrating conservancy of sequence motifs among lineages. However, differences were observed in the amino acid sequences of both proteins. The entire F gene of PPRV composed of 2405 nucleotides including the poly-(A) tail. The gene starts with the semi-conserved start gene sequence AGGG and ends with AAAC while the H gene of PPRV starts with usual semi conserved start signal of AGGR. The complete gene along with the poly (A) was 1954 nucleotides long as shown on figure 9 & 10 below. Considerable conservancy among the retrieved strains was observed, however, some regions exhibited differences (mutations) in some amino acids in various sequences.

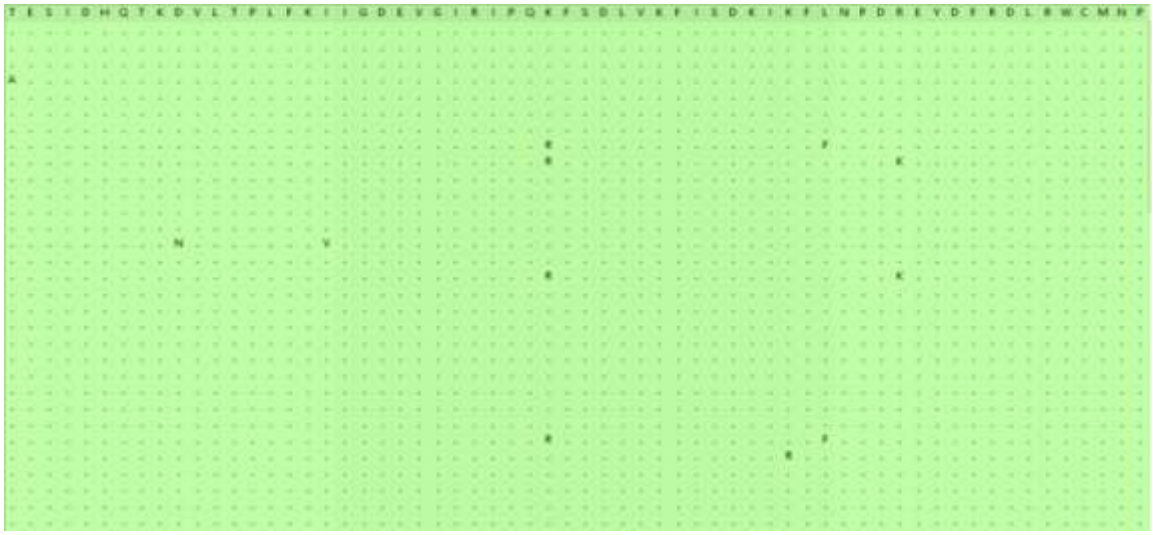

Figure 4.1: Section Showing Multiple Sequence Alignments (MSA) of the Retrieved Strains of the H Protein Using the Muscle Tool in MEGA 10.2.4 Software. Dots indicate conservancy of the retrieved strains. Letters, on the other hand, indicate no conservancy (Mutations)

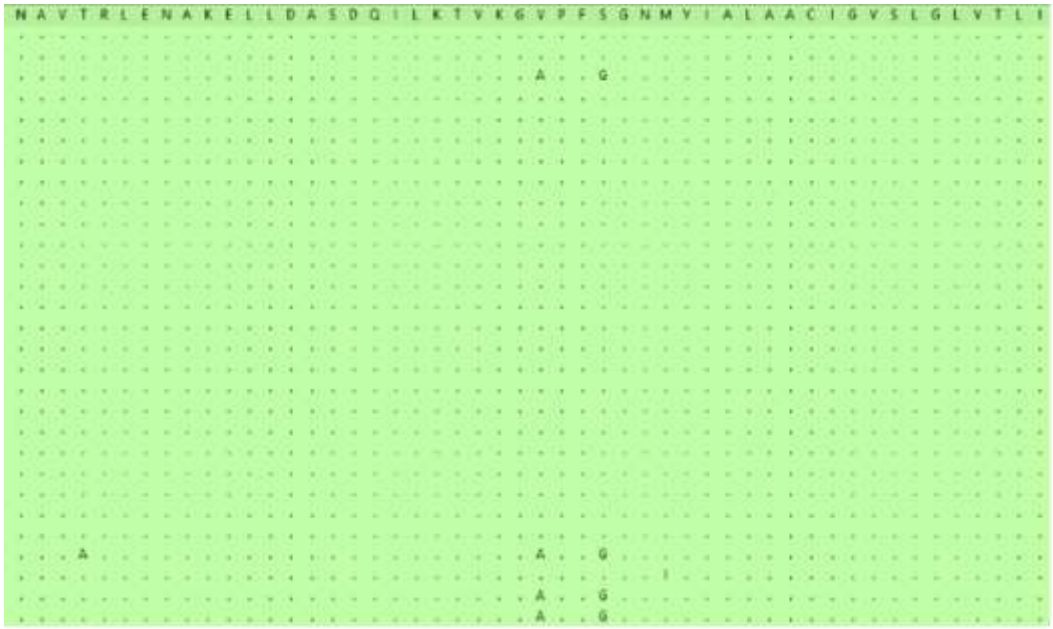

Figure 4.2: Multiple Sequence Alignments (MSA) of the Retrieved Strains of the F Protein Using the Muscle Tool in MEGA 10.2.4 Software

Dots indicate conservancy of the retrieved strains. Letters, on the other hand, indicate no conservancy (Mutations). Considerable conservancy among the retrieved strains was observed. However, some region exhibited differences (mutations) in some amino acids in various sequences.

4.2 Phylogenetic Evaluation

Close similarities were observed between the African, Asian and European strains, with higher similarities being observed between the Emiratis, with regard to the F protein, African, Asian and European strains were also clustered together Indicating close relatedness of the species that were collected from different countries within those continents. The close relationship between the Omanis, Emiratis and Ethiopian strains in both immunogenic proteins indicated the transfer of the H and F strain segments between these Nations. Phylogenetic analysis showed that the PPRV strain were genetically related to the lineage IV virus isolates. For the F gene, the sequence divergence of cloned gene and other selected genes ranged from 0.01% to 0.018%

within the tested genes species and in similarity it ranged from 98.2% to 99.0%. In the case of the H gene, similar results were also observed in divergence, ranging from 0.017% to 0.083% among lineage IV and others, and similarity varied from 91.7% to 98.3%. In a phylogenetic tree, each leaf node represented a species, each edge donates a relationship between the two neighbours and the length of an edge indicates the evolutionary distance between them (Figure 4.3 (A) and (B)) and denotes a relationship between the two neighbours. Length of an edge indicated the evolutionary distance between them (Pavlopoulos *et al.* 2010).

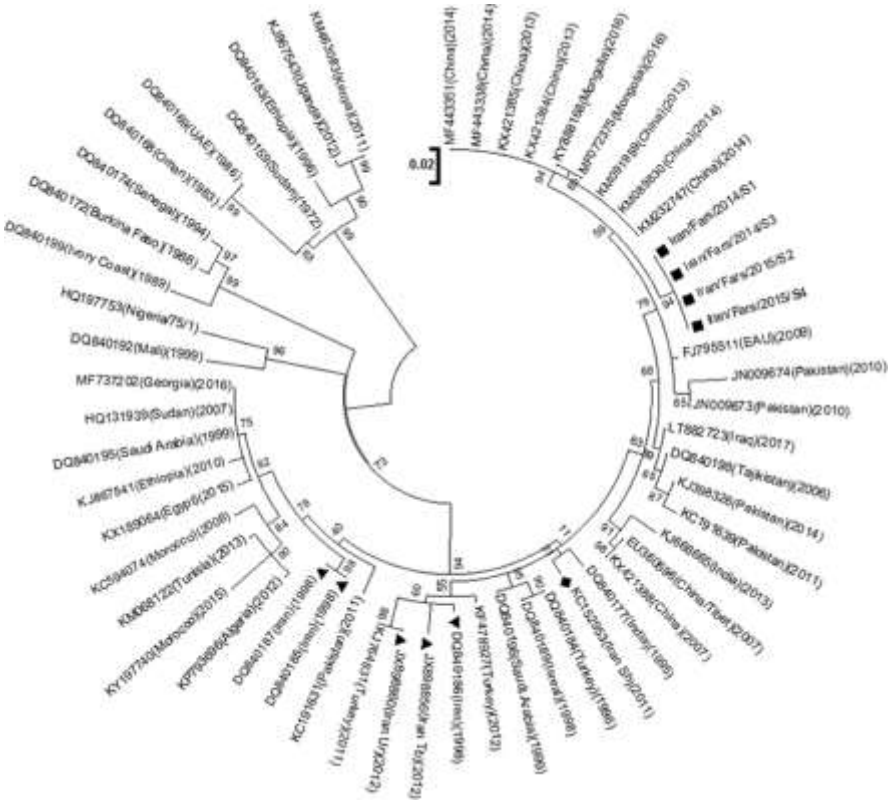

Figure 4.3: (A) - Phylogenetic Tree Showing Inferred Evolutionary History of 94 isolated Strains of the F Protein of PPRV

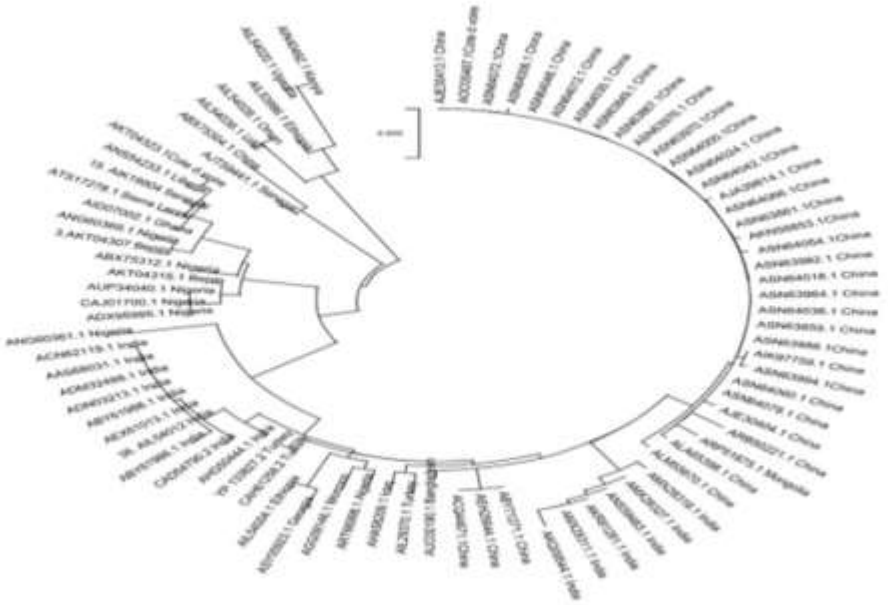

Figure 4.3: (B) Phylogenetic Tree Showing Inferred Evolutionary History of 82 isolated Strains of the H Protein of PPRV

4.3 Prediction of CTL Epitopes from the H and F Proteins Interact with MHC Class I (BoLA) Alleles

Two immunogenic epitopes were identified with 80.49% conservancy with a thresh hold limit of above 70%, and antigenicity score above the thresh hold value of 0.4 using vaxijen. (Adhikari, Tayebi, and Rahman 2018). The epitopes were also non-toxic and non-allergic and were predicted to bind with 30 of BoLA alleles (Table 4.1)

Table 4.1: Predicted CTL-Epitopes from the Hand F Proteins Interacting with MHC-1 (BoLA Alleles

Key: **NT**-None toxic, **NA**- None antigenic, **ALG**- Allergenic, **IMG**- Immunogenic, **Cons**-Conservancy,

No	**Epitope**	**Start**	**Stop**	**BA**	**PM**	**Casv**	**IMG**	**ALG**	**TOX**	**ANT**
F protein										
1	AQITAGVAL	125	133	BoLA-D 184	0.02	100%	0.21	NA	NT	0.80
				BoLA-HD6	0.1					
				BoLA-JSP.1	0.26					
				BoLA-T2C	0.49					
2	LAACIGSL	496	504	BoLA-JSP.1	0.12	100%	0.06	NA	NT	0.9
				BoLA-T2C	0.49					
3	VAILTFLFL	4	12	BoLA-JSP.1	1.3	100%	0.24	NA	NT	0.40
				BoLA-T2C	1.9					
4	KNVRPIQTL	92	100	BoLA-D184	0.96	100%	0.10	NA	NT	0.81
				BoLA-HD6	0.72					
				BoLA-JSP.1	0.05					
				BoLA-T2b	1.2					
				BoLA-T2C	1.7					
				BoLA 1:.00902	1.7					
5	KLMPNITAI	53	61	BoLA-D184	1.1	100%	0.11	NA	NT	0.85
				BoLA-HD6	0.27					
				BoLA-JSP.1	1.6					
				BoLA-T2C	0.12					
6	AAEISIQAL	222	230	BoLA-JSP.1	1.7	100%	0.06	NA	NT	1.17
				BoLA-T2C	0.75					
7	GTISNRFIL	369	377	BoLA-HD6	1.3	100%	0.10	NA	NT	0.81
				BoLA-JSP.1	0.5					
H protein										
1	SSYFYPVRL	549	557	BoLA-JSP.1	0.05	100%	0.17	NA	NT	0.63
				BoLA-T2C	0.37					
				BoLA-D 184	0.77					
				BoLA-2 012:01	1.3					
				BoLA 1:.00902	1.2					
2	SSYFYPVRL	316	324	BoLA-T2b	0.18	100%	0.18	NA	NT	0.57
				BoLA-JSP.1	0.87					

The predicted epitopes included $_{549}$SSYFYPVRL$_{557}$ and $_{316}$REPLVVVIL$_{324}$. Epitope $_{549}$SSYFYPVRL$_{557}$ exhibited an immunogenicity score of 0.16746 and an antigenicity score of 0.6308, whereas $_{316}$REPLVVVIL$_{324}$ recorded an immunogenicity score of 0.1769 and an antigenicity score of 0.5724. Higher scores are associated with an increased likelihood of eliciting an immune response (Adhikari, Tayebi, and Rahman, 2018). Among the identified epitopes, $_{549}$SSYFYPVRL$_{557}$ demonstrated the broadest binding affinity to MHC class I molecules, interacting with five bovine alleles, namely BoLA-JSP.1, BoLA-T2C, BoLA-2*012:01, BoLA-1:00902, and BoLA-D184. In contrast, $_{316}$REPLVVVIL$_{324}$ showed binding affinity to two bovine alleles, BoLA-T2b and BoLA-JSP.1. Furthermore, epitope mapping was performed to determine the spatial localization of the candidate epitopes on the three-dimensional structure of the H protein (Figure 4.4).

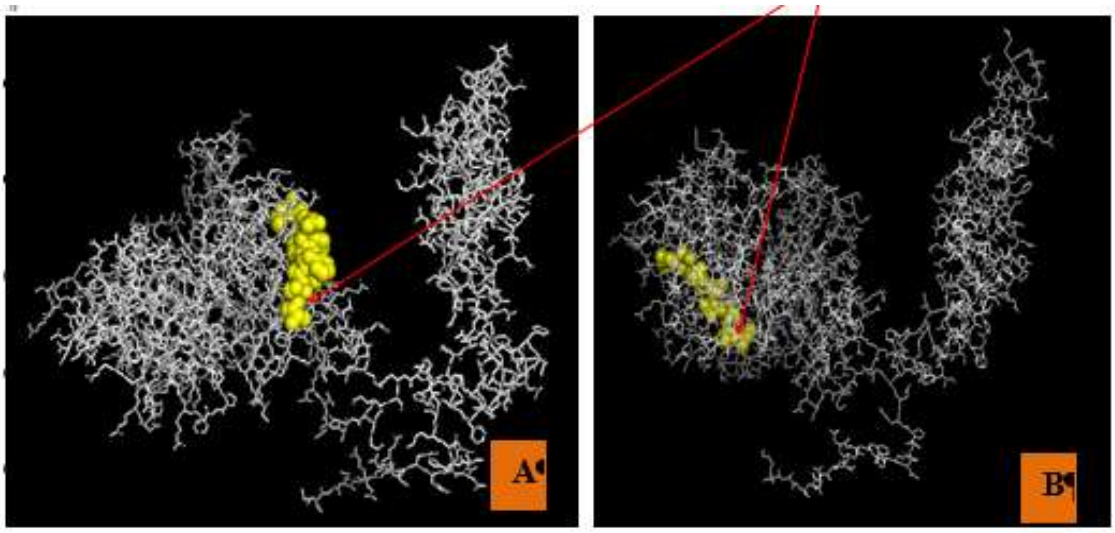

Figure 4.4: Three-Dimensional Representations of MHC-I T Cell Epitopes of the H Protein of PPRV during Epitope Mapping A - $_{549}$SSYFYPVRL$_{557}$ and B - $_{316}$REPLVVVIL$_{324}$. epitopes are represented by the yellow spheres while the bulk of the protein is represented as grey sticks.

Seven epitopes of the F protein were found to be immunogenic, antigenic, non-allergic, non-toxic and had a conservancy percentage of above 70% were selected

and predicted to bind to considerable number of BoLA alleles (Figure 4.5). These included: $_{125}$AQITAGVAL$_{133,}$ $_{496}$LAACIGVSL$_{504,}$ $_{4}$VAILTFLFL$_{12,}$

$_{92}$KNVRPIQTL$_{100,}$ $_{53}$KLMPNITAI$_{61}$, $_{222}$AAEISIQAL$_{230}$ and $_{369}$GTISNRFIL$_{377}$. They had immunogenicity scores of 0.20996, 0.05813, 0.23908, 0.10488, 0.10644, 0.0557 and 0.09571 respectively while their antigenicity scores were 0.7995, 0.8734, 0.4012, 0.8138, 08494 and 1.1573 respectively. Among them, $_{92}$KNVRPIQTL$_{100}$ showed the highest affinity to MHC class I molecules binding to six cow alleles which included BoLA-D 18.4, BoLA-HD6, BoLA-JSP.1, BoLA-T2b, BoLA 1:00902 and BoLA-T2C followed by $_{125}$AQITAGVAL$_{133}$ (BoLA-D 18.4, BoLA-HD6, BoLA-JSP.1, BoLA-T2C) and $_{53}$KLMPNITAI$_{61}$ (BoLA-D 18.4, BoLA-HD6, BoLA-JSP.1, BoLA-T2C) with four each, the rest of the epitopes showed affinity to two cow alleles each. Hence $_{92}$KNVRPIQTL$_{100}$ (**A**), $_{125}$AQITAGVAL$_{133}$ (**B**),$_{53}$KLMPNITAI$_{61}$(**C**), $_{496}$LAAC IGVSL$_{504}$ (**D**), $_{4}$VAILTFLFL$_{12}$ (**E**), $_{222}$AAEISIQAL$_{230}$ (**F**) and $_{369}$GTISNRFIL$_{377}$ (**G**) respectively were chosen as the candidate CTL epitopes (Figure 4.5).

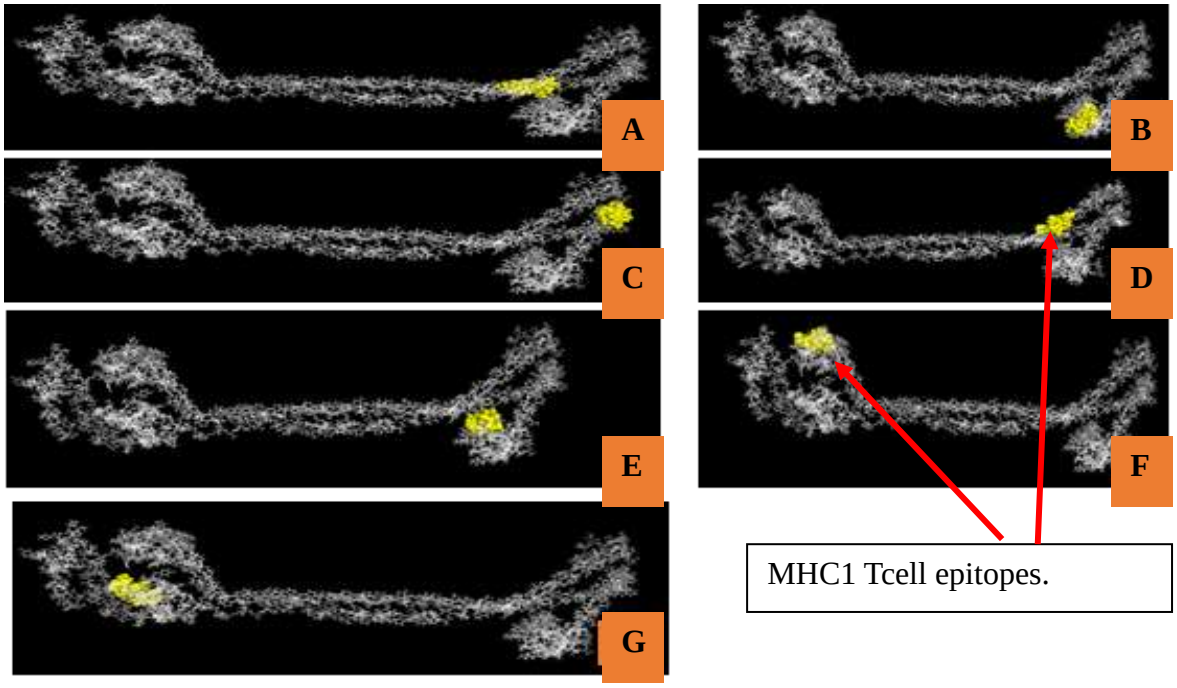

Figure 4.5: Seven Immunogenic Epitopes of the F Gene Found to be Antigenic,

Non-Allergic and Nontoxic with a Conservancy Percentage of Above 70%. Yellow colour

4.4 Analysis of Linier B Cell Epitopes of the H Protein

Based on BepiPred-2.0 method, a total of 17 B- cell epitopes with varied lengths were identified from the H protein of PPRV (Table 4.2). All the epitopes were non-toxic. 7 epitopes of the 17 were both antigenic and non-allergens as predicted by Vaxijen and AllerTOP v. 2.0 servers respectively. Further assessment was done by consideration of conservancy and surface accessibility. Three of the seven had high conservancy (100%) scores however, none of the three was surface accessible as predicted by IEDB tools for conservancy and Surface accessibility respectively. Therefore, none of the potential B cell epitopes qualified to undergo further analysis for hydrophobicity and flexibility. There was therefore no potential B cell epitope that passed the selection criteria in the H protein of PPRV. No candidate linear B cell epitope was identified.

Table 4.2: Potential Linier B Cell Epitopes of the H Protein

Start	End	Peptide	L(NT)	Antigenicity	Conservancy (%)	Toxicity (Y/N)	Allergenicity (Y/N)	Surface accessibility (Y/N)
5	21	RERINAFYKDNPHNKNH	17	0.3804	100.00%	Non toxin	Yes	No
72	87	SRLNTNIKLTESIDHQ	16	0.7233	0.00%	Non toxin	Yes	No
101	113	DEVGIRIPQKFSD	13	0.6401	100.00%	Non toxin	No	No
123	134	KFLNPDREYDFR	12	0.8441	100.00%	Non toxin	Yes	Yes
145	154	RVKINFDQFC	10	0.6702	100.00%	Non toxin	Yes	No
171	191	LNKSKKLQSLTLGPGTSCLGR	21	0.6131	0.00%	Non toxin	Yes	No
209	214	DLEMKH	6	3.0710	100.00%	Non toxin	Yes	No
236	249	RSDARDPSTDLGIG	14	1.2427	100.00%	Non toxin	No	No
262	267	DLGLGP	6	3.8964	100.00%	Non toxin	Yes	No
309	316	SERGVPKR	8	-0.5855	0.00%	Non toxin	No	No
329	346	PTLGGELYSILPTSDLMV	18	0.2905	0.00%	Non toxin	No	No
370	380	TDVRDLQNKGE	11	0.6422	100.00%	Non toxin	Yes	Yes
388	404	TRPPSFCNGTGSGPWSE	17	0.6260	100.00%	Non toxin	No	No
438	450	LSGMDLYNNPFSR	13	0.2084	100.00%	Non toxin	No	Yes
487	492	IRGPRG	6	-1.2409	100.00%	Non toxin	Yes	No
500	509	LSRRVDDDIK	10	0.6076	100.00%	Non toxin	No	No
590	596	TDEEVHM	7	0.6963	0.00%	Non toxin	No	No

Analysis of Linear B cell epitopes from the F protein. Based on the BepiPred-2.0 method, a total of 13 B cell epitopes of varied length were identified from the F protein of PPRV (Table 4.3). All the epitopes were non-toxic. 3 epitopes of the 13 were both antigenic and non-allergens as predicted by Vaxijen and AllerTOP v. 2.0 servers, respectively. All three had 100% conservancy. However, none of the 3 were surface accessible, therefore, none qualified to undergo further analysis for hydrophobicity and

flexibility. Just like in the H protein, there was no potential B cell epitope that passed the selection criteria in the F protein of PPRV. No candidate Linear B cell epitope was identified

Table 4.3: Potential Linier B Cell Epitopes of the F Protein

Start	End	Peptide	length	antigenicity	conservancy	toxicity	Allergenicity	S.Ace.
18	26	ACQIHWGNL	9	1.0493	100%	Non toxin	Non allergen	No
59	64	TAIDNC	6	-0.4880	100%	Non toxin	Allergen	No
66	74	KSEISKYKR	9	-0.6242	0%	Non toxin	Non allergen	Yes
92	106	KNVRPIQALTPGRRT	15	1.2323	0%	Non toxin	Allergen	No
214	224	GPSLRDPIAAE	11	0.4458	100%	Non toxin	Non allergen	No
239	251	NKILDKLGYSGED	13	0.2466	0%	Non toxin	Allergen	No
321	329	LISNFDETS	9	0.4696	100%	Non toxin	Allergen	No
340	349	SQNALYPMSP	10	0.6449	100%	Non toxin	Non allergen	No
367	373	VSGTISN	7	0.8571	100%	Non toxin	Allergen	No
432	437	EYPDSV	6	0.2341	100%	Non toxin	Allergen	Yes
439	461	LHKIDLGPAISLEKLDVGTNLGN	23	1.0155	100%	Non toxin	Non allergen	No
471	488	ELLDASDQILKTVKGVPF	18	0.5281	100%	Non toxin	Allergen	No
518	543	RNKEIPTPKINPGLKPDLTGTSKSYV	26	0.8635	0%	Non toxin	Non allergen	Yes

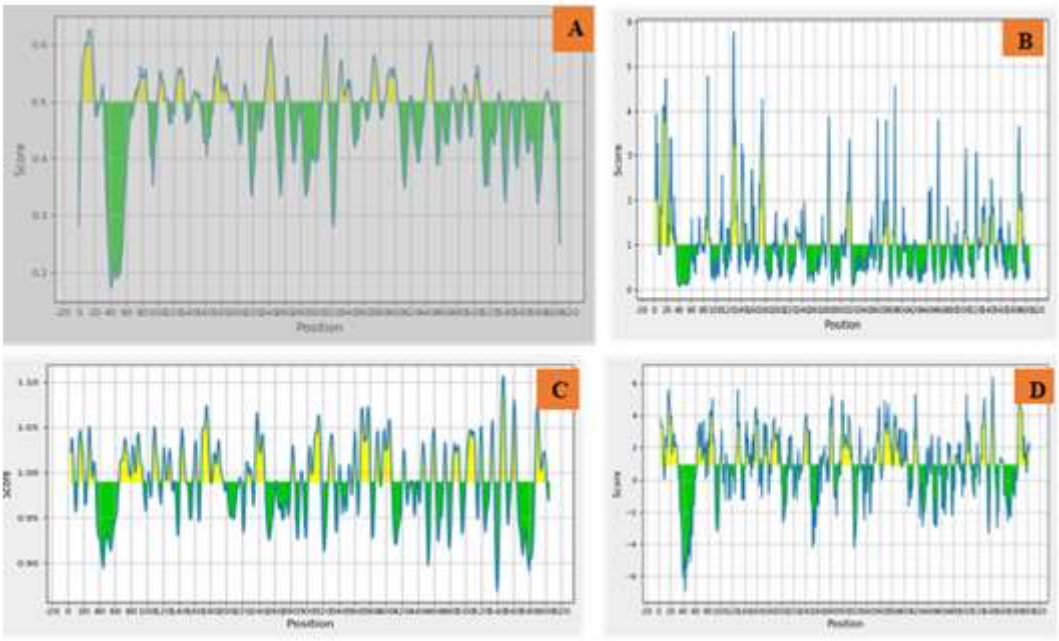

Figure 4.6: Prediction of B cell Epitopes by BepiPred Linear Epitope Prediction and Analysis of Surface Accessibility, Flexibility and Hydrophobicity, Respectively, for the H Protein of PPRV

Regions above the Threshold (Red Line) were proposed as a Part of the B Cell Epitope While Regions below the Threshold (Red Line) Were Not.

A BepiPred linear epitope prediction (Threshold 0.500,
B - Surface accessibility using Emini Surface (Threshold 1.00),
C - Flexibility using Karplus & Schulz (Threshold 0.989) and
D - Parker Hydrophilicity (Threshold 0.897).

4.5 Analysis of Linier B cell Epitopes from the F Protein

Based on BepiPred-2.0 method, a total of 13 B cell epitopes with varied length were identified from the F protein of PPRV (Table 4.3). Just like in the H protein, there was no potential B cell epitope that passed the selection criteria in the F protein of PPRV. Hence no candidate linier B cell epitope was identified (Figure 4.7).

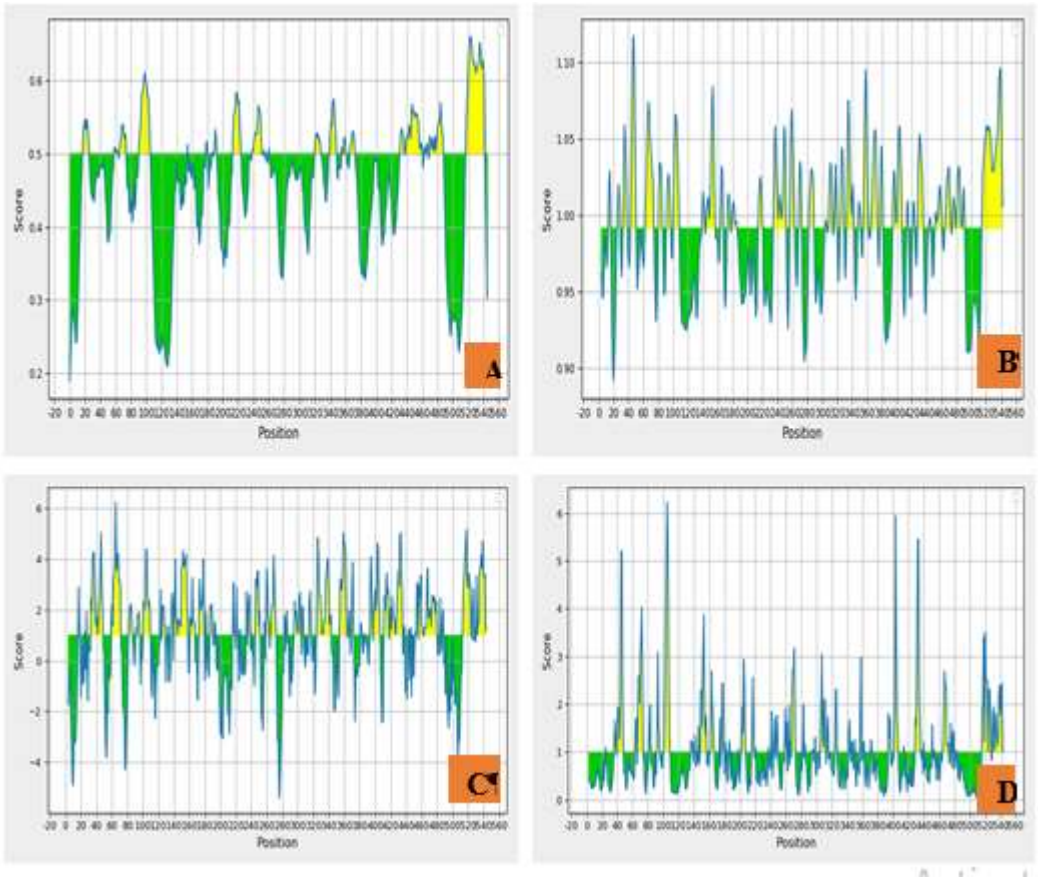

Figure 4.7: Prediction of B Cell Epitopes by BepiPred Linier Epitope Prediction and Analysis of Surface Accessibility, Flexibility and Hydrophobicity Respectively for the F Protein of PPRV

4.6 Analysis of Conformational B cell Epitopes from the H and F Protein

A total of 12 conformational B cell epitopes of the H protein and 6 of the F protein of PPRV were predicted. Five residues in the F protein had the highest score of above 0.96, for the H protein, 40 residues had the highest score of above 0.9. (Table 4.4) The threshold value for the scores was set at 0.5, indicating that most of the residues could be used as probable antigens

Table 4.4: Predicted Conformational B Cell Epitopes of the H Protein of PPR

No.	Residues	No. of residues	Score	3D structure
1.	M1, S2, A3, Q4, R5	5	0.963	Figure 4.8(a)
2.	R7, I8, N9, A10, F11,Y12, K13, D14, N15, P16	10	0.953	Figure 4.8(b)
3.	F46, L47, S48, L49, I50, G51, L52, L53, A54, I55, A56, G57, I58, R59, L60, H61, R62, A63, T64, V65, G66, T67, S68, E69, I70, Q71, S72, L74, N75, T76, N77, I78, E79, L80, T81, E82, S83, I84, D85, H86, Q87, T88, K89, D90, V91, L92, T93, P94, L95, F96, K97, I98, I99, G100, D101, V103, I107, F111, L114, V115, I118, S119, D120, K121, I122, K123, F124, L125, N126, P127, D128, R129, E130, Y131, D132, F133, R134, D135, L136	79	0.818	Figure 4.8(c)
4.	H17, N18, K19, N20, H21, R22, V23, I24, L25, D26, R27, R29, L30, V31, I32, E33, R145, V146, K147, I148, N149, F150, D151, Q152, F153, C154, E155, Y156, K157, A158, A159, V160, K161, S162, I163, E164, H165, I166, F167, E168, S169, P170, L171, N172	44	0.806	Figure 4.8(d)
5.	M212, K213, H214, N215, W235, R236, S237, D238, A239, R240, D241, P242, S243, T244, D245, L246, G247, I248, G249, H250, F251, L252, Y275, L276, T277, V278, N279, M280, S281, D282, D283, Y284, S302	33	0.708	Figure 4.8(e)
6.	E28, R34, P35, Y36, I37, L38, L39, G40, V41, L42, L43, V44, M45, W138, C139, N141, P142, P143, E144	19	0.696	Figure 4.8(f)
7.	T307, L308, G309, E310, G312, V313, P314, K315, R316, E317, V338, P340, T341, S342, D343, L344, M345, V346, E347, D371, V372, R373, D374, L375, Q376, N377, K378, G379, E380, C381, L382, V383, E384, A385, C386, K387, T388, R389, P390, P391, S392, C394, N395, G396, T397, G398, S399, G400, S403, E404, G405, R406, I407, P408, P433, E486, I487, R488, G489, P490, R491, G492, R493, C494, H495, E499	66	0.666	Figure 4.8(g)
8.	D418, L419, A420, S421, D422, P423, G424	7	0.609	Figure 4.8(h)
9.	N587, T588, I589, T590, D591, E592	6	0.608	Figure 4.8(i)
10.	T273, N325, L326, A327, G328, P329, T330, L331, G332, G333, E334	11	0.604	Figure 4.8(j)
11.	K173, S174, K175, K176, L177, Q178, S179, L180, T181, L189	10	0.579	Figure 4.8(k)
12.	F448, S449, R450, F472, P473, N474, R475	7	0.567	Figure 4.8(l)

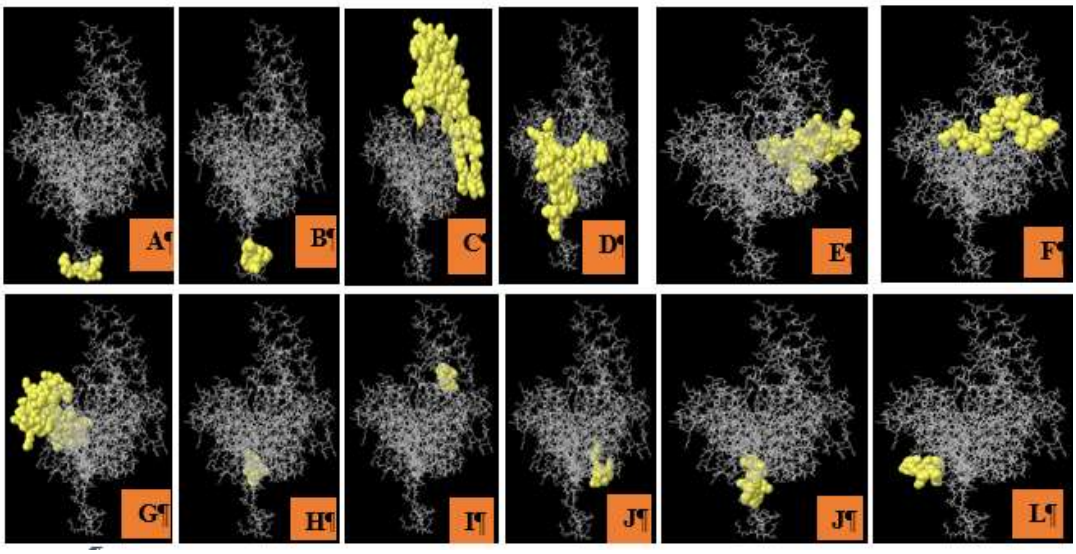

Figure 4.8: Twelve Conformational Structure of the Predicted B Cell Epitope of the H Protein the Epitopes Are Shown in Yellow

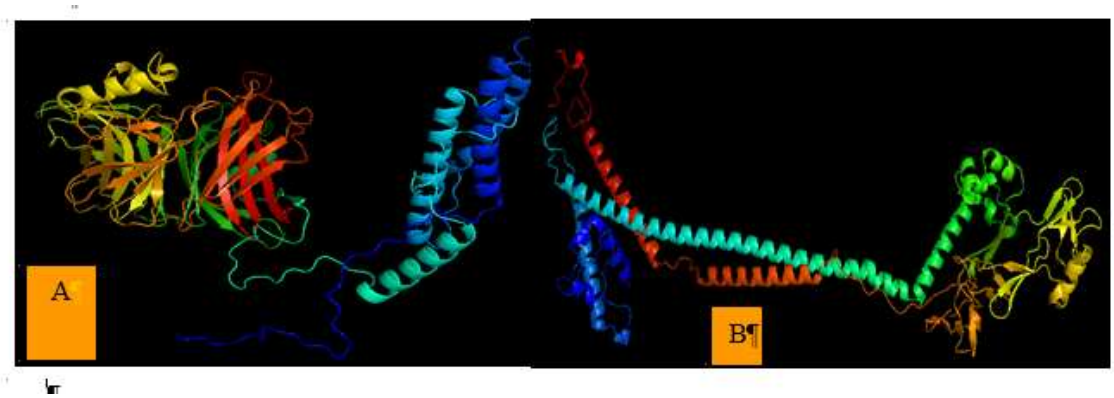

Figure 4.9: Three-Dimensional Structures of the H (A) and F (B) Proteins of PPRV Respectively Predicted by the raptorX Server, refined by Galaxy Refine and Visualized by PyMOL Molecular Graphics System

4.7 Construction of the Multi-Epitope Subunit Vaccine, Antigenicity, Toxicity, Allergenicity and Solubility Evaluation

Codon adaptation and *in silico* cloning: Codon sequence of the optimized vaccine was 620 nucleotides long, and its GC content and codon adaptation index (CAI) were

determined. GC content can be used as a criterion for selecting most suitable sequences for cloning and expression, as high or low GC content may affect stability and folding of the DNA molecule. GC content of cDNA sequence was found to be 52.2946 %, which was within the recommended range of 30–70 % for optimal translational efficiency. CAI was calculated to be 0.9926, which is also within the range of 0.8–1.0, indicating that the vaccine construct could be be expressed effectively in *E. coli*. Target sequence is highlighted yellow colour (Figure 4.10) in the clone, located between the restriction sites XhoI and BamHI The final vaccine peptide was constructed and consisted of 620 amino acid residues (Figure 4.10).

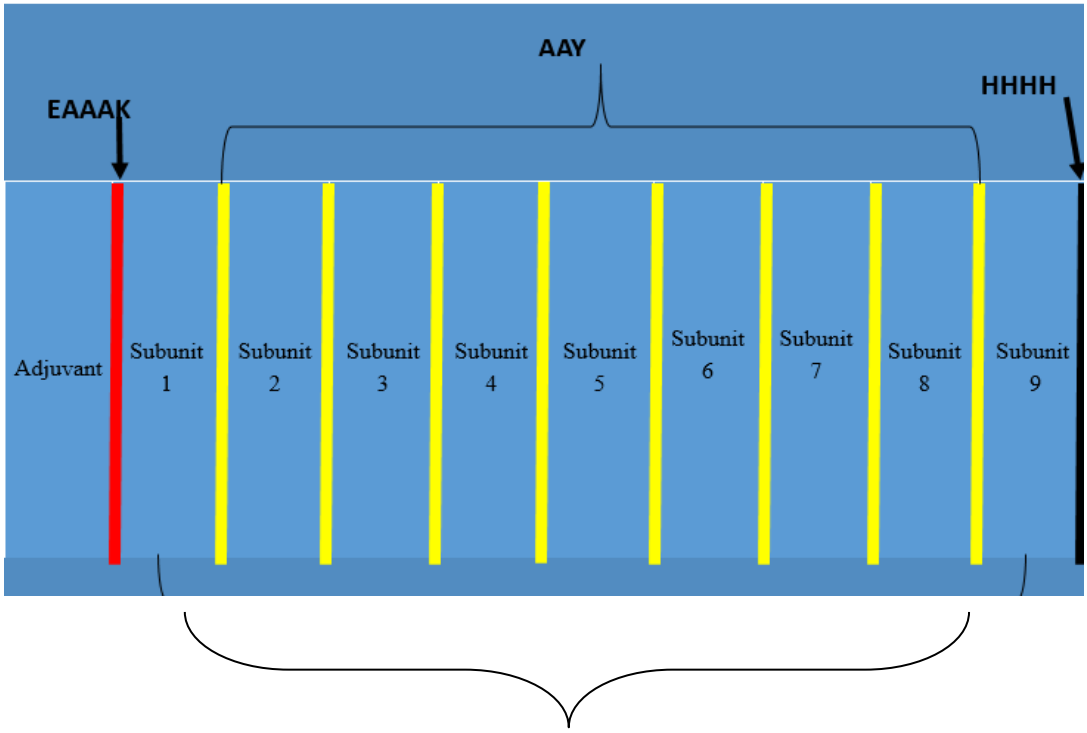

Figure 4.10: Schematic Illustration of Predicted Multiepitope Vaccine Construct

The vaccine was constructed using the predicted nine epitopes nine linked together by AAY linkers, an adjuvant linked using a EAAAK linker and 6His tag for identification and purification purposes. The final vaccine contains 620 amino acid residues. The candidate vaccine had a Vaxijen score of 0.5059 suggesting high

antigenicity. All the subunits of the vaccine candidate were predicted to be non-allergic and non-toxic (Gupta *et al.* 2013) The putative vaccine was soluble with a solubility probability of 0.558224 as predicted by the SolPro server (http://scratch.proteomics.ics.uni.edu) (Yang, Bogdan, and Nazarian, 2021). The quality score of the predicted model was also done by Galaxy refine (Table 4.5).

4.8 Prediction of the Secondary and Tertiary Structure of the Chimera

The secondary structure of the vaccine candidate predicted consisted of 52.4% alpha helix, 12.1% beta strand and 35.5%-coin residues. Among the 620 amino acid residues in the final vaccine, 51.6% were predicted to be exposed, 20.7% to be medium exposed while (28.2%) were predicted to be buried. A total of 70 amino acid residues were predicted to be located in disordered regions while 550 were predicted to be located in ordered regions. Model with the lowest Root-mean-square-deviation of atomic position (RMSD) score of 9.6982, was carried forward for refinement. The smaller the RMSD score of a predicted model the more likely it is of good quality (Wang *et al.*, 2017) .

Table 4.5: Quality Score of Predicted Vaccine Models by Galaxy Refine

Model	GDT-HA	RMSD	MolProbity	Clash score	Poor rotamers	Rama favored
Initial	1.0000	0.000	5.112	392.7	94.5	89.3
MODEL 1	0.9105	0.530	2.619	43.2	0.8	91.4
MODEL 2	0.9105	0.539	2.613	43.6	1.0	91.9
MODEL 3	0.9081	0.541	2.701	41.7	1.2	90.5
MODEL 4	0.9157	0.526	2.840	43.7	1.8	90.9
MODEL 5	0.9137	0.538	2.836	43.1	2.0	91

4.9 Evaluation of Antigenicity, Toxicity, Allergenicity, Solubility and of the Constructed Multi-Epitope Subunit Vaccine

A total of five refined models were predicted, and among the predicted models, model 1 was selected (Table 4.5) as the final vaccine model. The final vaccine peptide was constructed and consisted of 620 amino acid residues. The candidate

vaccine had a Vaxijen score of 0.5059, suggesting high antigenicity. All the subunits of the vaccine candidate were predicted to be non-allergic and non-toxic (Gupta et al., 2013). The putative vaccine was observed with a solubility probability of 0.558224 as predicted by the SolPro server (http://scratch.proteomics.ics.uni.edu) (Yang et al., 2021).

4.9.1 Analysis of the Physiochemical Properties of the Vaccine Candidate

The molecular weight (MW) of the constructed multi-epitope vaccine was 65361.99 Da with a theoretical isoelectric point (pI) of 5.70. The Grand Average of Hydropathy (GRAVY) was predicted to be -0.165 using Expasy's ProtPram (http://us.expasy.org/tools/protparam.html) (Gasteiger et al., 2003). The half-life was predicted as more than >10h in vivo in *E. coli* and >30h in vitro in mammalian reticulocytes. The vaccine was predicted as stable with an Instability Index of 21.20, with an estimated aliphatic index of the vaccine being predicted as 92.34 (Table 4.6).

Table 4.6: Evaluation of Antigenicity, Allergenicity, Toxicity and Physiochemical Properties of the Vaccine Candidate

Vaccine subunits	Epitope	Vaxijen score	AllerTOP result	Toxicity	Hydropathicity	Half-life in vivo	Half-life In vitro	Stability	pI	Molecular weight
Adjuvant		0.4932	NA	NT	-0.385	>10h	30h	Yes	4.91	52890.32
Subunit 1	92KNVRPIQTL100	0.8138	NA	NT	0.056	>10h	1.9h	No	8.31	1131.3
Subunit 2	125AQITAGVAL133	0.7995	NA	NT	1.478	>10h	4.4h	Yes	5.57	842.99
Subunit 3	53KLMPNITAI61	0.8494	NA	NT	0.756	3 min	1.3h	No	8.75	1000.26
Subunit 4	496LAACIGVSL504	0.8734	NA	NT	2.356	2 min	5.5h	No	5.52	846.05
Subunit 5	4VAILTFLFL12	0.4012	NA	NT	2.978	>10h	100h	No	5.49	1036.32
Subunit 6	222AAEISIQAL230	1.1573	NA	NT	1.156	>10h	4.4h	Yes	4	915.05
Subunit 7	369GTISNRFIL377	0.8098	NA	NT	0.633	>10h	30h	Yes	9.75	1020.2
Subunit 8	549SSYFYPVRL557	0.6308	NA	NT	0.056	>10h	1.9h	No	8.31	1131.3
Subunit 9	316REPLVVVIL324	0.5724	NA	NT	1.678	2 min	1h	No	6	1037.31
	Final vaccine	0.5059	NA	NT	-0.165	>10h	30h	Yes	5.7	65361.99

4.10 Subcellular Localization of Shortlisted Proteins

The nine proteins identified were then subjected to PSORTb version 3.0.2 (Yu et al., 2010) an online tool in order to identify subcellular localization. The proteins were found to be localised within the cytoplasm

4.11 Refinement of the Vaccine 3D Structure

The final vaccine score was 0.5, none toxic and none allergic. It had *in vivo* half-life of >10Hrs Hydrophobicity index of –0.165 and *in vitro* half-life of 30 Hrs. the stability index was 5.7 which was within the accepted range of less than ≤40. The GDI-HA scores for all the refined models reached a high of slightly above 0.9 The score ranges from 0 to 1, where 1.0 represents a perfect match to the experimental structure indicating that the refined protein model was exceptionally accurate and very close to the native experimental structure (Liu, et al., 2017). RSMD value of the predicted model was less than 0.6 indicating perfect stability and quality of the model. Usually, lower RMSD value usually suggests better stability and therefore better quality of the model (Liu, et al., 2017).

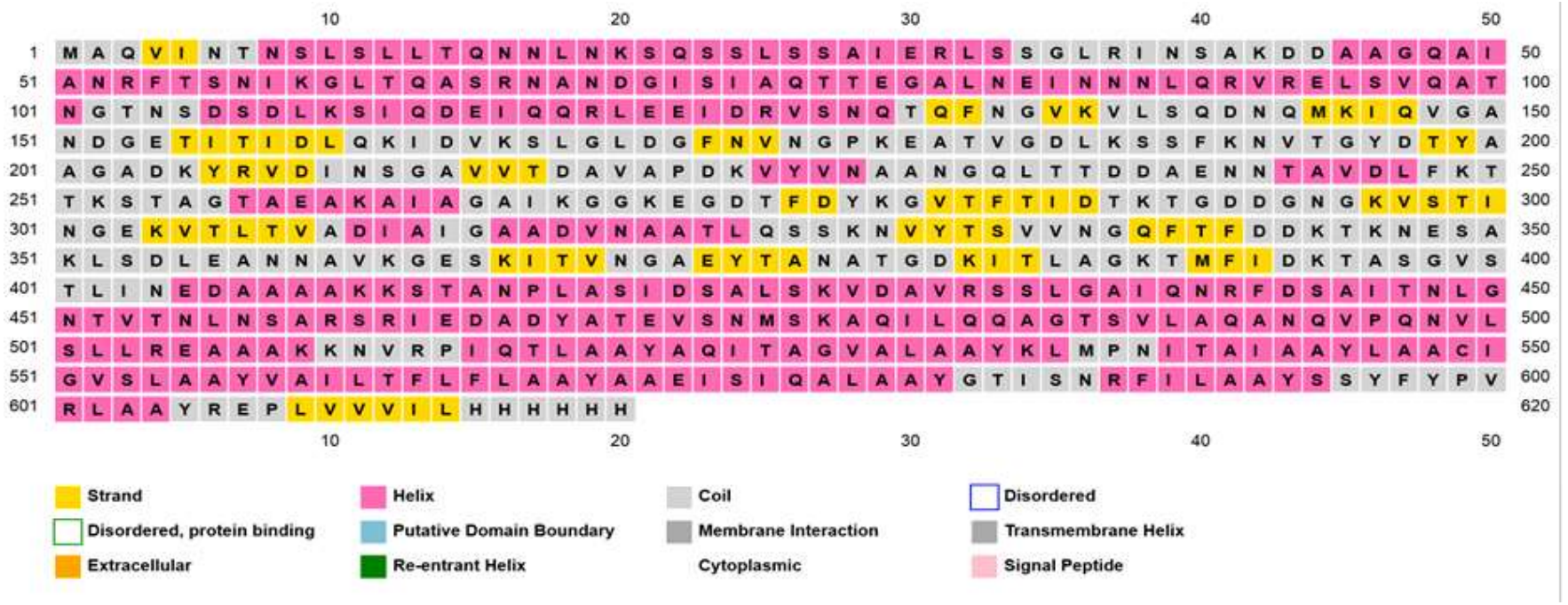

Figure 4.11: Features the Predicted by PSIPRED. The beta strand residues are coloured yellow, the alpha helix residues coloured pink and the coil residues coloured grey

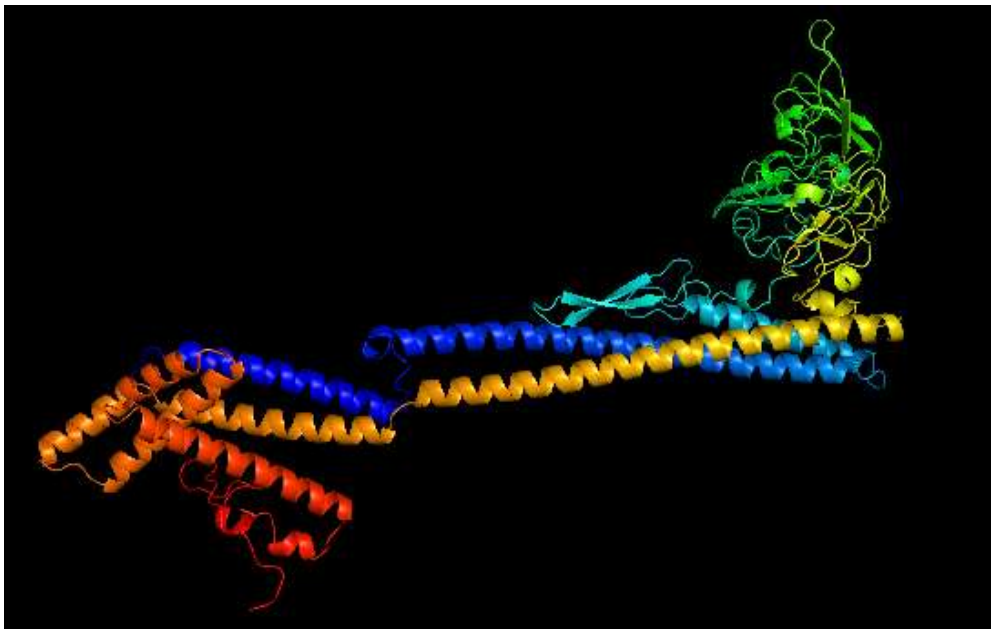

Figure 4.12: Refined Three-Dimensional Structure of the Vaccine Done by Galaxy Refine and Visualised by the PyMOL Molecular Graphics System

4.12 Validation of the Three-Dimensional Structure of the Vaccine

Ramachardan plot indicated 89.3% of the residues were in the most favoured region, 8.5% were in the allowed region, and 1.7% were in the disallowed region. The ERRAT quality factor was 84.4%. The A Z-score of the vaccine model was predicted as -6.75 using ProSA web server. This indicated that the predicted model was of a high-quality, reliable, and had a well-folded three-dimensional protein model (Figure 4.12)

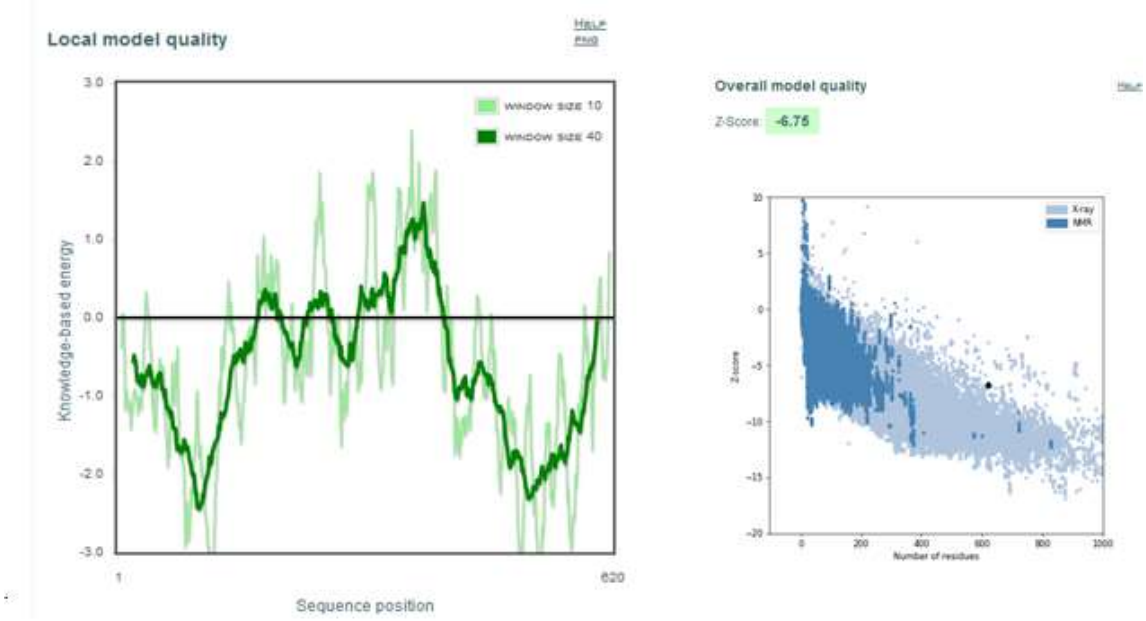

Figure 4.2: Structure Validation by ProSA-Web Showing (A) a Plot of the Structure's Residue Energies and (B) Its Z-Score. Predicted Z score of -6.75 lies within the score range. The negative values in the plot of the residues suggests absence of erroneous parts in the predicted model

4.13 Analysis of Physiochemical Properties of the Vaccine

The Grand Average of Hydropathy (GRAVY) was predicted to be -0.165, suggesting the vaccine was hydrophilic and can react with water because of the negative value. GRAVY index is usually a representation of the hydrophobicity of a peptide with a positive value representing a hydrophobic while a negative value representing a hydrophilic nature(Jaspard, Macherel, and Hunault 2012). The half-life was predicted as more than >10h in vivo in E. coli and >30h in vitro in mammalian reticulocytes. The vaccine was predicted as stable (Instability Index of 21.20) with an estimated aliphatic index of the vaccine being predicted as 92.34 indicating thermostability (Merkler et al., 1981).

4.14 Molecular Docking

The size (N) of the grid that was used in docking was 280, with the spacing between the grid cells being 1.2A. The ligand was indeed fixed during docking as predicted by the server (value of 1). In the output file, a value of 1 usually indicates the ligand was fixed while a value of 0 indicates the receptor was fixed during docking (Pierce et al., 2005). The initial location of the receptor in Euler angles was at -2.094395, 2.180315 and -1.357379 respectively. The initial rotation of the ligand in Euler angles was 2.380392, 2.500101 and -0.120466. The initial translation (X, Y and Z) to the centre of the receptor was 22.784, -63.756 and 22.966. On the other hand, the initial translation (X, Y, and Z) to the centre of the ligand was 102.168, 110.419 and 95.502. Complex 1 had the highest score (2600.133) and among all that were predicted it was chosen as the best model (Figure 4.14).

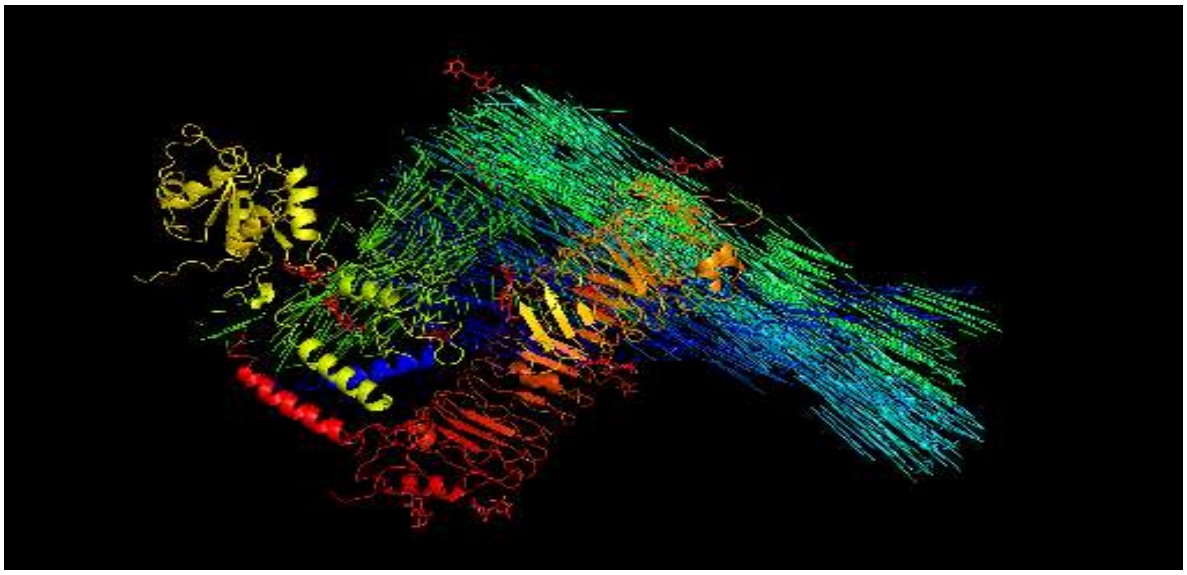

Figure 4.14: The Docked Complex of the Vaccine Model and the TLR5 Immune Receptor. The vaccine protein is represented as the cartoon structure while the rest of the residues is the TLR5 receptor. The score of this complex model is 2600.133 indicating good binding affinity.

4.15 Transformation Analysis

Transformation was observed to be successful, indicated by the growth of the transformed cells in presence of antibiotic *Kanamycin*. At a concentration of 50mg/ml. No growth was observed on the negative control plate that was inoculated with none transformed DH5αcells (Figure 4.15).

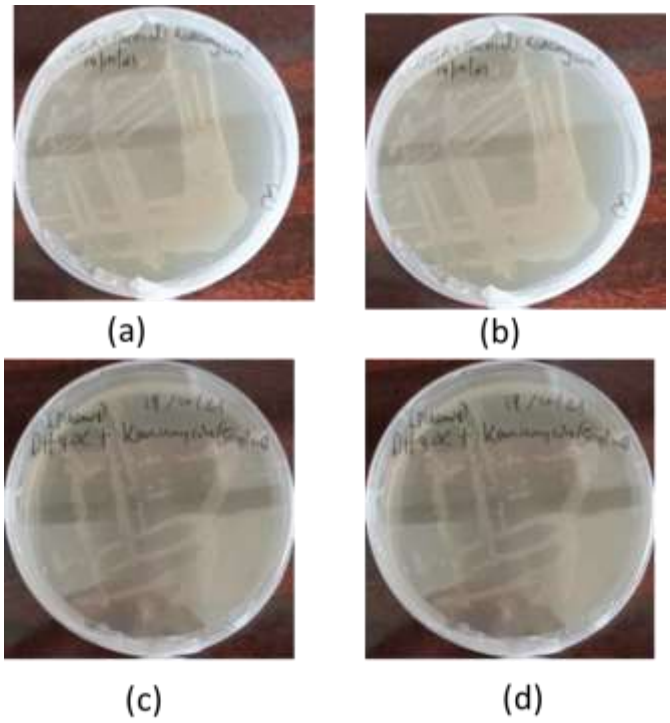

Figure 4.15: Transformed DH5-α E.coli Cells Cultured on Luria Broth (LB) with Agar Containing 50µg/ml Kanamycin.

4.16 Confirmation of Insert Using Agarose Gel Electrophoresis

The cloned fragment had a band size of approximately 72 KDa as visualized by the three bands in line (D). The non-transformed *E. coli* had a single band (Figure 4.16).

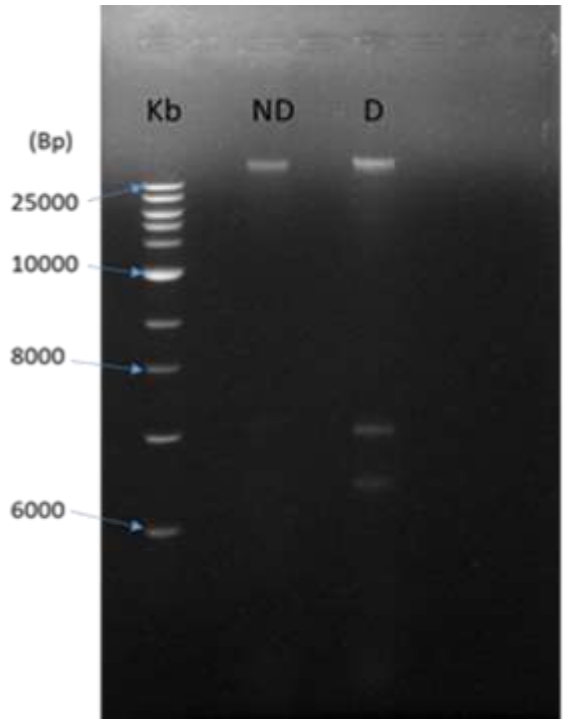

Figure 4.16: Visualized Agarose Gel After Electrophoresis. Lane 1= 1Kb DNA Ladder, lane ND =Control Lane Non-Transformed *E. coli* DH5α, lane D – Plasmid with the Insert

4.17 Determination of Protein Localization

The dot blot technique used indicated that the protein of interest was localized from the 3rd -6th aliquots while the rest of the aliquots had no protein of interest. Concentration on the SDS PAGE analysis confirmed the molecular weight of the desired protein to 72KDa (Figure 4.19).

Figure 4.17: Dot blot Technique Was Used to Determine to Protein Localization Those That Indicated a Signal Were Concentrated Using Poly-Ethyle Glycol (PEG) and Used for SDS Analysis.

4.18 Induction and Confirmation of Expressed Proteins Using IPTG

The intensity of the blots was shown to decrease with increased dilution. However, no reaction was observed in the negative control. Known positive sample of A New castle disease Virus (NCD virus) was used as shown in (Figure 4.18). These results showed specificity of the protein of interest and an indication of lack of cross reactivity with other Morbilliviruses. Which was an indication of the sensitivity and specificity of the protein of interest.

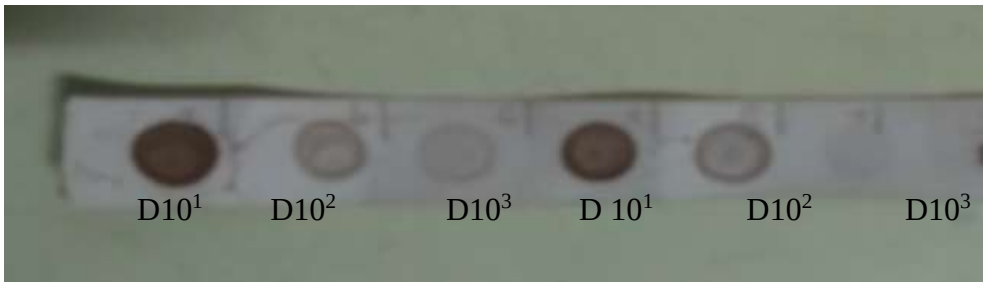

Figure 4.18: Immunoblotting Done to Determine the Protein Concentration from Expressed Samples

From the results there was no activity in the negative control, which indicated that our protein was specific to PPRV. The highest activity was shown in the neat sample and the activity went on fading with the dilution. of the purified (P) protein of interest The MW was confirmed to be ~72 KDa purification process was confirmed since no any other band was observed as compared to the (NP) non purified protein The none purified protein (NP) was observed to have different bands however the purified protein had only one band that was within the expected range of 72 KDa. The gel was further subjected to a western blot technique so as to reconfirm the immunological response of the purified band. Protein purity and Molecular weight was determined after purification using an SDS page gel. The protein of interest was confirmed to have a Mw of 72KDa (Figure 4.19).

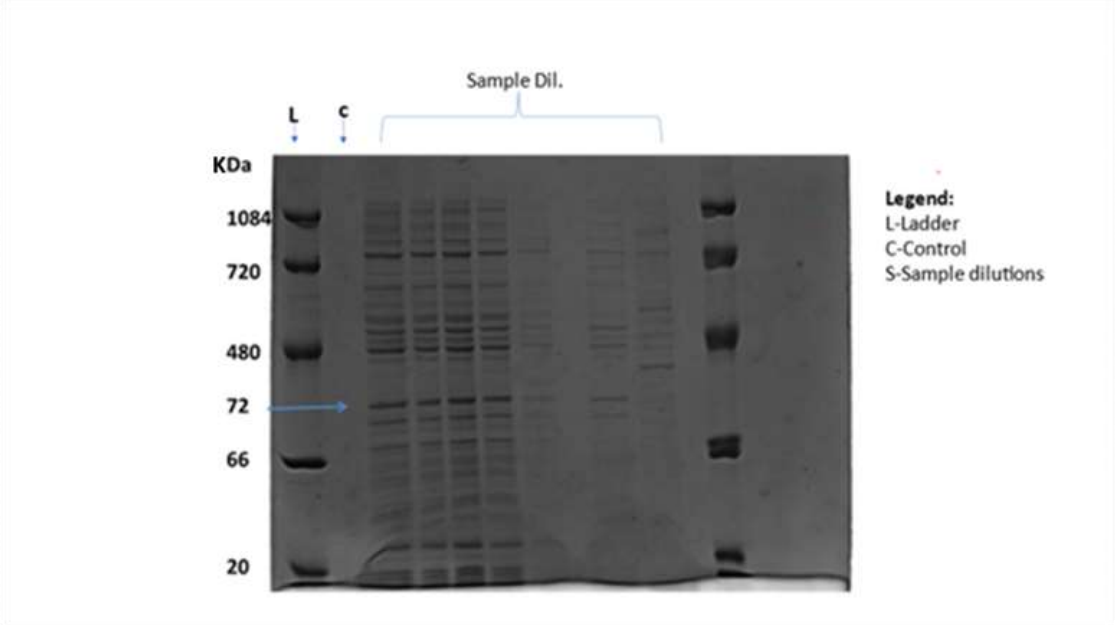

Figure 4.19: SDS PAGE Showing Different Fractions of the Protein Bands, Protein of Interest was seen at position 72KDa

4.19 Western Blot Analysis

This was performed to verify binding ability probing of the samples with secondary antibody after the transfer indicating that there is activity. The results showed that the expressed recombinant PPRV F/H protein when immunoblotted with a strong positive hyper immune serum (Antibodies) there was reaction that indicated sensitivity (Figure 4.20).

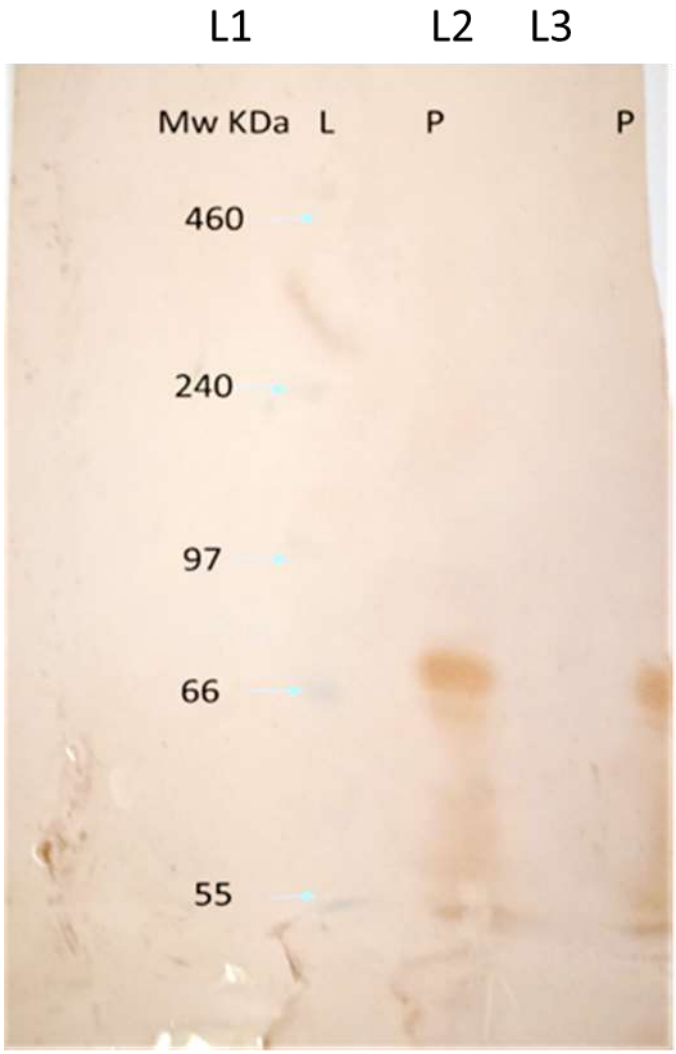

Figure 4.20: Electroblotting analysis of the Expressed Recombinant PPRV F/H Protein Immunoblotting with Standard Strong Positive Hyper Immune Serum

Lane 1: 0.5kd pre-stained marker Lane 2&3: purified sample (Thermo Scientific 26612) from the results above it was noted that the purified protein was able to recognize the PPR Virus antibodies when probed with hyper immune sera as shown in lane 2&3 hence indicating specificity to PPRVirus. The purified protein was later quantified for, *in vivo* studies to determine the immunogenicity.

4.2 Determination of the Protein Concentration of Interest

Protein concentration was found to be 4.45mg/ml indicating high concentration hence for *In-vivo* studies the protein had to be diluted further for *in-vivo* studies (Figure 4.21).

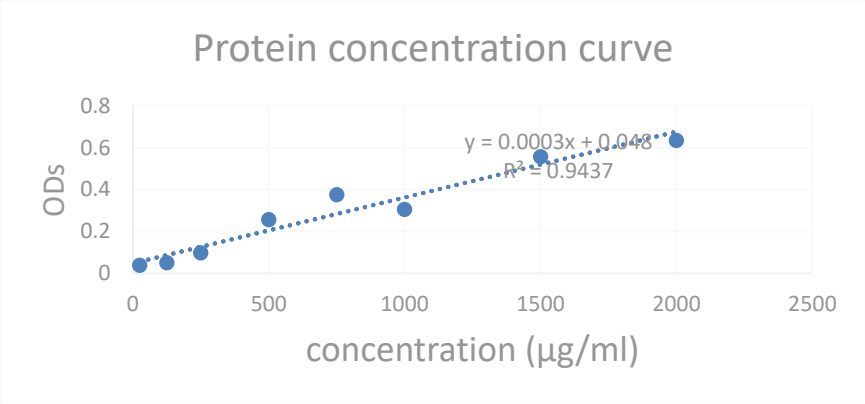

Figure 4.21: Determination of the Protein Concentration on the Purified Vaccine Candidate

Protein concentration was determined to be 4.45mg/ml indicating high concentration hence for *In-vivo* studies the protein had to be diluted further for *In-vivo* studies

4.2 In-*Vivo* Immunological Studies on the Purified Vaccine Candidates

The results showed that the humoral immune response to the subunit vaccine candidate was higher than that observed with the N/75 positive control vaccine. (Figure 4.22). The increased rate of seroconversion could be attributed to the specificity of the subunit vaccine candidate that was deemed to offer a much vigorous reaction (Figure 4.22). Seroconversion was not observed in the negative control group. An increase in antibody production was observed from day 21 after the boosting with the antigen this was observed in the test group and the positive control group. However, no reaction was observed in the control group that showed no response it was therefore clearly indicated that the response observed was due to vaccination with the specific antigen.

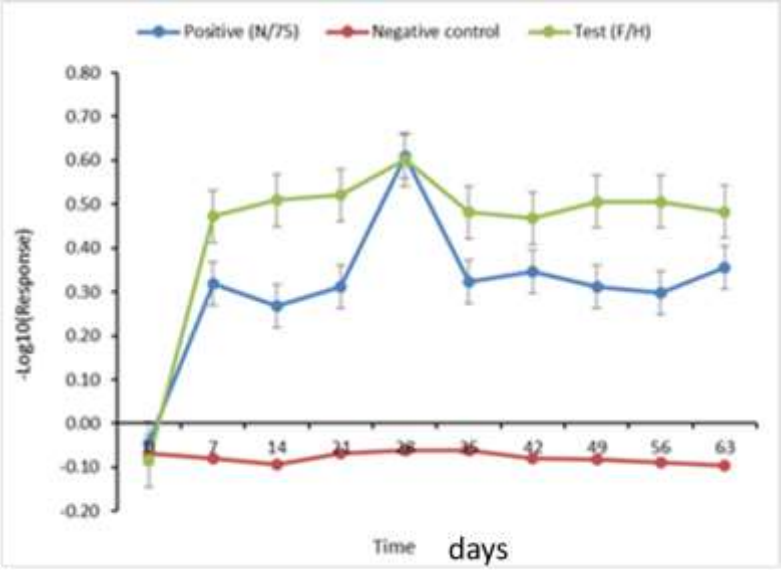

Figure 4.22: The mean group ELISA results showing the Antibody Titer Following Vaccination of Rabbits

(Blue): Positive control (N/75); (Red): Negative control; (Green): Test (F/H)]. There was negative correlation between Negative Control and Positive (N/75), but it is not statistically significant (r=-0.06, n=10, p = 0.870, which is much greater than 0.05). There was a statistically significant (p <0.001) between the positive control and the Test (vaccine) (F/H) and Positive (N/75), (r=+0.95, n=10, p <0.001).

CHAPTER FIVE

DISCUSSION

The present study employed an immunoinformatics and molecular biology approach to design, evaluate, express, and preliminarily validate a multiepitope subunit vaccine candidate against Peste des Petits Ruminants using the fusion (F) and hemagglutinin (H) proteins of the virus. The F and H proteins were selected because they are major surface glycoproteins involved in viral attachment, membrane fusion, and induction of host immune responses. Previous studies have demonstrated that these proteins contain highly immunogenic regions capable of eliciting both humoral and cellular immune responses, making them suitable targets for vaccine development.

5.1 Importance of Veterinary Vaccines

Veterinary vaccines have got an immense role in: protecting not only public health but also animal health, facilitating an efficient food production to feed the increasing human population as well as reducing morbidity and mortality in domesticated animals. Immunization is considered one of the most effective and safe methods of controlling infectious diseases and subsequently improving public health efficiently, quickly and cost-effectively. Vaccination in veterinary medicine, helps to greatly reduce the antibiotic resistance (Roth et al., 2011). Rabies vaccines that are applied in domesticated animals and wildlife, for example, have made tremendous steps in the fight against the disease all over the world, nearly eliminating human rabies, especially in developed countries (Roth et al., 2011). Rinderpest, on the other hand, became the second disease, after small pox, to be declared eradicated globally in the year 2011, after more than a decade of effort (Albina et al., 2013). This was following the establishment of Global Rinderpest Eradication Program (GREP), a flagship initiative of FAO's Emergency Prevention System for Transboundary Animal and Plant Pests and Diseases (EMPRES) that encompasses vaccination, trade restrictions, and surveillance (Yadav[b] et al., 2020).

5.2 Challenges in PPR Vaccine Development

PPR control and eradication is a priority for poverty alleviation due to its increased turnover on small ruminants' population and insufficient investment as well as political commitment for improving their health and productivity (Jones et al., 2016). Current vaccines against PPRV are live attenuated vaccines, which are mired with challenges that need to be addressed this includes: the requirement of a cold chain for their preservation, and the risk of reversion to virulence. Development of new vaccines starts with the identification of unique components of the microorganism capable of generating a protective immune response. With traditional techniques, this could be a long and arduous process, besides the difficulty of cultivating the microorganism in the laboratory. With traditional techniques, this could be a long and arduous process, besides the difficulty of cultivating the microorganism in the laboratory (Alan et al., 2010). Advancements in the field of bioinformatics and immunology have led to disciplines in vaccine design against diseases via computer-aided (in silico) epitope predictions. The new concept has been applied successfully in many studies, particularly in the development of vaccines targeting conserved regions within the genome of mutating pathogens (Gaafar et al., 2019). The continued spread of PPR has become an essential animal health concern in endemic countries despite the existence of an effective vaccine. Production of an effective vaccine is costly and can take years to be completed. Hence, researchers have tried for many years to minimize the cost and time for the development of vaccines. There are different strategies available for the design and development of effective and safe new-generation vaccines based on the Bioinformatics approaches. (Aparicio et al., n.d.) In the last decades, advances in genomics, genome sequencing, and annotation, coupled with the development of bioinformatics tools has revolutionized vaccine development strategy (Cunningham et al., 2017). Reverse vaccinology allows vaccines to be designed even for non-cultivable pathogens, it enables target proteins to be accessed even if they are only transiently expressed or scarce during infection. The strategy also considerably reduces the time required for the development of new vaccines. (Rappuoli 2000)This study adopted this methodology and selected proteins

with the best values for antigenicity, which is the ability of a proteins to be recognized by the immune system; hence, it is desirable to find the highest antigenicity value for the selection of the best potential vaccine candidates.

5.3 Multiple Sequence Alignment and Phylogenetic Analysis

The multiple sequence alignment analysis was done and demonstrated considerable conservancy among the retrieved strains of both the H and F proteins despite the presence of a few amino acid substitutions in some regions. Conserved regions within viral proteins are critical during vaccine development because they increase the likelihood of broad-spectrum protection against genetically diverse viral strains. The observed conservancy among the retrieved sequences suggests that the selected proteins are under strong evolutionary constraints due to their essential biological roles in viral infectivity and survival. Similar observations have previously been reported in morbilliviruses, where structural and functional proteins tend to remain highly conserved despite geographical diversity. Although mutations were observed in certain amino acid positions, these variations did not significantly alter the overall conservancy of the proteins. Such mutations may arise because of immune pressure, adaptation to different hosts, or environmental influences. However, the preservation of most conserved motifs indicates that the immunogenic regions of the proteins remain relatively stable and could therefore serve as reliable vaccine targets.

Phylogenetic analysis further demonstrated close genetic relationships among African, Asian, and European isolates, particularly between the Omani, Emirati, and Ethiopian strains. This finding may indicate transboundary transmission and circulation of lineage IV strains across continents through livestock trade and animal movement. The clustering of the strains into lineage IV is consistent with previous reports indicating the global expansion and predominance of lineage IV PPRV strains in Africa and Asia. The high percentage similarities observed among the strains further support the suitability of

designing a universal or broadly protective vaccine candidate targeting conserved regions within lineage IV viruses.

The low sequence divergence observed among the H and F genes also supports the relative genetic stability of these proteins. The F protein demonstrated particularly high similarity values ranging from 98.2% to 99.0%, indicating strong evolutionary conservation. Such conservancy is advantageous for epitope-based vaccine design because conserved epitopes are less likely to undergo immune escape mutations.

The multiple sequence alignment analysis demonstrated considerable conservancy among the retrieved strains of both the H and F proteins despite the presence of a few amino acid substitutions in some regions. Conserved regions within viral proteins are critical during vaccine development because they increase the likelihood of broad-spectrum protection against genetically diverse viral strains. The observed conservancy among the retrieved sequences suggests that the selected proteins are under strong evolutionary constraints due to their essential biological roles in viral infectivity and survival. Similar observations have previously been reported in morbilliviruses, where structural and functional proteins tend to remain highly conserved despite geographical diversity.

Although mutations were observed in certain amino acid positions, these variations did not significantly alter the overall conservancy of the proteins. Such mutations may arise because of immune pressure, adaptation to different hosts, or environmental influences. However, the preservation of most conserved motifs indicates that the immunogenic regions of the proteins remain relatively stable and could therefore serve as reliable vaccine targets.

Phylogenetic analysis further demonstrated close genetic relationships among African, Asian, and European isolates, particularly between the Omani, Emirati, and Ethiopian strains. This finding may indicate transboundary transmission and circulation of lineage IV strains across continents through livestock trade and animal movement. The

clustering of the strains into lineage IV is consistent with previous reports indicating the global expansion and predominance of lineage IV PPRV strains in Africa and Asia. The high percentage similarities observed among the strains further support the suitability of designing a universal or broadly protective vaccine candidate targeting conserved regions within lineage IV viruses.

The low sequence divergence observed among the H and F genes also supports the relative genetic stability of these proteins. The F protein demonstrated particularly high similarity values ranging from 98.2% to 99.0%, indicating strong evolutionary conservation. Such conservancy is advantageous for epitope-based vaccine design because conserved epitopes are less likely to undergo immune escape mutations.

5.4 Prediction and Evaluation of CTL Epitopes

The identification of conserved cytotoxic T lymphocyte (CTL) epitopes from the H and F proteins represents an important step toward the development of a cell-mediated immune vaccine candidate against PPRV. T-cell mediated immunity plays a major role in viral clearance by inducing the destruction of infected cells through MHC-I presentation pathways. In this study, selected epitopes demonstrated high conservancy, strong antigenicity, absence of allergenicity and toxicity, and favorable binding affinity toward multiple bovine leukocyte antigen (BoLA) alleles. The H protein epitope 549SSYFYPVRL557 exhibited broad MHC-I binding affinity with five BoLA alleles, suggesting its potential to induce immune responses in genetically diverse hosts. Broad allele coverage is desirable in epitope-based vaccine development because it increases population coverage and improves vaccine applicability across different breeds and geographical populations. Similarly, the F protein epitope 92KNVRPIQTL100 demonstrated the highest affinity toward six BoLA alleles, indicating strong immunogenic potential.

The high antigenicity scores observed among the shortlisted epitopes further support their potential to stimulate protective immune responses. According to

immunoinformatics principles, epitopes with high antigenicity and immunogenicity scores possess greater capacity to be recognized by host immune cells and initiate effective cellular immune responses. Additionally, the non-toxic and non-allergenic nature of the epitopes enhances their safety profile as vaccine candidates. Epitope mapping on the three-dimensional structures of the proteins revealed that the selected epitopes were spatially accessible within the protein structures (Heo and Feig 2020). Structural accessibility is important because exposed epitopes are more likely to interact effectively with immune receptors and antigen-presenting molecules. Therefore, the identified CTL epitopes may serve as promising candidates for inclusion in multiepitope vaccine constructs.

5.5 Linear and Conformational B-cell Epitope Prediction

The prediction of B-cell epitopes is important in vaccine development because B-cell epitopes stimulate antibody-mediated immune responses. In this study, several potential linear B-cell epitopes were identified from both the H and F proteins (Pourseif et al., 2018). However, none satisfied all the selection criteria simultaneously, particularly surface accessibility requirements. Surface accessibility is an important characteristic because antibody recognition primarily occurs on exposed protein surfaces.

The failure of the predicted linear B-cell epitopes to satisfy all screening criteria may indicate that the dominant antigenic determinants of the H and F proteins are conformational rather than linear. This observation agrees with previous findings that most viral neutralizing epitopes exist in conformational forms dependent on tertiary protein structure. Consequently, linear peptide vaccines alone may not fully mimic the natural antigenic conformation required for optimal antibody recognition.

In contrast, several conformational B-cell epitopes with high scores were identified in both proteins. The high scores obtained for many conformational residues suggest that the proteins possess structurally exposed antigenic regions capable of eliciting humoral immune responses. Conformational epitopes are generally considered more biologically

relevant because they better resemble the native structure of viral proteins recognized by antibodies during infection. Therefore, inclusion of structurally conserved conformational regions in vaccine design may improve immunogenicity and antibody specificity.

5.6 Construction and Evaluation of the Multiepitope Vaccine

The constructed multiepitope vaccine consisted of nine selected CTL epitopes linked using AAY linkers and fused with an adjuvant using the EAAAK linker. Linkers are important in multiepitope vaccine design because they facilitate proper epitope separation, folding, and processing by immune cells. The inclusion of an adjuvant was intended to enhance immunogenicity and stimulate stronger immune responses. The final vaccine construct demonstrated favorable immunological and physicochemical characteristics. The VaxiJen antigenicity score of 0.5059 indicated that the construct was likely antigenic and capable of inducing immune responses. Furthermore, the vaccine was predicted to be non-allergenic and non-toxic, suggesting its potential safety for administration.

The codon adaptation index (CAI) of 0.9926 and GC content of 52.29% indicated efficient codon optimization for expression in Escherichia coli. Codon optimization is important for enhancing translational efficiency, protein expression, and stability in heterologous hosts. The observed CAI value close to 1.0 suggests that the optimized sequence closely matched the codon usage preference of E. coli, thereby favoring high-level protein expression.

The predicted solubility of the vaccine construct also suggests suitability for recombinant expression and purification (Fakhoury, 2017). Soluble recombinant proteins are generally easier to purify and less likely to form inclusion bodies during expression (De Souza et al., 2012).

5.7 Structural analysis and Validation of the Vaccine Construct

Secondary structure analysis revealed that the vaccine construct contained a high proportion of alpha helices and coil regions. Alpha-helical structures are often associated with structural stability, while coil regions may enhance flexibility and antigen presentation. The presence of exposed residues within the construct further suggests accessibility to immune receptors.

The refined tertiary structure models demonstrated favorable quality parameters. Model 1 showed improved MolProbity scores, reduced clash scores, and high Ramachandran favored residues compared to the initial model, indicating substantial structural refinement. Lower RMSD values observed after refinement further support structural stability and reliability of the predicted model.

Validation using the Ramachandran plot, ERRAT, and ProSA further confirmed the quality of the predicted structure. The majority of residues falling within favored regions indicated acceptable stereochemical quality, while the ProSA Z-score of -6.75 suggested that the model was comparable to experimentally solved native proteins. Collectively, these findings indicate that the predicted vaccine structure was stable, properly folded, and structurally reliable.

5.8 Physiochemical Properties and Molecular Docking

The physicochemical analysis demonstrated that the vaccine construct possessed favorable biochemical properties. The negative GRAVY value indicated hydrophilicity, suggesting improved solubility and interaction with aqueous biological environments. The instability index below 40 further indicated that the vaccine construct was stable, while the high aliphatic index suggested thermostability.

Molecular docking analysis demonstrated strong interaction between the vaccine construct and the TLR5 immune receptor. Toll-like receptors play essential roles in

initiating innate immune responses through recognition of pathogen-associated molecular patterns. Strong binding affinity between the vaccine construct and TLR5 suggests the potential ability of the vaccine to activate downstream immune signaling pathways and stimulate adaptive immunity.

5.8.1 Physiochemical Properties and Molecular Docking

The physicochemical analysis demonstrated that the vaccine construct possessed favorable biochemical properties. The negative GRAVY value indicated hydrophilicity, suggesting improved solubility and interaction with aqueous biological environments. The instability index below 40 further indicated that the vaccine construct was stable, while the high aliphatic index suggested thermostability.

Molecular docking analysis demonstrated strong interaction between the vaccine construct and the TLR5 immune receptor. Toll-like receptors play essential roles in initiating innate immune responses through recognition of pathogen-associated molecular patterns. Strong binding affinity between the vaccine construct and TLR5 suggests the potential ability of the vaccine to activate downstream immune signaling pathways and stimulate adaptive immunity.

5.8.2 Recombinant Expression and Protein Characterization

Transformation of recombinant plasmids into DH5α E. coli cells was successful as confirmed by growth on kanamycin-containing media. The absence of growth in the negative control confirmed that antibiotic resistance was associated with successful plasmid uptake.

Agarose gel electrophoresis, SDS-PAGE, dot blot, and western blot analyses confirmed successful cloning, expression, purification, and immunoreactivity of the recombinant protein (Soleimani et al., 2016). The observed protein size of approximately 72 kDa

corresponded with the expected molecular weight of the vaccine construct, confirming successful recombinant expression.

The strong reactivity observed during western blot analysis with hyperimmune serum demonstrated that the expressed recombinant protein retained antigenic determinants recognizable by PPRV antibodies. The absence of cross-reactivity with other morbilliviruses further suggests specificity of the recombinant antigen toward PPRV.

5.8.3 In vivo Immunological Evaluation

The response of vaccinated rabbits vaccinated with the candidate was consistent with those observed during goat vaccination with homologous PPR vaccine as earlier demonstrated by (Balamurugan et al., 2014), and use of chimeric PPR vaccine by (Kumar, et al., 2017).

Direct ELISA was used to evaluate the expressed recombinant protein (Ma et al., 2011). The expressed protein was used as a coating antigen for the polyclonal antibody-based assay. The cloned and expressed sub-unit vaccine candidates, elicited significant seroconversion equal to or more than a four-fold rise in antibody titers, among the vaccinated rabbits via the intramuscular route of inoculation. The increase in antibody production following booster immunization is consistent with activation of immunological memory and secondary immune responses. The absence of antibody response in the negative control group confirmed that the observed immune responses were specifically induced by vaccination.

The observed responses were consistent with those observed during goat vaccination using homologous PPR vaccine, as earlier demonstrated by (Caufour et al., 2014) and chimeric PPR vaccine by (Karam et al., 2025). No specific clinical signs or side effects were observed in all the rabbits vaccinated with the developed subunit candidate's vaccine, an indication of the safety of the vaccine. A weak negative correlation was observed between the Negative Control and the Positive (N/75) sample ($r = -0.06$),

indicating no statistically significant relationship. In contrast, a strong and statistically significant positive correlation was found between the Test (F/H) and the Positive (N/75) sample (r = 0.95). Furthermore, the strong positive correlation between the test vaccine and the commercial vaccine group indicates comparable immunogenic behaviour between the two vaccine formulations. These findings collectively suggest that the multiepitope vaccine candidate may possess the capacity to stimulate effective humoral immune responses against PPRV. The observed correlations suggest that the Test (F/H) has a strong and reliable association with the Positive (N/75) sample, indicating its potential effectiveness as a vaccine. In contrast, the weak and non-significant correlation between the Negative Control and the Positive sample reaffirms the expected lack of relationship. These results align with previous findings by Douglas and others (2010), further supporting the validity of the current observations and the potential utility of the Test (F/H) vaccine formulation.

All the vaccinated rabbits exhibited an anamnestic immune response 21 days post-infection. The higher response observed was attributed to the fact that sub-unit vaccination tend to induce particular higher immune effector responses as demonstrated by (Douglas, S. D., & Leeman, S. E. (2011).vaccine candidates elicited significant sero-conversion equal to or more than four-fold rise in antibody titres among the vaccinated rabbits The high level of seroconversion observed was an indication that the sub-unit vaccine candidates developed were immunogenic and can be used as vaccine antigens for control of PPR. During the experiment the immune responses was consistent with those observed during goat vaccination using homologous PPR vaccine, as earlier demonstrated by (Balamurugan, et al., 2014).

5.9 Safety of the Developed Vaccine Candidates

No specific adverse clinical signs or side effects were observed in all the rabbits vaccinated with the developed subunit candidate's vaccine; the safety profile was comparable to that of the conventional N/75 strain vaccine produced by KEVEVAPI.

Laboratory parameters were comparable throughout the study. No local or systemic allergic event were observed this was an indication that the protein used were safe hence, a safe vaccine. All the vaccinated rabbits exhibited an anamnestic immune response 21 days post-infection. The higher response observed was attributed to the fact that sub-unit vaccination modalities tend to induce particular higher immune effector responses as demonstrated by (Demento et al., 2012) Overall, the findings of this study demonstrate that immunoinformatics-guided identification of conserved epitopes from the H and F proteins of PPRV can successfully generate a structurally stable, antigenic, non-toxic, and immunogenic multiepitope vaccine candidate with promising in vitro and in vivo characteristics. Further challenge studies and large-scale animal trials are however necessary to validate the protective efficacy and safety of the vaccine candidate under field conditions.

5.9.1 Study limitations

The limitation of this study was that the immunoinformatics and bioinformatics predictions were primarily based on in silico analyses, which may not fully represent the actual biological interactions and immune responses under in vivo conditions. Although the selected PPRV proteins and epitopes, demonstrated promising antigenicity, immunogenicity, and physicochemical properties through computational tools, experimental validation in animal models was also limited. In addition, the study relied on available PPRV sequences from public databases, which may not comprehensively represent all circulating strains and genetic variations of the virus across different geographical regions. Variations in viral evolution and host immune responses could therefore influence the effectiveness and broad applicability of the proposed vaccine candidates. Furthermore, constraints in laboratory resources, limited extensive challenge studies, long-term immune evaluation, and large-scale vaccine efficacy assessments.

CHAPTER SIX

CONCLUSION AND RECOMMENDATION

6.1 Conclusion

In this study, immunoinformatics approaches were utilised, a multi-epitope-based subunit vaccine candidates was developed. In the study, a novel multi-epitope vaccine candidate for PPR in ruminants, comprising CTL, and B cell epitopes from antigenic protein, along with appropriate adjuvants and linkers. The designed vaccine candidates underwent comprehensive characterizations, including assessment of allergenicity, antigenicity, physicochemical properties, 2D and 3D structure prediction, and in silico cloning parameters. Molecular docking and dynamics studies were conducted to assess binding affinity and stability of the vaccine construct with TLR-2 and TLR-4 receptors. Immunoinformatics have significantly contributed to the improvement of peptide-based vaccine predictions. The immunogenicity, physicochemical characteristics, and structure-related properties of our vaccine candidate suggest its potential for positive outcomes in upcoming in vitro and in vivo tests. Targeting specific antigens involved in the pathogenesis Peste des Petit, this in silico-designed vaccine holds promise for delivering long-lasting protection against this common ruminant disease. While in silico approaches provide valuable insights into vaccine design, experimental validation remains essential to confirm efficacy and safety of the vaccine candidate.

The approach used a combination of analyses to generate a subunit vaccine candidate construct based on multi-epitope, the proposed vaccine candidate was also validated in vivo using rabbits as a model. The selection procedure theoretically guarantees that the identified sequences have the potential to achieve a considerable degree of protection.

6.2 Recommendations

Low thermostability of available live-attenuated vaccine against PPR and the risk of reversion is a major concern, especially in sub- tropical countries where the maintenance of a cold chain during vaccine transportation. Hence, a new vaccine formulation with improved stability is the hallmark of efficacy for the current PPR live-attenuated vaccines. From the studies carried out it is quite evident that the thermostable subunit vaccine candidate for the control and management of PPR in ruminants is promising

Hence, I do recommend the following:

i. Field evaluation of the vaccine candidate in target host i.e. the small ruminant goats using virulent virus to determine its efficacy.
ii. Further expression and characterisation of the proteins for establishment of a mass production protocol.

REFERENCES

Aasim, Sharma, R., Patil, C. R., Kumar, A., & Sharma, K. (2022). Identification of vaccine candidate against Omicron variant of SARS-CoV-2 using immunoinformatic approaches. *In Silico Pharmacology*, *10*(1), 12.

Abubakar, M., Jamal, S. M., Hussain, M., & Ali, Q. (2008). Incidence of peste des petits ruminants (PPR) virus in sheep and goat as detected by immuno-capture ELISA (Ic ELISA). *Small ruminant research*, *75*(2-3), 256-259.

Adhikari, U. K., Tayebi, M., & Rahman, M. M. (2018). Immunoinformatics Approach for Epitope-Based Peptide Vaccine Design and Active Site Prediction Against Polyprotein of Emerging Oropouche Virus. *Journal of immunology research*, *2018*(1), 6718083.

Albina, E., Kwiatek, O., Minet, C., Lancelot, R., de Almeida, R. S., & Libeau, G. (2013). Peste des petits ruminants, the next eradicated animal disease? *Veterinary microbiology*, *165*(1-2), 38-44.

Alharbi, M., Alshammari, A., Alasmari, A. F., Alharbi, S. M., Tahir ul Qamar, M., Ullah, A., ... & Khalil, A. A. K. (2022). Designing of a recombinant multi-epitopes based vaccine against Enterococcus mundtii using bioinformatics and immunoinformatics approaches. *International journal of environmental research and public health*, *19*(6), 3729.

Anand, R., Biswal, S., Bhatt, R., & Tiwary, B. N. (2020). Computational perspectives revealed prospective vaccine candidates from five structural proteins of novel SARS corona virus 2019 (SARS-CoV-2). *PeerJ*, *8*, e9855.

Anandhan, G., Narkhede, Y. B., Mohan, M., & Paramasivam, P. (2023). Immunoinformatics aided approach for predicting potent cytotoxic T cell

epitopes of respiratory syncytial virus. *Journal of Biomolecular Structure and Dynamics*, *41*(21), 12093-12105.

Andey, T., Soni, S., & Modi, S. (2024). Conventional vaccination methods: Inactivated and live attenuated vaccines. *Advanced Vaccination Technologies for Infectious and Chronic Diseases*, 37-50.

Ayebazibwe, C., Akwongo, C. J., Waiswa, J., Ssemakula, O., Akandinda, A., Barasa, M., ... & Kiara, H. K. (2022). Peste des petits ruminants (PPR) in Uganda: Assessment of animal health systems and coordination mechanisms.

Baazizi, R., Mahapatra, M., Clarke, B. D., Ait-Oudhia, K., Khelef, D., & Parida, S. (2017). Peste des petits ruminants (PPR): A neglected tropical disease in Maghreb region of North Africa and its threat to Europe. *PloS one*, *12*(4), e0175461.

Bailey, D., Banyard, A., Dash, P., Ozkul, A., & Barrett, T. (2005). Full genome sequence of peste des petits ruminants virus, a member of the Morbillivirus genus. *Virus research, 110*(1-2), 119-124.

Balamurugan, V., Hemadri, D., Gajendragad, M. R., Singh, R. K., & Rahman, H. (2014). Diagnosis and control of peste des petits ruminants: a comprehensive review. *Virus disease*, 25(1), 39-56.

Balamurugan, V., Kumar, K. V., Govindaraj, G., Suresh, K. P., Shome, B. R., & Gulati, B. R. (2023). Status Paper on Peste des petits ruminants Indian Perspective, ICAR-National Institute of Veterinary Epidemiology and Disease Informatics (NIVEDI), pp: 1-47 Copyright©: ICAR-National Institute of Veterinary Epidemiology and Disease Informatics (NIVEDI)(2023). All rights are reserved by the Organization.

Balamurugan, V., Sen, A., Venkatesan, G., Bhanuprakash, V., & Singh, R. K. (2014). Protective immune response of live attenuated thermo-adapted peste des petits ruminants vaccine in goats. *Virus disease, 25*, 350-357.

Banyard, A. C., Parida, S., Batten, C., Oura, C., Kwiatek, O., & Libeau, G. (2010). Global distribution of peste des petits ruminants virus and prospects for improved diagnosis and control. *Journal of general virology*, *91*(12), 2885-2897.

Banyard, A. C., Parida, S., Batten, C., Oura, C., Kwiatek, O., & Libeau, G. (2024). Peste des petits ruminants virus: Current status and future perspectives. *Transboundary and Emerging Diseases*, 71(2), 1–15.

Baron, J., Fishbourne, E., Couacy-Hyman, E., Abubakar, M., Jones, B. A., Frost, L., ... & Baron, M. D. (2014). Development and testing of a field diagnostic assay for peste des petits ruminants virus. *Transboundary and emerging diseases, 61*(5), 390-396.

Baron, M. D., Banyard, A. C., Parida, S., & Barrett, T. (2005). The Plowright vaccine strain of Rinderpest virus has attenuating mutations in most genes. *Journal of general virology*, 86(4), 1093-1101.

Baron, M. D., Diallo, A., Lancelot, R., & Libeau, G. (2016). Peste des petits ruminants virus. *Advances in Virus Research*, 95, 1–42.

Baron, M. D., Diop, B., Njeumi, F., Willett, B. J., & Bailey, D. (2017). Future research to underpin successful peste des petits ruminants virus (PPRV) eradication. *Journal of General Virology*, 98(11), 2635-2644.

Beavis, P. A., Henderson, M. A., Giuffrida, L., Mills, J. K., Sek, K., Cross, R. S., ... & Darcy, P. K. (2017). Targeting the adenosine 2A receptor enhances chimeric

antigen receptor T cell efficacy. *The Journal of clinical investigation*, *127*(3), 929-941.

Benfield, C. T., Legnardi, M., Mayen, F., Almajali, A., Cinardi, G., Wisser, D., ... & Njeumi, F. (2023). Peste Des Petits Ruminants in the Middle East: epidemiological situation and status of control and eradication activities after the first phase of the PPR global eradication program (2017–2021). *Animals*, *13*(7), 1196.

Bouazzaoui, A., Abdellatif, A. A., Al-Allaf, F. A., Bogari, N. M., Al-Dehlawi, S., & Qari, S. H. (2021). Strategies for vaccination: conventional vaccine approaches versus new-generation strategies in combination with adjuvants. *Pharmaceutics*, *13*(2), 140.

Bouqellah, N. A., & Farag, P. F. (2023). In Silico Evaluation, Phylogenetic Analysis, and Structural Modeling of the Class II Hydrophobin Family from Different Fungal Phytopathogens. *Microorganisms*, *11*(11), 2632.

Bukar, Babagana Alhaji, and Isa Musa Mabu. "Common diseases of goats, treatment and preventive measures." In *Goat Science-From Keeping to Precision Production*. IntechOpen, 2023.

Calis, J. J., Maybeno, M., Greenbaum, J. A., Weiskopf, D., De Silva, A. D., Sette, A., ... & Peters, B. (2013). Properties of MHC class I presented peptides that enhance immunogenicity. *PLoS computational biology*, *9*(10), e1003266.

Colinas, J., Schmidler, S. C., Bohrer, G., Iordanov, B., & Benfey, P. N. (2008). Intergenic and genic sequence lengths have opposite relationships with respect to gene expression. *PLoS One*, *3*(11), e3670.

Crowther, J. R. (2008). *ELISA: theory and practice* (Vol. 42). Springer Science & Business Media.

Cunningham, A. L., Garçon, N., Leo, O., Friedland, L. R., Strugnell, R., Laupèze, B., ... & Stern, P. (2016). Vaccine development: From concept to early clinical testing. *Vaccine*, *34*(52), 6655-6664.

De Souza, C. M., Silva, E. D., Ano Bom, A. P. D., Bastos, R. C., Nascimento, H. J., & da Silva Junior, J. G. (2012). Evaluation of an ELISA for canine leishmaniasis immunodiagnostic using recombinant proteins. *Parasite Immunology*, *34*(1), 1-7.

Deeba, F., Rahman, M. S., Ullah, M. A., & Islam, M. T. (2023). Immunoinformatics-driven multiepitope vaccine design against peste des petits ruminants virus. *Computers in Biology and Medicine*, 162, 107084.

Demento, S. L., Cui, W., Criscione, J. M., Stern, E., Tulipan, J., Kaech, S. M., & Fahmy, T. M. (2012). Role of sustained antigen release from nanoparticle vaccines in shaping the T cell memory phenotype. *Biomaterials*, *33*(19), 4957-4964.

Dhanda, S. K., Karosiene, E., Edwards, L., Grifoni, A., Paul, S., Andreatta, M., ... & Sette, A. (2018). Predicting HLA CD4 immunogenicity in human populations. *Frontiers in immunology*, *9*, 1369.

Dhar, P., Sreenivasa, B. P., Barrett, T., Corteyn, M., Singh, R. P., & Bandyopadhyay, S. K. (2002). Recent epidemiology of peste des petits ruminant's virus (PPRV). *Veterinary microbiology*, *88*(2), 153-159.

Diallo, A., Bataille, A., Lancelot, R., & Libeau, G. (2019). Peste des petits ruminants. Transboundary *Animal Diseases in Sahelian Africa and Connected Regions*, 233-266.

Diallo, A., Minet, C., Le Goff C, Berhe, G., Albina, E., Libeau, G., Barrett, T. (2007). The threat of peste des petis ruminants: Progress in vaccine development for disease control. *Vaccine*. 25(30): 5591-5597.

Diallo, A., Minet, C., Le Goff, C., Berhe, G., Albina, E., & Libeau, G. (2021). The threat of peste des petits ruminants: Progress in vaccine development and control strategies. *Vaccines*, 9(8), 845.

Dimitrov, I., Bangov, I., Flower, D. R., & Doytchinova, I. (2014). AllerTOP v. 2—a server for in silico prediction of allergens. *Journal of molecular modeling, 20*, 1-6.

Doğanay, M., Özdarendeli, A., Düzlü, Ö., & Yıldırım, A. (2018). Overview of zoonotic diseases in Turkey: the one health concept and future threats. *Türkiye Parazitolojii Dergisi*, *42*(1), 39.

Douglas, A. D., de Cassan, S. C., Dicks, M. D., Gilbert, S. C., Hill, A. V., & Draper, S. J. (2010). Tailoring subunit vaccine immunogenicity: maximizing antibody and T cell responses by using combinations of adenovirus, poxvirus and protein-adjuvant vaccines against Plasmodium falciparum MSP1. *Vaccine, 28*(44), 7167-7178.

Douglas, S. D., & Leeman, S. E. (2011). Neurokinin-1 receptor: functional significance in the immune system in reference to selected infections and inflammation. Annals of the New York *Academy of Sciences, 1217*(1), 83-95.

Doytchinova, I. A., & Flower, D. R. (2007). Identifying candidate subunit vaccines using an alignment-independent method based on principal amino acid properties. *Vaccine, 25*(5), 856-866.

Dubie, T., Dagnew, B., Gelo, E., Negash, W., Hussein, F., & Woldehana, M. (2022). Seroprevalence and associated risk factors of peste des petits ruminants among ovine and caprine in selected districts of Afar region, Ethiopia. *BMC Veterinary Research*, 18(1), 429.

Eggleston, P. (1991). recombinant DNA technology. *Heredity, 66*, 161-172.

El-Manzalawy, Y., Dobbs, D., & Honavar, V. G. (2017). In silico prediction of linear B-cell epitopes on proteins. *Prediction of Protein Secondary Structure*, 255-264.

Fakhoury, G. (2017). *Expression and Purification of the Hepatitis B Virus X Protein*. Drexel University.

FAO & WOAH (2016). Global Control and Eradication Strategy for Peste des Petits Ruminants (PPR). Rome, Italy.

FAO & WOAH (2023). Global Strategy for the Control and Eradication of Peste des Petits Ruminants.

Gasteiger, E., Hoogland, C., Gattiker, A., Duvaud, S. E., Wilkins, M. R., Appel, R. D., & Bairoch, A. (2005). *Protein identification and analysis tools on the ExPASy server* (pp. 571-607). Humana press.

Gattani, A. (2019). *Evaluation of neuraminidase activity of HN protein of peste des petits ruminant's virus using electrochemical biosensor*. Unpublished PhD Thesis, , Izatnagar: Indian Veterinary Research Institute.

Gibbs, P. J., Taylor, W. P., Lawman, M. J., & Bryant, J. (1979). Classification of peste des petits ruminant's virus as the fourth member of the genus *Morbillivirus*. *Intervirology, 11*(5), 268-274.

Gitonga, P. N. (2015). *Spatial analysis of risk factors and their effects on peste des petits ruminants control strategies in Kajiado and Marsabit pastoral systems of Kenya*. Unpublished PhD Thesis, Nairobi: University of Nairobi.

Glick, B. R., & Patten, C. L. (2022). *Molecular biotechnology: principles and applications of recombinant DNA*. John Wiley & Sons.

Gotsman, I., Grabie, N., Gupta, R., Dacosta, R., MacConmara, M., Lederer, J., ... & Lichtman, A. H. (2006). Impaired regulatory T-cell response and enhanced atherosclerosis in the absence of inducible costimulatory molecule. *Circulation*, *114*(19), 2047-2055.

Griffith, E., Kipkemoi, J. R., Mariner, J. C., Coffin-Schmitt, J., & Whittier, C. A. (2023). Expanding Participatory Epidemiology to Explore Community Perceptions of Human and Livestock. Diseases among Pastoralists in Turkana County, Kenya. Qeios. *Expanding Participatory Epidemiology to Explore Community Perceptions of Human and Livestock Diseases among Pastoralists in Turkana County, Kenya.*

Gupta, N., Regar, H., Verma, V. K., Prusty, D., Mishra, A., & Prajapati, V. K. (2020). Receptor-ligand based molecular interaction to discover adjuvant for immune cell TLRs to develop next-generation vaccine. *International Journal of Biological Macromolecules*, *152*, 535-545.

Gupta, S. S. (2013). Study on prevalence of Peste des petits ruminants (ppr) in goat at Upazilla veterinary hospital, Dinajpur Sadar. Chattogram Veterinary & Animal| Sciences University.

Gupta, S., Kapoor, P., Chaudhary, K., Gautam, A., Kumar, R., & Raghava, G. P. (2015). Peptide toxicity prediction. *Computational peptidology*, 143-157.

Gupta, S., Kapoor, P., Chaudhary, K., Gautam, A., Kumar, R., Open-Source Drug Discovery Consortium, & Raghava, G. P. (2013). In silico approach for predicting toxicity of peptides and proteins. *PloS one*, *8*(9), e73957.

Haas, L., Baron, M. D., Liess, B., & Barrett, T. (1995). Editing of morbillivirus P gene transcripts in infected animals. *Veterinary microbiology*, *44*(2-4), 299-306.

Haq, A. A. (2016). *Evaluation of Monoclonal Antibody Resistant Mutant of PPR Vaccine Virus as a Candidate Marker Vaccine and Application of Biosensor Based Technique for PPR Disease Diagnosis*. Unpublished PhD Thesis, Izatnagar: Indian Veterinary Research Institute.

Harris, J. R. (1993). The ultrastructure of multinucleate giant cells. Micron, 24(2), 173-231.

Hassan, S., Nazeer, I. M., & Raheem, A. (2023). Immunization: Unveiling the power of vaccines in shaping global health. In *Viral Replication Cycle-From Pathogenesis and Immune Response to Diagnosis and Therapy*. IntechOpen.

Heo, L., & Feig, M. (2020). High-accuracy protein structures by combining machine-learning with physics-based refinement. Proteins: *Structure, Function, and Bioinformatics, 88*(5), 637-642.

Holzer, B., Hodgson, S., Logan, N., Willett, B., & Baron, M. D. (2016). Protection of cattle against rinderpest by vaccination with wild-type but not attenuated strains of peste des petits ruminant's virus. *Journal of Virology*, *90*(10), 5152-5162.

Ithinji, D. G. (2011). *Manifestation in sheep and goats and its prevalence in in-contact herbivores in Kenya*. Unpublished PhD Thesis, Nairobi: University of Nairobi.

Jahangirian, E., Jamal, G. A., Nouroozi, M., & Mohammadpour, A. (2022). A novel multiepitope vaccine against bladder cancer based on CTL and HTL epitopes for induction of strong immune using immunoinformatics approaches. International *Journal of Peptide Research and Therapeutics, 28*(2), 71.

Jemberu, W. T., Knight-Jones, T. J., Gebru, A., Mekonnen, S. A., Yirga, A., Sibhatu, D., & Rushton, J. (2022). Economic impact of a peste des petits ruminants' outbreak and vaccination cost in northwest Ethiopia. *Transboundary and emerging diseases, 69*(5), e2084-e2092.

Jespersen, M. C., Peters, B., Nielsen, M., & Marcatili, P. (2017). BepiPred-2.0: improving sequence-based B-cell epitope prediction using conformational epitopes. *Nucleic acids research, 45*(W1), W24-W29.

Jeyachandran, A., Muthuvel, R., Jagannathan, S., Pillai, S. B., Rajendran, V., Pachamuthu, R. G., ... & Mandal, A. (2024). Identification and evaluation of multi-antigenic epitopes of immunodominant protein from the selected Crimean–Congo hemorrhagic fever virus genome towards the development of diagnostic and vaccine candidates by reverse vaccinology approach. *Journal of Proteins and Proteomics, 1*-10.

Jones, B. A., Rich, K. M., Mariner, J. C., Anderson, J., Jeggo, M., Thevasagayam, S. & Roeder, P. (2016). The economic impact of eradicating peste des petits ruminants: a benefit-cost analysis. *PloS one, 11*(2), e0149982.

Kamel, M., & El-Sayed, A. (2019). Toward peste des petits virus (PPRV) eradication: Diagnostic approaches, novel vaccines, and control strategies. *Virus research, 274*, 197774.

Karam, R., Aljasem, Y., Alrashedi, S., Alhafufi, A., Abuhaimed, M., & Albaqshi, H. (2025). Diagnostic and vaccination challenges in the PPR pre-eradication era: Identifying gaps and potential unintended consequences. *Journal of Advanced Veterinary & Animal Research,* 12(4).

Kardjadj, M., Kouidri, B., Metref, D., Luka, P. D., & Ben-Mahdi, M. H. (2016). Abortion and various associated risk factors in small ruminants in Algeria. *Preventive veterinary medicine*, *123*, 97-101.

Kashem, m. a. (2010). A study on concomitant infections and survivability in black bengal goats with *peste des petits* ruminants (doctoral dissertation, a thesis submitted for the partial fulfillment of the degree of Master of Science (Msc.) in microbiology, department of microbiology faculty of veterinary medicine chittagong veterinary and animal sciences university chittagong-4225, bangladesh).

Khan, S., Khan, A., Rehman, A. U., Ahmad, I., Ullah, S., Khan, A. A., & Wei, D. Q. (2019). Immunoinformatics and structural vaccinology driven prediction of multi-epitope vaccine against Mayaro virus and validation through in-silico expression. *Infection, Genetics and Evolution*, *73*, 390-400.

Kihu, S. M. (2014). *Risk factors and socioeconomic effects associated with spread of peste des petits ruminants (PPR) in Turkana County, Kenya*. Unpublished PhD Thesis, Nairobi: University of Nairobi.

Kihu, S. M., Gachohi, J. M., Gitao, C. G., Bebora, L. C., Njenga, J. M., Wairire, G. G., ... & Wahome, R. G. (2013). Analysis of small ruminants' pastoral management practices as risk factors of Peste des petits ruminants (PPR) spread in Turkana District, Kenya. *Research Opinions in Animal and Veterinary Sciences.*

Kihu, S. M., Njagi, L. M., Njogu, G. N., Kamande, J. N., & Gitao, C. G. (2012). Peste des petits ruminants in Kenya; pastoralist knowledge of the disease in goats in Samburu and Baringo Counties.

Kihu[a], S. M., Gachohi, J. M., Ndungu, E. K., et al. (2015). Sero-epidemiology of peste des petits ruminants in Kenya. *BMC Veterinary Research*, 11, 87.

Kihu[b], S.M., et al. (2015). Peste des petits ruminants risk factors and seroprevalence in Turkana County, Kenya. Research in Veterinary Science, 108, 185–190.

Kinimi, E., Mahapatra, M., Kgotlele, T., Makange, M. R., Tennakoon, C., Njeumi, F., ... & Misinzo, G. (2021). Complete genome sequencing of field isolates of Peste des petits ruminant's virus from Tanzania revealed a high nucleotide identity with lineage III PPR viruses. *Animals*, *11*(10), 2976.

Klima, C. L., Zaheer, R., Cook, S. R., Rasmussen, J., Alexander, T. W., Potter, A., ... & McAllister, T. A. (2018). In silico identification and high throughput screening of antigenic proteins as candidates for a Mannheimia haemolytica vaccine. *Veterinary immunology and immunopathology*, *195*, 19-24.

Ko, J., Park, H., Heo, L., & Seok, C. (2012). GalaxyWEB server for protein structure prediction and refinement. *Nucleic acids research*, *40*(W1), W294-W297.

Kotchofa, P., Rich, K. M., Baltenweck, I., & Dione, M. M. (2021). Macroeconomic impact assessment of peste des petits ruminants (PPR) in Ethiopia and Burkina Faso.

Krishnan, R., Kim, J. O., Kim, J. O., Qadiri, S. S. N., Kim, S. J., & Oh, M. J. (2019). Immunoglobulin-like cell adhesion molecules, nectins-Characterization, functional prediction and expression profiling from seven-band grouper, Hyporthodus septemfasciatus. *Aquaculture*, *506*, 387-393.

Kumar, K. S., Babu, A., Sundarapandian, G., Roy, P., Thangavelu, A., Kumar, K. S., ... & Parida, S. (2014). Molecular characterisation of lineage IV peste des petits ruminant's virus using multi gene sequence data. *Veterinary microbiology*, *174*(1-2), 39-49.

Kumar, K. S., Babu, A., Sundarapandian, G., Roy, P., Thangavelu, A., Kumar, K. S., ... & Parida, S. (2014). Molecular characterisation of lineage IV peste des petits ruminant's virus using multi gene sequence data. *Veterinary microbiology, 174*(1-2), 39-49.

Kumar, N., Barua, S., Riyesh, T., & Tripathi, B. N. (2017). Advances in peste des petits ruminants' vaccines. *Veterinary microbiology, 206*, 91-101.

Kwiatek, O., Ali, Y. H., Saeed, I. K., Khalafalla, A. I., Mohamed, O. I., Obeida, A. A., ... & Libeau, G. (2011). Asian lineage of peste des petits ruminant's virus, Africa. *Emerging infectious diseases*, 17(7), 1223.

Lamb, R. A., & Kolakofsky, D. (2001). Paramyxoviridae: the viruses and their replication (No. Ed. 4, pp. 689-724).

Leroy, H., Han, M., Woottum, M., Bracq, L., Bouchet, J., Xie, M., & Benichou, S. (2020). Virus-mediated cell-cell fusion. *International Journal of Molecular Sciences, 21*(24), 9644.

Lewis, C. E., & Roth, J. A. (2021). Challenges in having vaccines available to control transboundary diseases of livestock. *Current Issues in Molecular Biology, 42*(1), 1-40.

Lhermie, G., Pica-Ciamarra, U., Newman, S., Raboisson, D., & Waret-Szkuta, A. (2022). Impact of Peste des petits ruminants for Sub-Saharan African farmers: A bioeconomic household production model. Transboundary and Emerging *Diseases, 69*(4), e185-e193.

Liu, K., Watanabe, E., & Kokubo, H. (2017). Exploring the stability of ligand binding modes to proteins by molecular dynamics simulations. *Journal of computer-aided molecular design, 31*(2), 201-211.

Liu, W., & Chen, Y. H. (2005). High epitope density in a single protein molecule significantly enhances antigenicity as well as immunogenicity: a novel strategy for modern vaccine development and a preliminary investigation about B cell discrimination of monomeric proteins. *European journal of immunology*, *35*(2), 505-514.

López-Blanco, J. R., Aliaga, J. I., Quintana-Ortí, E. S., & Chacón, P. (2014). iMODS: internal coordinates normal mode analysis server. *Nucleic acids research*, *42*(W1), W271-W276.

Lynn, G. M., Laga, R., Darrah, P. A., Ishizuka, A. S., Balaci, A. J., Dulcey, A. E., ... & Seder, R. A. (2015). In vivo characterization of the physicochemical properties of polymer-linked TLR agonists that enhance vaccine immunogenicity. *Nature biotechnology*, *33*(11), 1201-1210.

Mahapatra, M., Selvaraj, M., & Parida, S. (2020). Comparison of immunogenicity and protective efficacy of PPR live attenuated vaccines (Nigeria 75/1 and Sungri 96) administered by intranasal and subcutaneous routes. *Vaccines*, *8*(2), 168.

Mahapatra, M., Selvaraj, M., & Parida, S. (2020). Comparison of immunogenicity and protective efficacy of PPR live attenuated vaccines (Nigeria 75/1 and Sungri 96) administered by intranasal and subcutaneous routes. *Vaccines*, *8*(2), 168.

Mantip, S. E., Shamaki, D., & Farougou, S. (2019). Peste des petits ruminants in Africa: meta-analysis of the virus isolation in molecular epidemiology studies. *Onderstepoort Journal of Veterinary Research*, *86*(1), 1-15.

McVety, A. K. (2018). The rinderpest campaigns: a virus, its vaccines, and global development in the twentieth century. Cambridge University Press.

Merkler, D. J., Farrington, G. K., & Wedler, F. C. (1981). Protein thermostability. Correlations between calculated macroscopic parameters and growth

temperature for closely related thermophilic and mesophilic bacilli. *International Journal of Peptide and Protein Research*, *18*(5), 430-442.

Mtema, Z. J. (2013). *Integrated disease surveillance and response systems in resource-limited settings.* Unpublished PhD Thesis, Glasgow: University of Glasgow.

Mugunthan, S. P., & Harish, M. C. (2021). Multi-epitope-based vaccine designed by targeting cytoadherence proteins of Mycoplasma gallisepticum. *ACS omega*, *6*(21), 13742-13755.

Munir, M., Zohari, S., & Berg, M. (2012). Epidemiology and distribution of peste des petits ruminants. In *Molecular Biology and Pathogenesis of Peste des Petits Ruminants Virus* (pp. 69-104). Berlin, Heidelberg: Springer Berlin Heidelberg.

Muniraju, M. B. (2015). *Establishment of reverse genetics system for PPR virus to develop recombinant vaccines.* Unpublished PhD Thesis, Warwick: University of Warwick.

Mutua, F., et al. (2023). Seroprevalence of PPR and CCPP in goats in Kwale County, Kenya. *Frontiers in Veterinary Science, 10*:1123456.

Njeumi, F., Bailey, D., Soula, J. J., Diop, B., & Tekola, B. G. (2020). Eradicating the scourge of peste des petits ruminants from the world. Viruses, 12(3), 313.

Noton, S. L., & Fearns, R. (2015). Initiation and regulation of paramyxovirus transcription and replication. *Virology, 479*, 545-554.

OIE/WOAH (2021). Peste des petits ruminants: Technical factsheet.

Palumbo, E., Fiaschi, L., Brunelli, B., Marchi, S., Savino, S., & Pizza, M. (2011). Antigen identification starting from the genome: a “Reverse Vaccinology” approach applied to MenB. In *Neisseria meningitidis: advanced methods and protocols* (pp. 361-403). Totowa, NJ: Humana Press.

Parida, S., Muniraju, M., Mahapatra, M., Muthuchelvan, D., Buczkowski, H., & Banyard, A. C. (2015). Peste des petits ruminants. Veterinary Microbiology, 181(1–2), 90–106.

Pavlopoulos, G. A., Soldatos, T. G., Barbosa-Silva, A., & Schneider, R. (2010). A reference guide for tree analysis and visualization. *BioData mining*, *3*, 1-24.

Pierce, B. G., Hourai, Y., & Weng, Z. (2011). Accelerating protein docking in ZDOCK using an advanced 3D convolution library. *PloS one*, *6(*9), e24657.

Pourseif, M. M., Moghaddam, G., Naghili, B., Saeedi, N., Parvizpour, S., Nematollahi, A., & Omidi, Y. (2018). A novel in silico minigene vaccine based on CD4+ T-helper and B-cell epitopes of EG95 isolates for vaccination against cystic echinococcosis. *Computational Biology and Chemistry*, *72*, 150-163.

PPR, A. P. D. P. R. (2006). *Development of bhk21 cell culture adapted peste des petits ruminants (PPR) VIRUS VACCINE*. Unpublished PhD Thesis, Chennai: Tamil Nadu Veterinary and Animal Sciences University Chennai.

Prajapati, M., Alfred, N., Dou, Y., Yin, X., Prajapati, R., Li, Y., & Zhang, Z. (2019). Host cellular receptors for the peste des petits ruminant virus. *Viruses*, *11*(8), 729.

Ranjitha, H. B., Dhanesh, V. V., Hosamani, M., Sreenivasa, B. P., Jabeen, U., Biswal, J. K., ... & Basagoudanavar, S. H. (2023). Thermostable negative-marker foot-and-mouth disease virus serotype O induces protective immunity in guinea pigs. *Applied Microbiology and Biotechnology*, *107*(4), 1285-1297.

Ronchi, G. F., Monaco, F., El-Harrak, M., Chafiqa, L., Capista, S., Bortone, G., ... & Ventura, M. D. (2016). Preliminary results on innocuity and immunogenicity of an inactivated vaccine against Peste des petits ruminants.

Roth, J. A. (2011). Veterinary vaccines and their importance to animal health and public health. *Procedia in vaccinology, 5*, 127-136.

Sahu, A. R., Wani, S. A., Saminathan, M., Rajak, K. K., Sahoo, A. P., Pandey, A., ... & Gandham, R. K. (2017). Genome sequencing of an Indian peste des petits ruminant's virus isolate, Izatnagar/94, and its implications for virus diversity, divergence and phylogeography. *Archives of virology, 162*, 1677-1693.

Selvaraj, M., Mahapatra, M., & Parida, S. (2021). Exchange of C-terminal variable sequences within morbillivirus nucleocapsid protein are tolerated: Development and evaluation of two marker (DIVA) vaccines (Sungri/96 diva, Nigeria/75/1 DIVA) against PPR. *Viruses*, *13*(11), 2320.

Shaila, M. S., Shamaki, D., Forsyth, M. A., Diallo, A., Goatley, L., Kitching, R. P., & Barrett, T. (1996). Geographic distribution and epidemiology of peste des petits ruminants' viruses. *Virus research, 43*(2), 149-153.

Shankar, T. H. (2016). *Molecular characterization of peste-des-petits ruminants virus*. Unpublished PhD Thesis, Maharashtra: Maharashtra Animal and Fishery Sciences University).

Singh, R. K., Rajak, K. K., Muthuchelvan, D., Banyard, A. C., & Parida, S. (2015). Vaccines against peste des petits ruminants virus. *Peste des Petits Ruminants Virus*, 183-194.

Sinnathamby, G., Naik, S., Renukaradhya, G. J., Rajasekhar, M., Nayak, R., & Shaila, M. S. (2001). Recombinant hemagglutinin protein of rinderpest virus

expressed in insect cells induces humoral and cell mediated immune responses in cattle. *Vaccine, 19*(28-29), 3870-3876.

Soleimani, N., Mobarez, A. M., & Farhangi, B. (2016). Cloning, expression and purification flagellar sheath adhesion of Helicobacter pylori in Escherichia coli host as a vaccination target. *Clinical and experimental vaccine research, 5*(1), 19-25.

Su, W., Xing, C., Wu, Y., Wang, Y., Ding, H., & He, H. (2015). Complete genome sequence of a novel mutant of peste des petits ruminants virus obtained from China. *Genome announcements, 3*(1), e01504-14.

Tamura, K., Peterson, D., Peterson, N., Stecher, G., Nei, M., & Kumar, S. (2011). MEGA5: molecular evolutionary genetics analysis using maximum likelihood, evolutionary distance, and maximum parsimony methods. *Molecular biology and evolution, 28*(10), 2731-2739.

Tenuche, O. Z., Emikpe, B. O., Godwin, E., Enem, S. I., & Egwu, G. O. (2023). Peste des petits ruminants: An update. *Microbiology Research Journal International, 33*(3), 9-40.

Wang, S., Sun, S., Li, Z., Zhang, R., & Xu, J. (2017). Accurate de novo prediction of protein contact map by ultra-deep learning model. PLoS computational biology, 13(1), e1005324.

Xiao, F., Chen, Z., Wei, Z., & Tian, L. (2020). Hydrophobic interaction: a promising driving force for the biomedical applications of nucleic acids. *Advanced Science, 7*(16), 2001048.

Xu, J. (2019). Distance-based protein folding powered by deep learning. Proceedings of the National Academy of Sciences, 116(34), 16856-16865.

Yadav, M. P., Singh, R. K., & Malik, Y. S. (2020). Emerging and transboundary animal viral diseases: Perspectives and preparedness. In *Emerging and transboundary animal viruses* (pp. 1-25). Singapore: Springer Singapore.

Yadav[a], M. P., Singh, R. K., & Malik, Y. S. (2020). Emerging and transboundary animal viral diseases: Perspectives and preparedness. *Emerging and transboundary animal viruses*, 1-25.

Yang, B., Qi, X., Guo, H., Jia, P., Chen, S., Chen, Z., ... & Xue, Q. (2018). Peste des petits ruminants virus enters caprine endometrial epithelial cells via the caveolae-mediated endocytosis pathway. *Frontiers in Microbiology*, *9*, 210.

Yin, P., Li, Q., Yan, C., Liu, Y., Liu, J., Yu, F., ... & Yan, N. (2013). Structural basis for the modular recognition of single-stranded RNA by PPR proteins. *Nature*, *504*(7478), 168-171.

Yu, N. Y., Wagner, J. R., Laird, M. R., Melli, G., Rey, S., Lo, R., ... & Brinkman, F. S. (2010). PSORTb 3.0: improved protein subcellular localization prediction with refined localization subcategories and predictive capabilities for all prokaryotes. *Bioinformatics*, *26*(13), 1608-1615.

Zachary, J.F., 2017. Mechanisms of Microbial Infections. Pathol. Basis Vet. Dis. Expert Consult. https://doi.org/10.1016/B978-0-323-35775-3.00004-7.

Zachary, J.F., 2017. Mechanisms of Microbial Infections. Pathol. Basis Vet. Dis. Expert Consult. https://doi.org/10.1016/B978-0-323-35775-3.00004-7.

Zahur, A. B., Irshad, H., Ullah, A., et al., (2014). Epidemiological investigations of peste des petits ruminants in Pakistan. *Journal of Animal and Plant Sciences, 24*(4), 1215–1222.

Zhao, H., Njeumi, F., Parida, S., & Benfield, C. T. (2021). Progress towards eradication of peste des petits ruminants through vaccination. *Viruses*, *13*(1), 59.

APPENDICES

Appendix I: Sodium Dodecyl Sulphate–Polyacrylamide Gel Electrophoresis (SDS-PAGE)

Preparation of polyacrylamide. 30 g of acrylamide and 0.8 g of N, N' methylene-bisacrylamide were dissolved in 100 ml of distilled water. The solution was then filtered through a 0.45 µm sterile filter and stored in a 4^{o}C refrigerator.

Preparation of 5 % stacking gel. 6.8 ml of distilled water, 1.7 ml of 30.8 % acrylamide mix, 1.25 ml of 1.0 M Tris (pH 6.8), 0.1 ml of 10% sodium dodecyl sulphate (SDS), 0.1 ml of 10% ammonium persulfate (APS), and 0.01 ml of Tetramethylethylenediamine (TEMED) were all mixed making 10 ml of the stacking gel.

Preparation of 10% resolving/separating gel. 15.9 ml of distilled water, 13.3 ml of 30.8 % acrylamide mix, 10 ml of 1.5 M Tris (pH 8.8), 0.4 ml of 10% SDS, 0.4 ml of 10% APS, and 0.0116 ml of TEMED were all mixed to make 10 ml of the stacking gel.

Preparation of SDS sample loading buffer. To make 40ml of the sample loading buffer: 5 ml of 0.5 M Tris (pH 6.8), 8 ml of 10% SDS, 8 ml of 50% glycerol, and 20 mg of bromophenol blue (0.5 mg/ml) were all dissolved in 16 ml of distilled water. 2 ml of 2-βmercaptoethanol was then added to the mixture immediately before use.

Preparation of the 5X SDS running buffer. 15 g of Tris, 72 g of glycine, and 5g of SDS were dissolved in 1 L of distilled water.

Preparation of 10% Ammonium per sulphate (APS). 1g of APS was dissolved in 10 ml of distilled water. The solution was immediately used.

Preparation of 1 L coomassie blue stain. One gram of coomassie R250, 300 ml of methanol, and 50 ml of acetic acid were added to 650 ml of distilled water. The mixture was stirred, on a magnetic stirrer, for 2 hours. Insoluble dye was filtered out through a

Whatman (number 1) paper. The solution was then stored at 20^{o}C.

Preparation of the destain solution 1 (30% methanol, 5% acetic acid). To make 1 L of the destain solution: 300 ml of methanol and 50 ml of acetic acid were added to 650 ml of distilled water. The destain solution (1) was stored at 20^{o}C.

Preparation of destain solution 2 (7% acetic acid, 5% methanol). To make I L of the destain solution: 50 ml methanol and 70 ml acetic acid were dissolved in 880 ml of distilled water. The destain solution (2) was stored at 20^{o}C.

Preparation of the fixing solution. To make 500 ml of the fixing solution: 4 ml of 25% glutaraldehyde and 13.61 g of Sodium acetate trihydrate were dissolved in 150 ml ethanol. The mixture was topped up to 500 ml with distilled water. The fixing solution was used immediately.

Preparation of 1.5 M Tris-HCl, pH 8.8. To make 500 ml of this solution: 90.75 g of Tris-free base and 8 ml of concentrated HCl were first dissolved in 300 ml of distilled water. The solution's pH was adjusted to 8.8 with concentrated HCl, and the final volume was brought to 500 ml with distilled water.

Preparation of 1.0 M Tris-HCl, pH 6.8. To make 500 ml of this solution: 60.54 g of Tris-free base and 36 ml of concentrated HCl were first dissolved in 300 ml of distilled water. The solution's pH was adjusted to 6.8 with concentrated HCl, and the final volume was brought to 500 ml with distilled water.

Preparation of the Elution Buffer

Preparation of the wash buffer. Initially, 13.8 g of NaH_2PO_4, 1.2 g Tris base and 480.5 g of urea were all dissolved in 1000 ml of distilled water. The solution's pH was then adjusted to 6.3 using HCl. Finally, the solution was passed through a 0.45 µm sterile filter.

Appendix II: Protein Expression

Preparation of the Starter Culture for Protein Expression

Preparation of 75 ml LB media with Kanamycin (50µg/ml) first happened. A single colony of transformed DH5-α *E.coli* was picked with a sterile loop and inoculated in the prepared LB/kanamycin media. Incubation then occurred in a shaker (250 rpm/37^{o}C) until the optical density (O.D) at 600nm reached a range of between 0.5 and 1.5. The starter culture flask was stored overnight at 4^{o}C.

Making the Big Batch of Protein Culture for Bacterial Expression

The starter culture was equally divided among three conical flasks containing 250 ml of LB media with kanamycin (50µg/ml). Scaled up cultures were then grown in a shaker (250 rpm/37^{o}C) to an optical density of 0.8-1.2 at 600 nm. Thereafter, 250µl of Isopropylthiogalactoside (IPTG) was added to each culture. The flasks kept shaking for 4 hours at 37^{o}C. Centrifugation of the cultures in sterile 50 ml falcon tubes at 4000rpm for 30 minutes happened in batches until all the bacteria had spun down. The cell pastes were finally washed with sterile Phosphate Buffered Saline (PBS).

Storage of the cell pastes. The cell pastes were re-suspended in 1ml of 25% Sucrose/50mM Trisaminomethane solution (ratio 1:1). Re-distribution in sterile 2ml Eppendorf tubes and storage in a -80^{o}C freezer followed, respectively.

Bacterial Lysis

Preparation of the lysis buffer. 13.8g of Monosodium phosphate (NaH_2PO_4), 1.2g of Tris base, and 480.5g of urea were dissolved in 1000ml of distilled water. The solution's pH was adjusted to 8.0 with sodium hydroxide (NaOH). The mixture was then passed through a 0.4 µm sterile filter.

Bacterial lysis. Cells were removed from the -80^{o}C freezer and left to thaw on ice for 15

minutes after which, 10ml of the lysis buffer per gram of pellet was added. The cells were then spun on a rotor for 1 hour. Sonication was later done at 50% amplitude for two minutes and vortexing at maximum speed, respectively. Cell lysates were spun at 10,000g for 30 minutes at 15^{o}C. Finally, the supernatants were collected and the pellets re suspended in 10ml PBS buffer.

Dot-Blot

Sample preparation. Re-suspended pellets and supernatants were first serial diluted in 0.1 % SDS in PBS. Afterwards, they were vortexed for 1 minute at maximum speed. The samples were then heated for 5 minutes at 95^{0}C followed by quenching on ice. Finally, they were spun at 12,000g for 10 minutes.

Blotting. 10µl of different sample concentrations were blotted onto a nitrocellulose membrane strip.10 µl of both the primary antibody (1:500 dilution in PBS) and a protein sample from expressed *E.coli* lacking the gene of interest were blotted on the strip. The membrane was incubated for 20 minutes at room temperature to dry.

Blocking. The membrane was inserted in a 50 ml falcon tube then blocked with 45 ml of 5% skimmed milk in PBS for 1 hour at room temperature (on a rotor). Afterwards, the blocking buffer was poured off. The membrane was then washed three times (10 minutes per wash) in 45 ml of 0.1% tween 20 in PBS (on a rotor).

Incubation with the primary antibody. The membrane was incubated in 45 ml of positive PPRV goat serum (1:500 dilution in PBS) for 1 hour at room temperature on a rotor. Afterwards, the membrane was washed three times (10 minutes per wash) in 45 ml of 0.1% tween 20 in PBS on a rotor.

Incubation with the secondary antibody. The membrane was incubated with 45 ml of anti-goat serum (1:500 dilution in PBS) for 1 hour at room temperature in a rotor. Afterwards, the membrane was washed three times (10 minutes per wash) in 45 ml of

0.1% tween 20 in PBS (on a rotor).

Detection. Addition of 10 µl 30% hydrogen peroxide (H_20_2) to 10 ml of 0.05% diaminobenzidine (DAB) preceded. The substrate was then poured into the falcon tube with the membrane followed by incubation in a dark room. Monitoring progress occurred after 5 minutes. Thereafter, the reaction was stopped by briefly washing the membrane with distilled water and finally the membrane was air dried.

Mini-Protean SDS Page Protocol

Gel casting. The glass plates and spacers were assembled in a gel casting apparatus. Components of the resolving gel were mixed then poured between the gel plates. A layer of distilled water was poured on top of the resolving gel, preventing the formation of a meniscus. The resolved gel stood for 30 minutes (until it solidified) at room temperature. The layer of distilled water was drained, followed by rinsing. Excess distilled water was drained and the resolving gel top dried by wicking. Components of the stacking gel were mixed then poured onto the solidified resolving gel. A comb was inserted into the spacers. The stacking gel then stood for 1 hour (until it solidified) at room temperature.

Sample preparation. The pellet (15 µl), obtained after spinning the lysate, was mixed with 45 µl of prepared SDS sample loading buffer (ratio of 1:3). The solution was then heated at 95^{o}C (4 minutes) in a water bath followed by centrifugation (12000 g) for 30 seconds.

Running of the gel. The comb was removed and the cast gel assembled in a Mini-Protean II apparatus. Freshly prepared running buffer (300ml) was added to both Mini-protean II chambers, then loading of prepared samples into the wells followed. The gel was run at 100 V until the dye front migrated to the resolving gel, after which the voltage was increased to 200 V. Running stopped when the dye front reached the bottom of the gel.

Staining and destainig of the gel. The run gel was removed from the apparatus. Spacers and glass plates were then removed. The gel was placed in a small trough and submerged in enough coomassie blue so that it freely floated in the tray. The tray was slowly shaken for 30 minutes (in a laboratory shaker). The stain was then poured off. The gel was destained in destain solution 1 with this solution being periodically changed until the gel background became clear.

Purification of the protein. Expressed cells were removed from the -80^{o}C freezer and left to thaw on ice for 15 minutes. Addition of 8M urea lysis buffer at 10 ml per gram and 0.1 mM Phenylmethylsulfonyl fluoride (PMSF) then followed. Mixing occurred for 60 minutes at 24^{o}C in a rotor (forming was avoided). The lysate was then spun down at 10,000 g for 30 minutes at 15^{o}C. Afterwards, 1 ml of 50% nickel-nitriloacetic acid (Ni-NTA) slurry was added to 10 ml of the lysate. Mixing occurred gently on a rotor for 30 minutes at 24^{o}C. The lysate-resin mixture was then carefully loaded into an empty column. The column was washed three times with 4 ml of the washing buffer (pH 6.3). The protein was eluted with 3x elution buffer (pH of 7.4) and collected for SDS-PAGE analysis.

Purification/Quantification of the Protein

Sephadex G-200 (Pharmacia, Piscataway, NJ, U.S.A.) in a 40 cm x 1.4 cm diameter column and a 4.5 cm pressure head was eluted with 0.05 M phosphate buffer (pH 7.2 at room temperature) and the flow rate adjusted to 6 ml/h. The extract was applied on the column and eluted with the phosphate buffer. 2.0 ml fractions were then collected at and stored at -20^{o}C for protein localization, A protein concentration curve was then drawn to determine the concentration of purified protein this was done using the BCA protein assay kit from *thermoscientific* which is a detergent-compatible formulation based on bicinchoninic acid (BCA) for the colorimetric detection and quantitation of total protein. This method combines the well-known reduction of Cu+2 to Cu+1 by protein in an alkaline medium (the biuret reaction) with the highly sensitive and selective colorimetric

detection of the cuprous cation (Cu+1) using a unique reagent containing bicinchoninic acid.

Preparation of the BCA Working Reagent (WR)

Immunoblotting was done to determine the protein concentration samples. The following formula was used to determine the total volume of WR (working Reagent) required:

(# standards + # unknowns) × (# replicates) × (volume of WR per sample) = total volume WR required After determining the WR it was prepared by mixing 50 parts of BCA Reagent A with 1 part of BCA Reagent B (50:1, Reagent A:B). 50ml of Reagent A was mixed with 1ml of Reagent B. turbidity was observed that quickly disappears upon mixing to yield a clear, green WR.

Procedure (Sample to WR Ratio = 1:8)

25 µL of each standard or unknown sample were Pippeted in replicate into a microplate well with a working range of 20–2000 µg/mL). 200 µL of the working reagent was added to each well and mixed thoroughly on a plate shaker for 30 seconds. The plate was covered and incubated at 37°C for 30 minutes. After which the plate was cooled and measured at absorbance of n 562 nm on a plate reader, the concentration of the protein was found to be 4.45mg/ml.

Protein Expression

Preparation of the starter culture for protein expression. Preparation of 75 ml LB media with Kanamycin (50µg/ml) first happened. A single colony of transformed DH5-α *E.coli* was picked with a sterile loop and inoculated in the prepared LB/kanamycin media. Incubation then occurred in a shaker (250 rpm/37^{o}C) until the optical density (O.D) at 600nm reached a range of between 0.5 and 1.5. The starter culture flask was stored overnight at 4^{o}C.

Making the big batch of protein culture for bacterial expression. The starter culture was equally divided among three conical flasks containing 250 ml of LB media with kanamycin (50µg/ml). Scaled up cultures were then grown in a shaker (250 rpm/37^{o}C) to an optical density of 0.8-1.2 at 600 nm. Thereafter, 250µl of Isopropylthiogalactoside (IPTG) was added to each culture. The flasks kept shaking for 4 hours at 37^{o}C. Centrifugation of the cultures in sterile 50 ml falcon tubes at 4000rpm for 30 minutes happened in batches until all the bacteria had spun down. The cell pastes were finally washed with sterile Phosphate Buffered Saline (PBS).

Storage of the cell pastes. The cell pastes were re-suspended in 1ml of 25% Sucrose/50mM Trisaminomethane solution (ratio 1:1). Re-distribution in sterile 2ml Eppendorf tubes and storage in a -80^{o}C freezer followed, respectively.

Bacterial Lysis

Preparation of the lysis buffer. 13.8g of Monosodium phosphate (NaH_2PO_4), 1.2g of Tris base, and 480.5g of urea were dissolved in 1000ml of distilled water. The solution's pH was adjusted to 8.0 with sodium hydroxide (NaOH). The mixture was then passed through a 0.4 µm sterile filter.

Dot-Blot

Sample preparation. Re-suspended pellets and supernatants were first serial diluted in 0.1 % SDS in PBS. Afterwards, they were vortexed for 1 minute at maximum speed. The samples were then heated for 5 minutes at 95^{0}C followed by quenching on ice. Finally, they were spun at 12,000g for 10 minutes.